Stratigraphy, sedimentology, and paleontology of the lower Eocene San Jose Formation in the central portion of the San Juan Basin, northwestern New Mexico

by Larry N. Smith and Spencer G. Lucas

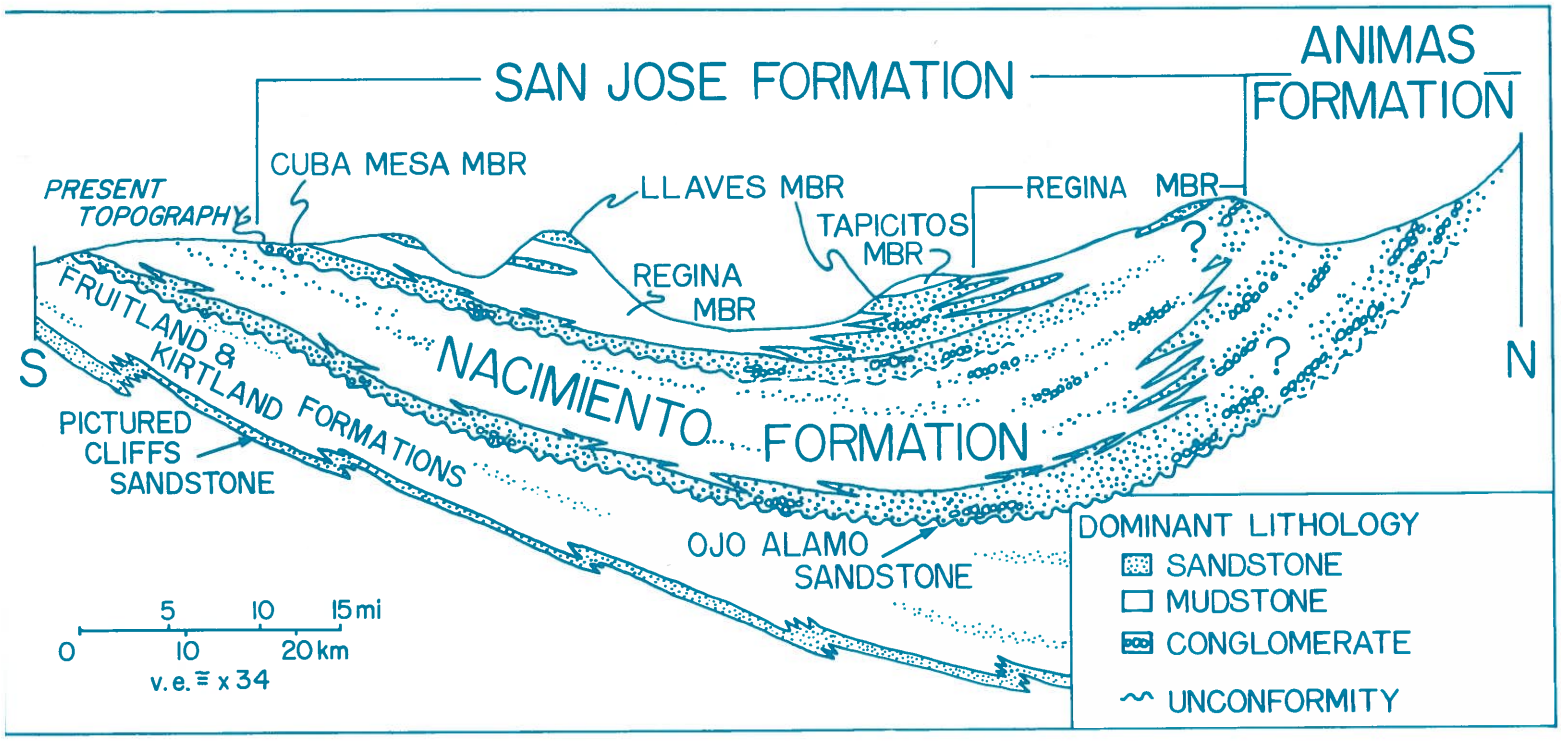

BULLETIN 126 New Mexico Bureau of Mines & Mineral Resources 1991

A DIVISION OF
NEW MEXICO INSTITUTE OF MINING & TECHNOLOGY

Bulletin 126

New Mexico Bureau of Mines & Mineral Resources

A DIVISION OF

NEW MEXICO INSTITUTE OF MINING & TECHNOLOGY

Stratigraphy, sedimentology, and paleontology of the lower Eocene San Jose Formation in the central portion of the San Juan Basin, northwestern New Mexico

Larry N. Smith' and Spencer G. Lucas²

'Shell Western E. & P., Inc., P.O. Box 527, Houston, Texas 77001;
'New Mexico Museum of Natural History, 1801 Mountain Road NW, Albuquerque, New Mexico 87104

SOCORRO 1991

Original Printing

Published by Authority of State of New Mexico, NMSA 1953 Sec. 63-1-4
Printed by University of New Mexico Printing Services, August 1991

Available from New Mexico Bureau of Mines & Mineral Resources, Socorro, NM 87801

Contents

Figures

Tables

Plate (in pocket)

Abstract—The lower Eocene San Jose Formation in the central portion of the San Juan Basin of New Mexico consists of the Cuba Mesa, Regina, Llaves, and Tapicitos Members. Well-log data indicate that, from its 100 m thickness, the Cuba Mesa Member thins towards the center of the basin and pinches out to the northeast by latitude 36° 40' N, longitude 107° 19' W. The Regina Member crops out most extensively in the study area and decreases in sandstone-to-mudrock ratio to the north. The Llaves and Tapicitos Members occur only in the highest locales of the area, are thin due to erosion, and are not mappable as separate units.

Well-log data and 1275 m of measured sections in the Regina, Llaves, and Tapicitos Members indicate that strata in the study area are made up of approximately 35% medium- to coarse-grained sandstone and 65% fine-grained sandstone and mudrock. Sedimentology and sediment-dispersal patterns in the study area suggest deposition by generally south-flowing streams that had sources to the northwest, northeast, and east. Low-sinuosity, sand-bedded, braided(?) streams shifted laterally across approximately 1 km wide channel belts to produce sheet sandstones that are prominent throughout the formation. Levees separated channel environments from floodplain and local lacustrine areas. Avulsion relocated channels periodically to areas on the floodplain, resulting in the typically disconnected sheet sandstones within muddy overbank sediments of the Regina Member.

Fossil plants from lacustrine strata of the Regina Member at Santos Peak are the only flora described from the San Jose Formation. They indicate a humid, forested environment in the depositional basin. Fossil vertebrates from the Regina Member include the mammal taxa *Phenacolemur praecox, Oxyaena forcipata, Ectoganus gliriformis, Esthonyx bisulcatus, Coryphodon molestus, Hyopsodus miticulus, Phenacodus primaevus,* and *Hyracotherium angustidens.* These taxa support correlation with the Almagre local fauna of the Regina Member in the east-central San Juan Basin. They are thus indicative of a middle Wasatchian (Lysitean) age, about 53 Ma.

Introduction

The San Jose Formation of the San Juan Basin is the most extensively preserved and exposed Eocene rock-stratigraphic unit in New Mexico. The formation has yielded one of the largest and most diverse vertebrate faunas of early Eocene age collected in North America. The southern and southeastern outcrop area of the San Jose has received the most geologic study (e.g. Simpson, 1948; Baltz, 1967; Lucas et al., 1981). These previous studies included descriptions of fossils and local physical stratigraphic studies (Simpson, 1948; Haskin, 1980; Lucas et al., 1981; and references cited therein) and regional stratigraphy and mapping (Baltz, 1967; Mytton, 1983; Manley et al., 1987). Strata correlative to the San Jose in the northern and northeastern San Juan Basin, Colorado, were described and mapped (Baltz, 1953; Barnes, 1953; Barnes et al., 1954; Dunn, 1964) before the details of the stratigraphy of the San Jose were worked out to the south (Baltz, 1967). More complete discussions of these and other earlier works are presented below.

In this paper we report on the stratigraphy and paleontology of that part of the San Jose Formation that lies between its southern and northern outcrop areas. We also include a discussion of the sedimentology of these strata, a subject which, except for Smith (1988), has not been reported for any part of the San Jose Formation. This study of the San Jose is part of an effort to decipher the basin-wide stratigraphy of the unit, which will help to determine the (1) paleogeographic controls on the distribution of facies throughout the basin, (2) stratigraphic relationships between the contiguous Paleocene Animas and Nacimiento Formations and the San Jose, (3) stratigraphic relationships between members of the San Jose (Baltz, 1967: 56), (4) completeness of the rock record in the northern versus the southern San Juan Basin, and (5) physical stratigraphy of paleontological sites.

The area (Fig. 1) has been targeted for study because (1) fossil vertebrates have been collected but not described from this area, (2) fossil-leaf floras, which are uncommon in the San Jose, are located in this area, (3) the four-quadrangle area is adjacent to previous geologic maps that delineate four members of the formation, (4) excellent outcrops and closely spaced well logs are available for study, and (5) north-to-south facies changes in the San Jose are evident in this and adjacent areas.

The goals of the present study include presentation of stratigraphic, sedimentologic, and paleontologic data on the four-quadrangle region, evaluation of the applicability of the stratigraphy of Baltz (1967) outside of his study area, and discussion of the accumulation of the San Jose Formation in the central San Juan Basin. Physical stratigraphy is presented in the form of a geologic map and surface and subsurface data along cross sections. The subsurface work extends outside of the present map area to show regional correlations. Sedimentologic and paleocurrent information from within the map area provide a basis for discussion of the types of environments responsible for deposition of the rock units. Systematic description of fossils found in the study area and their biochronologic significance are included. We conclude with a general discussion of the stratigraphy of the San Jose Formation.

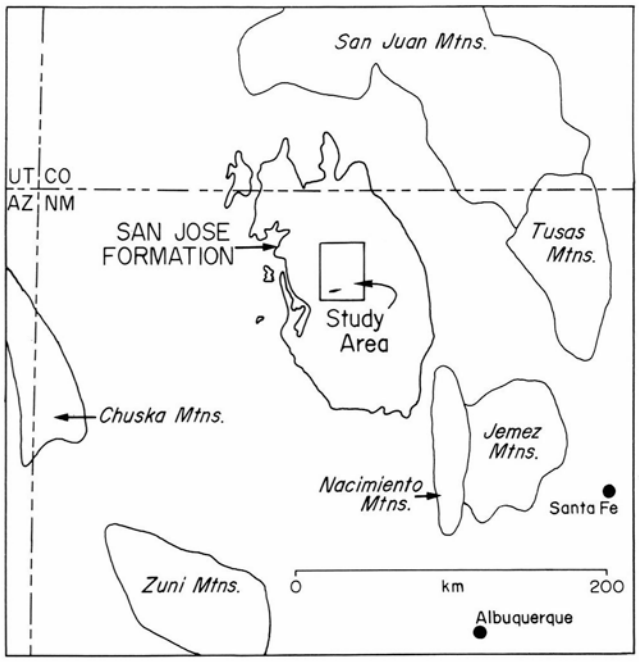

FIGURE 1—Location map of study area.

Acknowledgments

This study of the San Jose Formation depended on the fundamental observations of a number of geologists who

worked in the San Juan Basin, especially E. H. Baltz, Jr. We are grateful to those who have published stratigraphic and paleontologic data so that we could incorporate their work. We especially thank E. H. Baltz, Jr. for his published contributions and correspondence, and G. R. Scott for a preprint of the Aztec 1° x 2° quadrangle and his comments on the San Juan Basin stratigraphy.

Financial support for field and laboratory work was provided by the New Mexico Bureau of Mines & Mineral Resources. Additional support that contributed to data acquisition was provided to LNS by the New Mexico Geological Society, the Geological Society of America (research grant 3497-85), the Department of Geology of the University of New Mexico, and the Donald L. Smith Research Grant awarded by the Rocky Mountain Section of the Society of Economic Paleontologists and Mineralogists.

We also thank Dr. Robyn Wright for her comments and discussion on sedimentology and her review of an earlier draft of this report; Dr. Les McFadden for his advice on paleopedology; Ken Kietzke for running samples for microfossils; Cornelis Klein for generously allowing us to use his photography equipment and microscope; and S. Cather, R. Chamberlin, and L. Krishtalka for helpful reviews of an earlier version of this report.

Structure of the San Juan Basin

The study area is located in the geographic center of the central basin region of the San Juan Basin (Fig. 2). Structurally, the area is in the southwestern part of the central basin, a northeast-dipping structural ramp that slopes from the Zuni uplift, across the Chaco slope, and toward the northeastern axis of the basin, as defined by the elevation of the Upper Cretaceous Huerfanito bentonite bed (Fassett and Hinds, 1971: fig. 15). The structurally lowest part of the basin, as defined by Cretaceous rocks, is in a northwest-trending oval 10 km north of the present map area (Thaden and Zech, 1984). The structure of the base of the Paleocene Ojo Alamo Sandstone (Fig. 2) shows little north-to-south tilt and minor east dip in the study area. Thus, the study area is west-southwest of the Paleogene axis of the San Juan Basin. Dips greater than 5° in the San Jose Formation are restricted to outcrops along a 2-10 km wide belt to the east and to some of the unit's northern occurrences in Colorado. No faults exist in the central and western parts of the San Jose except for those related to rock slumps along some canyon walls.

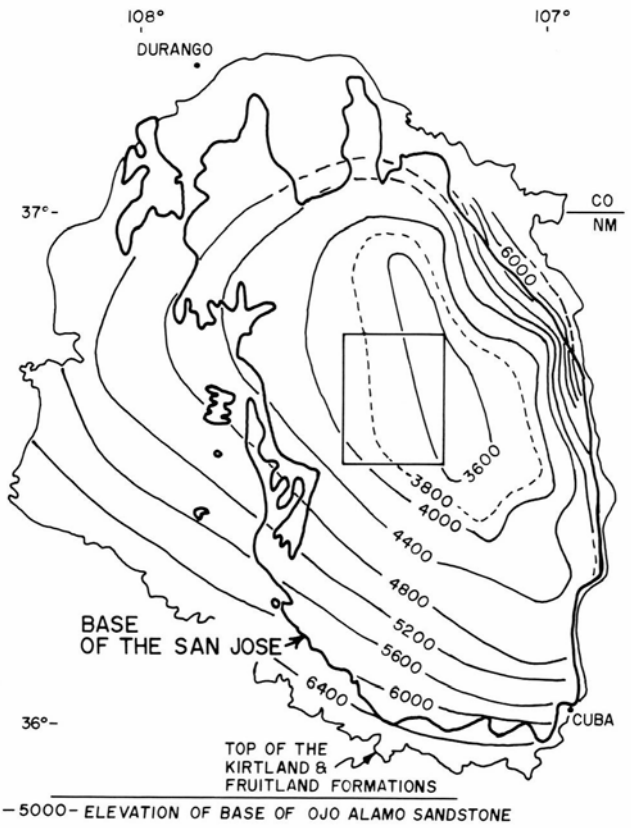

FIGURE 2—Structure contour map of central San Juan Basin. Modified from Fassett and Hinds (1971), with study area indicated by rectangle.

Stratigraphy

Previous studies

Stratigraphy of the Paleocene Ojo Alamo, Nacimiento, and Animas Formations—The stratigraphic sequence of Paleogene rocks in the eastern part of the San Juan Basin is shown diagrammatically in Fig. 3. The Ojo Alamo Sandstone (sensu Baltz et al., 1966) and Nacimiento Formation (sensu Simpson, 1948) have been studied and named for outcrops in the southern part of the San Juan Basin. The Ojo Alamo Sandstone is a nearly basin-wide, sheet-like sandstone that is as much as 120 m thick (Fassett and Hinds, 1971; Sikkink, 1987). The Nacimiento Formation is a sequence of varicolored beds of sandstone and mudrock that attains a thickness of as much as 530 m (Baltz, 1967). The Nacimiento contains Puercan and Torrejonian fossils that indicate an early Paleocene (Daman equivalent) age of deposition (Lucas and Ingersoll, 1981; Sloan, 1987). A north-to-south decrease in grain size in the formation has been recognized in well logs (Baltz, 1967: 38-39) and surface sections (Tsentas et al., 1981).

The Animas Formation (sensu Barnes et al., 1954) was named for strata in the northern part of the San Juan Basin that occupy a stratigraphic position similar to that of the Ojo Alamo and Nacimiento Formations. The Animas includes two members, the lower McDermott Member of Late Cretaceous age (Upper Cretaceous McDermott Formation of Reeside, 1924) and an informal upper member that contains Paleocene plant fossils (Knowlton, 1924). The upper member of the Animas also includes the late Paleocene (Thanetian equivalent) Tiffany vertebrate fauna (Granger, 1917; Simpson, 1935 a, b, c) indicating a younger age for these strata than recognized for any Nacimiento strata to the south. The Animas strata comprise a generally fining-upward sequence of volcaniclastic conglomerates and sandstones, with arkosic conglomerates and sandstones near the top. The upper member of the Animas has been shown to interfinger with the Nacimiento in its eastern (Dane, 1946) and western (Barnes et al., 1954) outcrop belts. Subsurface correlation of these formations has not been carried out in any detail because of the difficulty of recognizing their contact on electric logs (Fassett and Hinds, 1971: 33).

The nature of the contact between the lower Eocene San Jose Formation and the Nacimiento Formation north of latitude 36° 45' N has been described as conformable (Barnes et al., 1954; Stone et al., 1983: 25-26), whereas at latitude 36° N it has been shown to be unconformable (Baltz, 1967; Lucas et al., 1981). The transitional nature of the contact from conformable to unconformable has not been analyzed or discussed in any detail. Contact relationships between the San Jose and Animas Formations in the northernmost San Juan Basin have been shown to be intertonguing (Smith, 1988). The presence of Tiffanian strata indicates that upper Paleocene strata are preserved below and/or laterally adjacent to the San Jose Formation in Colorado. Upper Paleocene strata may have been eroded (Baltz, 1967: 87), not deposited, or are represented by unfossiliferous sandstones

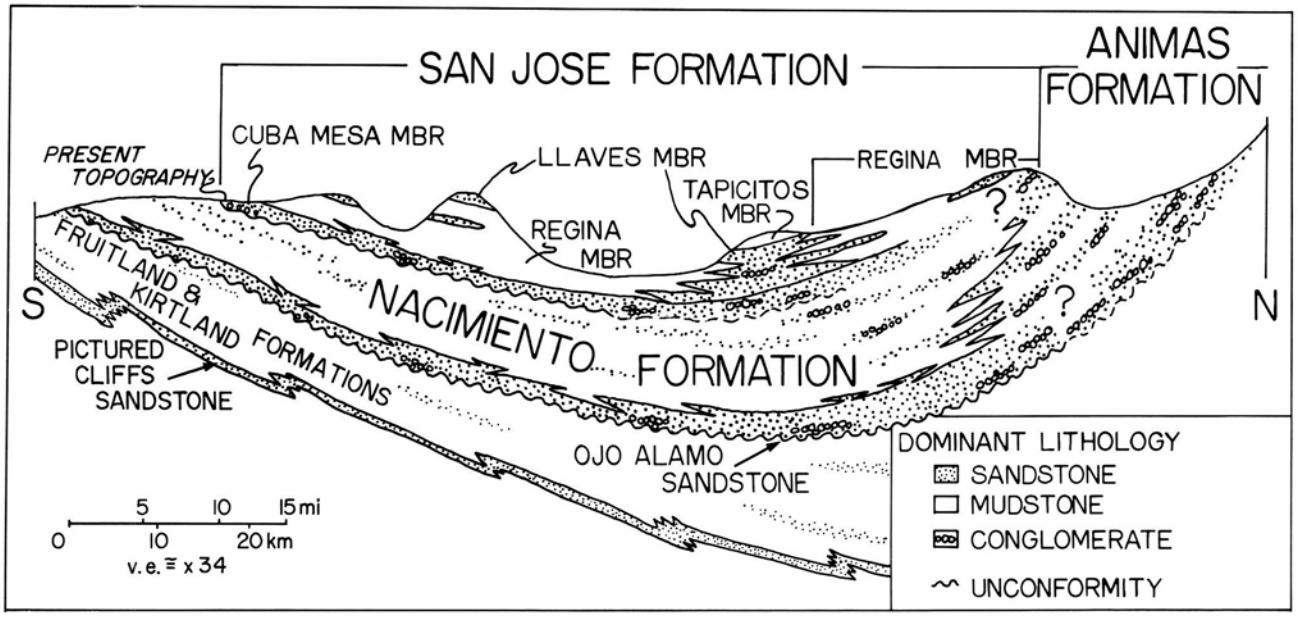

FIGURE 3—Diagrammatic north–south cross section showing the physical stratigraphy of the uppermost Cretaceous and lower Tertiary strata in the San Juan Basin (modified from Smith et al., 1985).

of the basal Cuba Mesa Member of the San Jose Formation in the southern part of the basin.

Stratigraphy of the Eocene San Jose Formation—The San Jose Formation was named by Simpson (1948) for a mudrock-dominated sequence of strata in the southeastern San Juan Basin that contains early Eocene fossil vertebrates (Lucas et al., 1981). Baltz (1967) mapped the base of the formation to include a pervasive sandstone-dominated sequence that rests in slight-to-moderate angular unconformity on the Paleocene Nacimiento Formation in the southern San Juan Basin. Baltz (1967) defined four members of the San Jose in the southeastern outcrop area (Fig. 3). He also recognized an "unnamed member," composed mostly of mud-rock, north of the Llaves Member and suggested that it is time- and facies-equivalent of, but not laterally continuous with, the Regina Member (Baltz, 1967: 56). Stratigraphic data included in the present report and Smith (1988) indicate the necessity for some modifications to Baltz's work outside of the southeastern portion of the San Juan Basin (Fig. 4).

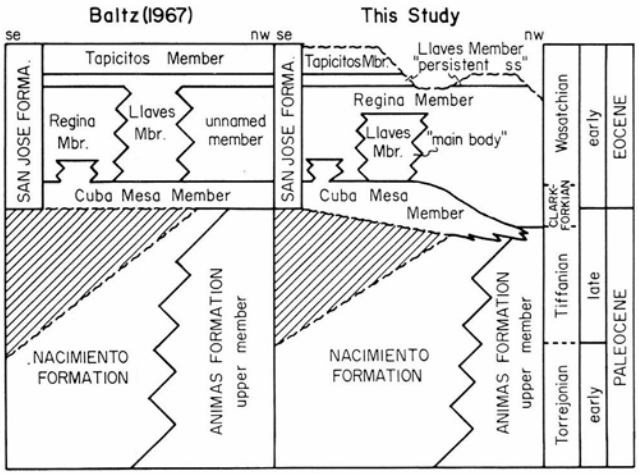

FIGURE 4—Comparison of Baltz's (1967: 86) nomenclature for the San Jose Formation with that of this report (modified from Smith, 1988). The separation of two parts of the Llaves Member, shown on the right, occurs east of the study area; only the "persistent sandstone" occurs in the study area.

Geologic mapping of the members of the San Jose Formation has been carried out in the southwestern outcrop areas of the formation (Mytton, 1983) by extension of Baltz's (1967) contacts. We correct the position of the basal San Jose contact on our map after a mapping error from Dane and Bachman's (1957) map was perpetuated on the maps of, or in, Dane and Bachman (1965), Fassett and Hinds (1971), Clemons (1982), and Stone et al. (1983). To some extent, the origin of this mapping error may have been due to the presence of arkosic sandstones similar in lithology to the basal San Jose strata in the underlying Nacimiento Formation in the west-central and northern parts of the San Juan Basin. The Regina and Cuba Mesa Members have been mapped by reconnaissance to the west and northwest of the present map area by Manley et al. (1987) (Fig. 5).

Correlation of Paleogene strata in the San Juan Basin by well-log interpretation has been carried out by Baltz (1967), Fassett and Hinds (1971) (Ojo Alamo Sandstone only), Brimhall (1973), and Stone et al. (1983). None of these studies were intended to analyze facies changes within members of the San Jose. These previous workers portrayed the members of the San Jose Formation as continuous and consistent with the formal stratigraphy of Baltz (1967), with some lateral changes in thickness.

Methodology

Outcrop stratigraphy—Members of the San Jose Formation were mapped with aerial photographs (USGS VANJ-1962) on the Santos Peak, Vigas Canyon, Gobernador, and Fourmile Mesa 71/2 min. topographic quadrangle maps. It became apparent that subsurface stratigraphy must be incorporated with field mapping to evaluate accurately contacts between the intertonguing members of the formation. Because structural dips on the rock bodies are below the measurement error of standard field equipment, regional mapping of continuous sandstone beds and trigonometric solutions of gently dipping sandstone beds in the subsurface had to be employed to evaluate structural tilt from assumed original positions of horizontality.

Stratigraphic sections were measured with a 1.5 m staff and Brunton compass. Long stratigraphic sections (100-400 m) are only 0.5 to 7% different from topographic relief along

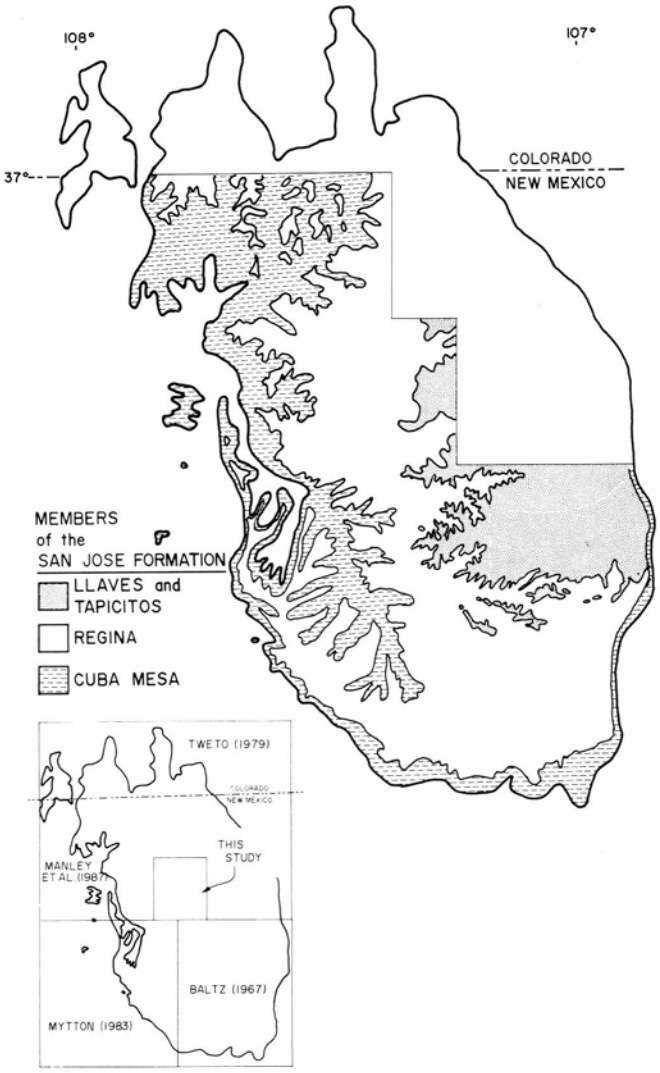

FIGURE 5—Geologic map of distribution of the members of the San Jose Formation. Note that the entire northern half of the San Jose Formation in New Mexico was mapped by Manley et al. (1987); however, members were not differentiated in that area.

sections as estimated from topographic maps. Two- and three-dimensional outcrop faces were studied with the use of photographic panoramas to analyze local relationships between beds; these panoramas are discussed in the sedimentology section of this report.

Subsurface stratigraphy—Subsurface data for the area consist mostly of spontaneous potential (SP), resistivity, and conductivity electric logs, and a few gamma-ray radioactivity logs. Resistivity and SP logs were used for correlation; gamma-ray and conductivity logs were consulted when available to confirm correlations. One to four electric logs from wells drilled for hydrocarbons are available for most sections in each township of the study area. The well log with the longest Paleogene sequence in each section along cross sections was selected for correlation. The positions of the wells were orthogonally projected onto cross-section lines over an average distance of 920 m, resulting in an average apparent spacing along cross-section lines of 1.5 km for the 87 well logs employed (Fig. 6). This relatively close spacing of well logs was deemed necessary for consistent correlation of members of the San Jose Formation.

Beds were picked based on deviation of resistivity and SP values from mudrock base-lines (after Dresser-Atlas, 1975). Beds as thin as 1.5 m were picked on working copies of the logs. Interpretations of sedimentary facies of beds picked on well logs are based on (1) comparison and correlations of measured outcrop sections with nearby well logs, (2) comparison of bed thickness in subsurface and surface sections, and (3) evaluation of the magnitude of deviation of electric signals from mudrock base-lines.

Four electric logs have been correlated to nearby stratigraphic sections to corroborate electric-log interpretations made in this report (Fig. 7). The correlations in Fig. 7 show a positive relation between increasing grain size and value of resistivity and SP. Higher porosities in some beds are probably due to either coarser grain sizes or lesser amounts of cement in pores relative to other parts of the logs. The lower values of resistivity in some coarse-grained sandstone beds (Fig. 7) may be due to locally greater volumes of pore-filling cement. For example, in the section with the greatest amount of sandstone, MS-4 (Fig. 7), very coarse-grained sandstones with abundant gravel-sized mudrock ripups correlate to beds with resistivities that are lower than medium-to-coarse-grained sandstones that do not have mudrock ripups. The presence of mudrock ripups in channel sequences may affect the hydrologic properties of the beds and decrease resistivity by locally increasing the amount of intergranular clay and silt through infiltration.

Beds indicated by high resistivity and negatively skewed SP, relative to the base-lines, are interpreted to be sandstones or siltstones with relatively salt-laden water in pores. (Dresser-Atlas, 1975). Positively skewed SP values occur locally on the logs, suggesting the presence of relatively fresh water, as in the Kaime Ranch aquifer of the Nacimiento Formation (Brimhall, 1973). Many rock sequences show extremely high resistivity on electric logs, e.g. much of the Ojo Alamo Sandstone (Fassett and Hinds, 1971: 6). An extremely high value of resistance for each log studied in the present report was chosen arbitrarily to be equal to 70% of the maximum normal resistance value on that log. Strata that have resistivities higher than this value are interpreted to have higher porosities relative to other sandstones on the log.

Kantorowicz (1985) demonstrated for terrestrial channel sandstones that more laterally continuous beds will commonly have greater porosity than more discontinuous channel-sandstone bodies because much sandstone cementation is due to flushing depositional water from surrounding mudrock. More continuous beds will tend to transmit meteoric water that dilutes depositional water. This relationship may help to explain why the Ojo Alamo Sandstone and Cuba Mesa Member have high resistivities and SP values relative to some Regina Member sandstones that have the same texture. Thus, if the continuity of sandstone beds has controlled diagenesis in the San Jose Formation and the high resistivities are measures of porosity, beds with extremely high resistivities should be more easily correlated than those with lower resistivities and be useful for evaluation of lateral changes in rock-stratigraphic units.

The locations of stratigraphic-unit boundaries in the subsurface were picked and correlated based on (1) correlation with, and reinterpretation of, contacts mapped on the surface (Baltz, 1967; Mytton, 1983; present study); (2) correlation with, and reinterpretation of, previous subsurface work in the region (Baltz, 1967; Fassett, 1968; Fassett and Hinds, 1971; Brimhall, 1973; Stone et al., 1983), and (3) dips along cross-section lines measured from elevations of marker beds, such as the bases of the Ojo Alamo Sandstone and Cuba Mesa Member of the San Jose Formation.

Stratigraphy of the San Jose Formation and subjacent strata in the study area

The San Jose Formation is made up of beds of sandstone and mudrock that can typically be shown to be lenticular

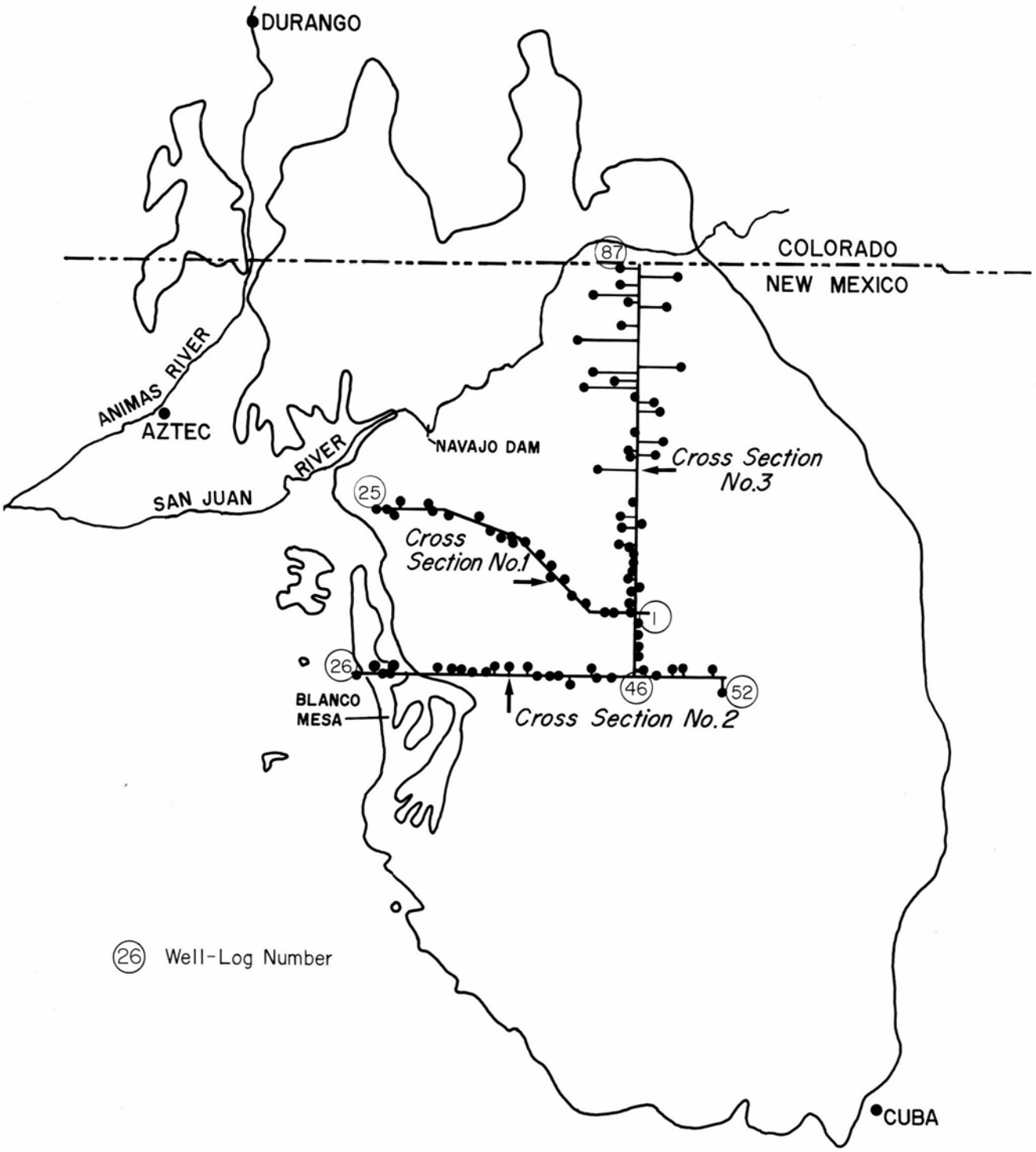

FIGURE 6—Locations of well logs and cross sections (see Appendix 1).

over outcrop to basin-wide scales. Baltz (1967) originally defined the Cuba Mesa and Llaves Members to include sandstone tongues that trace into or correlate with the main bodies of these sandstone-dominated units. Sandstones with lithologies identical to the Cuba Mesa and Llaves Members, but surrounded by mudrock of the Regina or Tapicitos Members, were assigned to the mudrock-dominated units by Baltz (1967). We adopt this nomenclatural method in the present report.

Cuba Mesa Member and subjacent strata—The Cuba Mesa Member of the San Jose Formation has been traced in outcrop (Baltz, 1967: pl. 1; Mytton, 1983) and in subcrop (Baltz, 1967: pl. 5) from its type locality near Cuba, New Mexico, to the southwestern boundary of the present map area. At the Cuba Mesa Member type locality and in outcrops west of the present study area (e.g. on Blanco Mesa, along Manzanares Canyon, and along the San Juan River near Navajo Dam: Figs. 5, 6, Pl. 1), the unit consists of white-to-yellow, thickly bedded, locally conglomeratic, very coarse- and coarse-grained arkosic sandstone with minor mudrock lenses (Fig. 8). The Nacimiento Formation beneath the Cuba Mesa Member in the above-mentioned outcrops contains arkosic sandstones that are similar in lithology to those of the Cuba Mesa Member (Baltz, 1967: 56). The base of the Cuba Mesa Member in its western outcrop area is picked at the base of a laterally continuous, thickly bedded arkosic

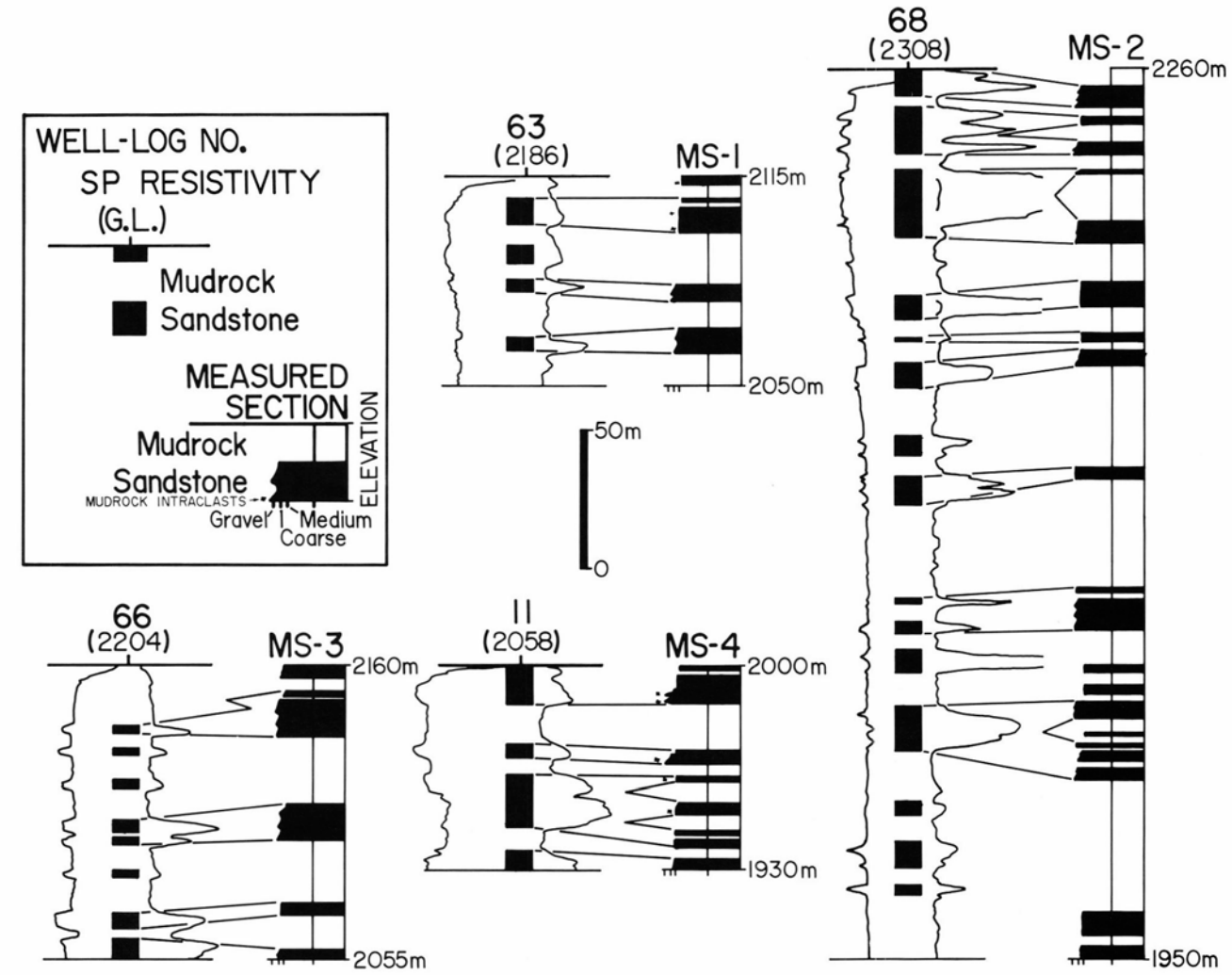

FIGURE 7—Correlations between four well logs and nearby stratigraphic sections of the Regina, Llaves, and Tapicitos Members of the San Jose Formation. Locations of stratigraphic sections and nearby well logs are shown in Fig. 9.

sandstone (the base of the Wasatch Formation of Reeside, 1924: 40-41). In outcrops west of the study area, the Cuba Mesa Member is overlain by mudrocks that we consider to be of the Regina Member at elevations near 1930 m at Navajo Dam, 1930 m in Manzanares Canyon, and 2085 m on Blanco Mesa. To assess the upper and lower contacts of the Cuba Mesa Member, we have correlated the strata in the present study area with outcrops outside of the area by the use of electric logs (Pl. 1, in pocket).

The locations of cross sections 1, 2, and 3 and well logs employed in this report are shown in Fig. 6. The cross sections are in Pl. 1 (in pocket). Cross-section lines and well-log locations are also shown on the geologic map of the present study area (Fig. 9). Location and ownership information for individual well logs are compiled in Appendix 1.

Representative electric logs that show subsurface correlations of Paleogene strata across the southern part of the study area with outcrops and subsurface data to the west are depicted in Fig. 10. The well logs shown in Fig. 10 are

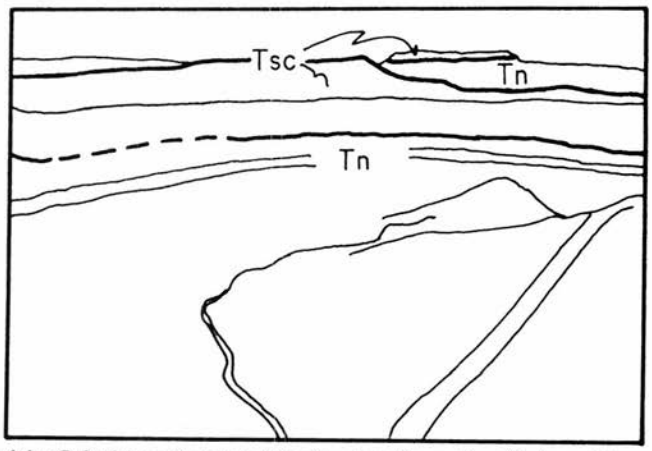

FIGURE 8—Low-angle oblique aerial view looking west-southwest, of the Cuba Mesa Member of the San Jose Formation (Tsc) overlying the Nacimiento Formation (Tn) west of the study area (secs. 22 and 23, T26N, R5W).

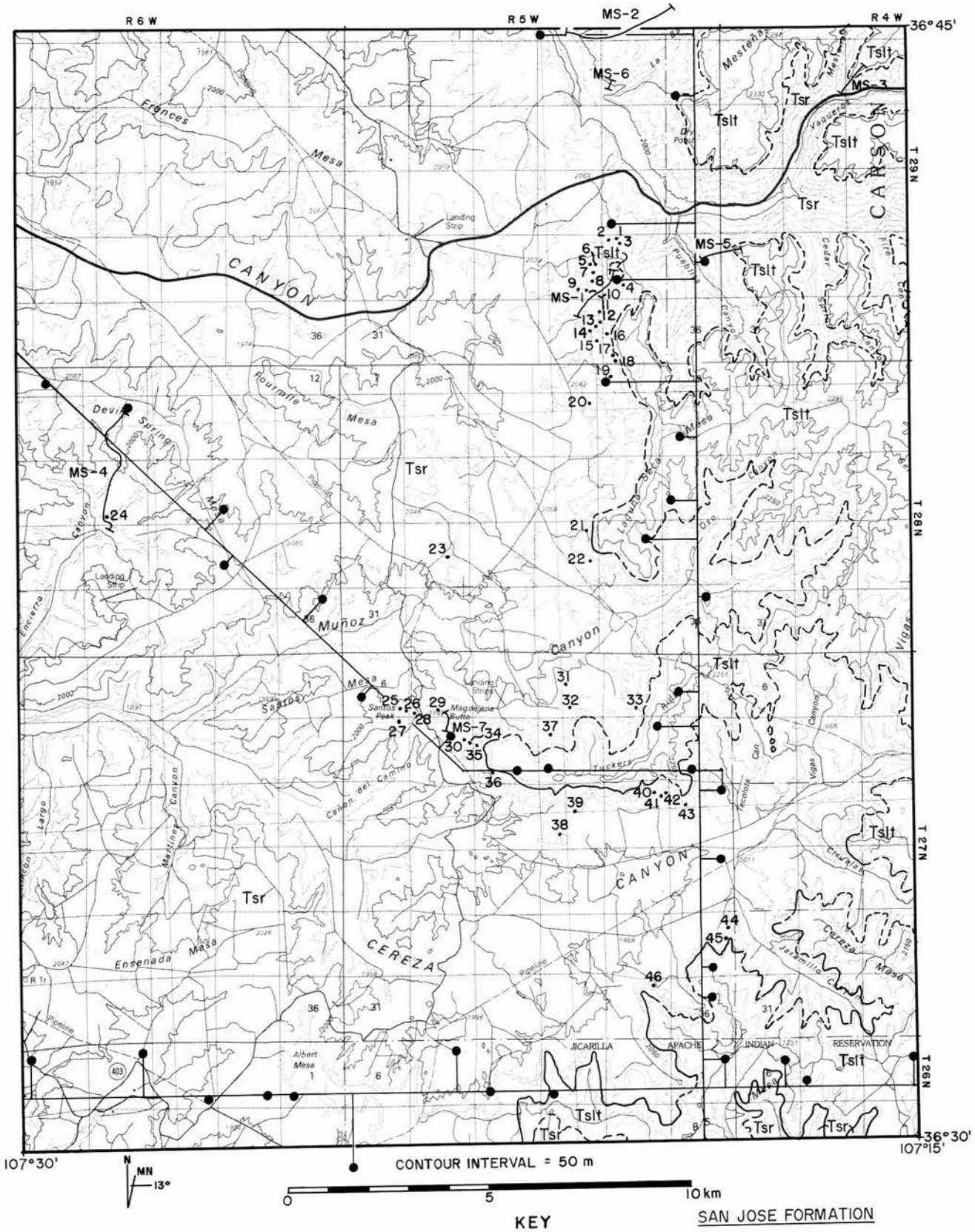

FIGURE 9—Geologic map of study area showing locations of stratigraphic sections, well-log cross sections, and paleontological sites. Topographic base is from the U.S.G.S. Navajo Reservoir 30 × 60 min. quadrangle.

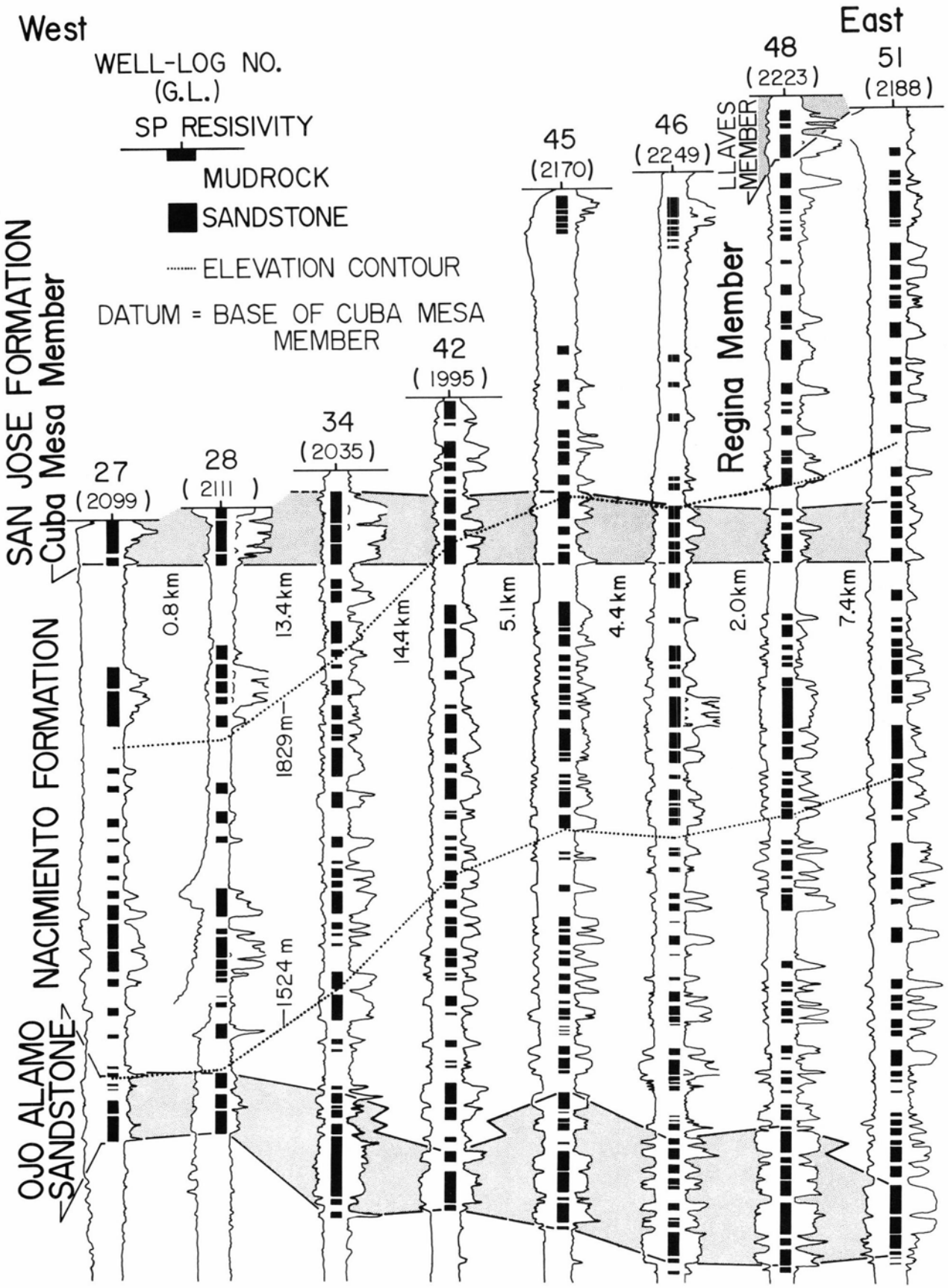

FIGURE 10—Representative well logs along cross section 2, showing correlation of Paleogene units. Distance between well logs is given in kilometers.

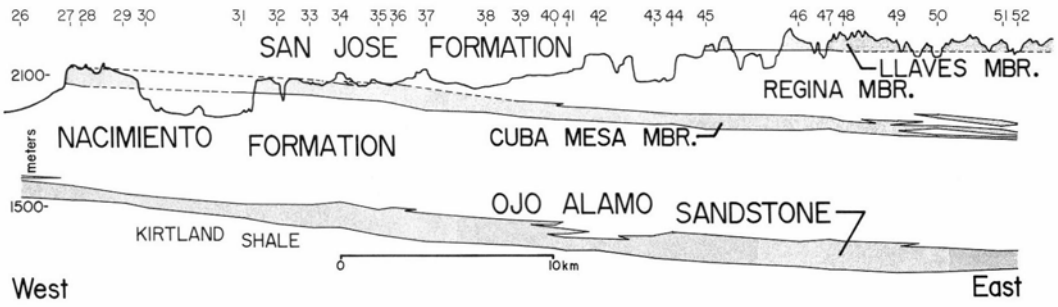

FIGURE 11—Paleogene stratigraphy along cross section 2, generalized from Pl. 1 (in pocket).

eight of the 27 well logs that were used to construct cross section 2 in Pl. 1, which is depicted in generalized form in Fig. 11. The contact between the Cuba Mesa Member of the San Jose Formation and the Nacimiento Formation was chosen as a datum for Fig. 10 to show the slight angular relation between the Cuba Mesa Member and the Ojo Alamo Sandstone along this 46 km long cross section. In Fig. 11 and Pl. 1, which utilize mean sea level as a datum, an apparent eastward dip of approximately 0.35° is evident. The interval including the Ojo Alamo and Nacimiento Formations is slightly thicker in the east, toward the basin center. The Cuba Mesa is a coarse, sandstone-dominated unit that is as much as 90 m thick in the western and central part of cross section 2 (Fig. 11, Pl. 1). In the four easternmost logs (well logs 49 to 52), the Cuba Mesa Member thins dramatically by intertonguing with mudrock.

Well log 45 (Figs. 10, 11) is interpreted as it was by Baltz (1967: pl. 5). Mytton (1983) mapped the top of the Cuba Mesa Member 30-50 m higher than shown in the vicinity of well log 38 in Fig. 11 and Pl. 1. The westernmost well log in Fig. 11 is the same as well log 218 of Stone et al. (1983: sheet 4). Based on the correlations presented above (Figs. 10, 11, Pl. 1), we pick the base of the Cuba Mesa 250 m higher in elevation than did Stone et al. (1983: sheet 4, well log 218) on the same well log. Based on our correlation of the base of the San Jose Formation along the axis of the San Juan Basin, the San Jose Formation reaches a maximum thickness of 608 m (Smith 1988: well log 177), which is significantly less than the 811 m thickness reported by Stone et al. (1983: well log 219).

The Cuba Mesa Member along a northwest-to-southeast cross section (cross section 1) shows a minor eastward apparent dip of 0.06° (Fig. 12, Pl. 1). The Cuba Mesa Member below Manzanares Mesa is thick relative to the rest of the cross section, reaching at least 100 m at well log 25. Correlation of the base of the Cuba Mesa Member is complicated in the northwestern part of the cross section by an abundance of sandstone in the upper Nacimiento Formation. Topographic relief on the base of the Cuba Mesa Member between well logs 16 and 25 (Fig. 12, P1. 1) could be due to erosion of the Nacimiento Formation during deposition of the Cuba Mesa in this area. The Cuba Mesa Member thins by intertonguing with mudrock to the southeast, toward the center of the San Juan Basin (Fig. 12). The electric-log signatures suggest that this thinning is accompanied by a southeastward-fining of grain size (Pl. 1). The interval represented by the Ojo Alamo and Nacimiento Formations thickens slightly toward the basin center along cross section 1, as it does in cross section 2 (Pl. 1).

North-to-south correlation of the Ojo Alamo through San Jose Formations is shown in Fig. 13. The seven well logs in Fig. 13 are representative of the 30 logs that were used to construct cross section 3 (Fig. 14, Pl. 1). The irregularity of the base of the Ojo Alamo Sandstone on this cross section is due to the locations of wells off the cross-section line and to eastward dip of the unit (Figs. 2, 6). The Cuba Mesa Member thins from 46 m at well log 46 by intertonguing with mudrock to a pinchout by well log 63. Correlations of the Cuba Mesa near its northern pinchout on cross section 3 are shown schematically; the member likely splits into lenticular sandstones in this area. In this area (between Carrizo [Cereza] and La Jara canyons) the Regina Member of the San Jose comes to lie on the Nacimiento Formation in apparent conformable contact. Thickness changes in the interval including the Ojo Alamo and Nacimiento Formations cannot be evaluated because the uppermost Nacimiento Formation and Regina Member are indistinguishable on electric logs. North-to-south facies changes in the Nacimiento Formation are evident on cross section 3 where a south-thinning wedge or relatively coarse-grained sandstone intertongues with mudrock and relatively fine-grained sandstone near the base and top of the formation (Fig. 13, Pl. 1). This north-to-south decrease in grain size in the Nacimiento Formation is similar to that recognized by Baltz (1967) and Tsentas et al. (1981).

In summary, the Cuba Mesa Member is a distinct 40 to 100 m thick sheet sandstone in the west-central portion of the San Juan Basin. It thins toward the center of the basin by intertonguing with mudrock of the Regina Member of the San Jose Formation and the upper Nacimiento Formation. The Cuba Mesa Member pinches out toward the basin center where the sheet sandstone is replaced laterally by

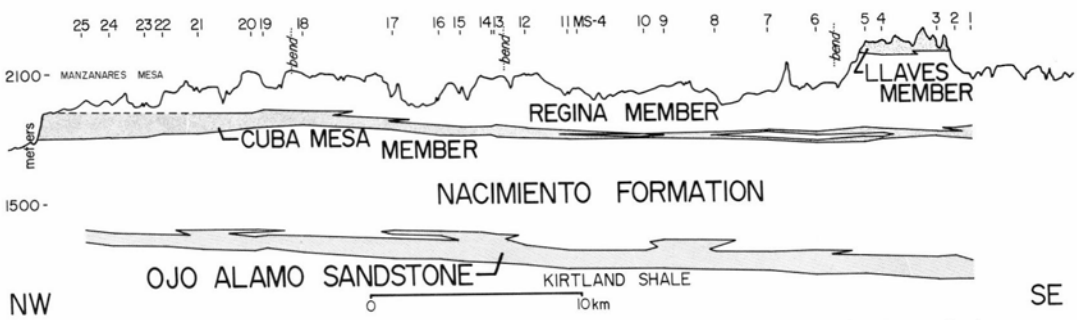

FIGURE 12—Paleogene stratigraphy along cross section 1, generalized from Pl. 1 (in pocket).

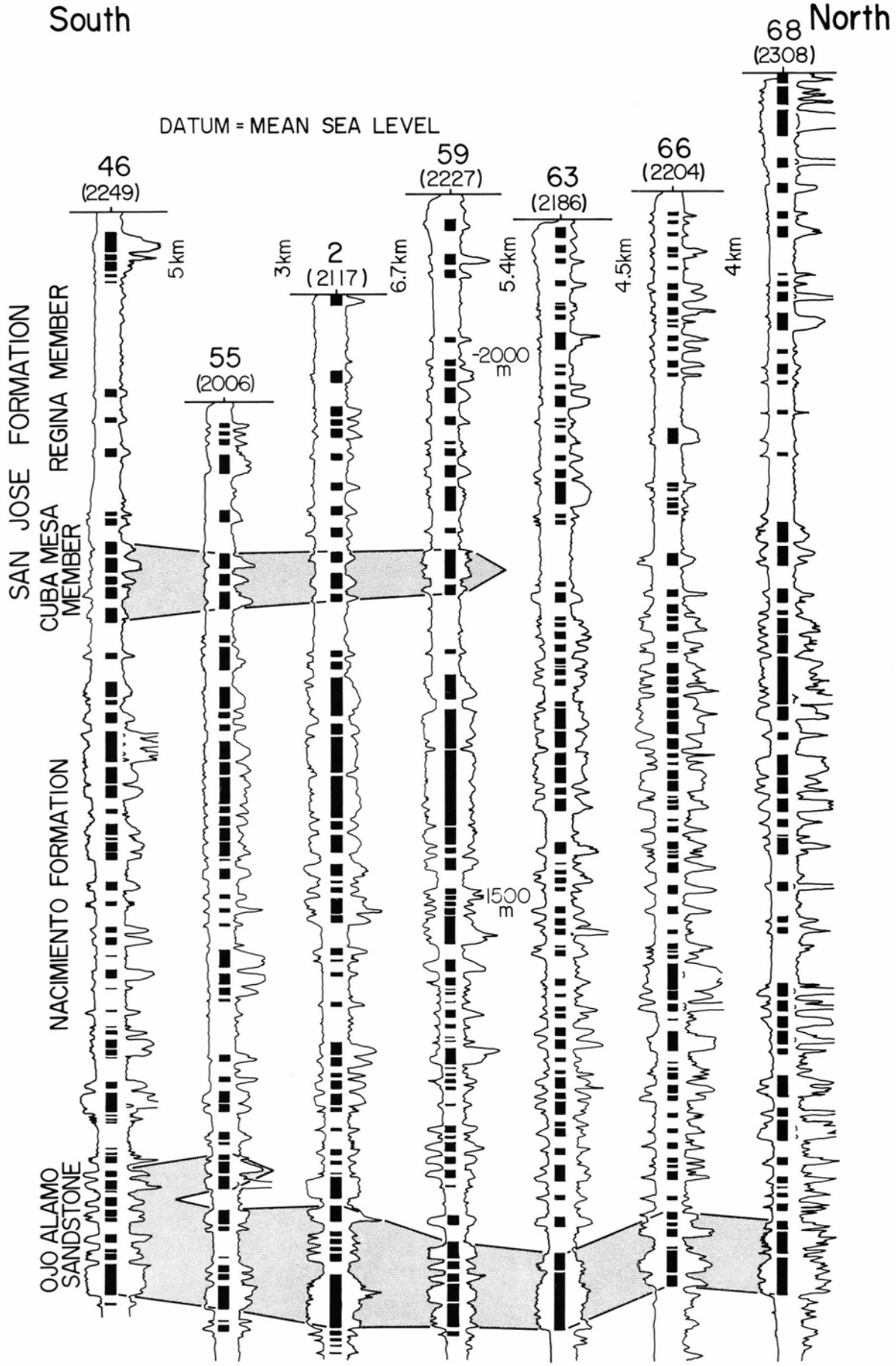

FIGURE 13—Representative well logs along cross section 3, showing correlation of Paleogene units. See Fig. 10 for explanation.

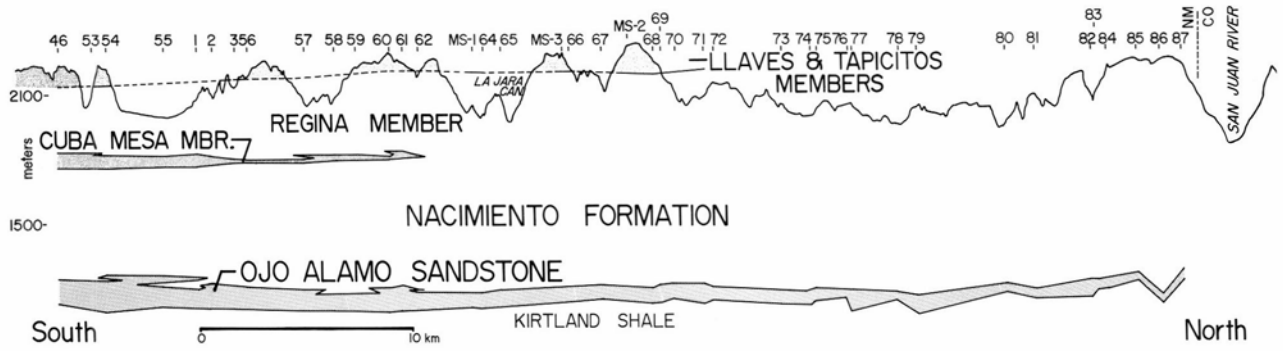

FIGURE 14—Paleogene stratigraphy along cross section 3, generalized from Pl. 1 (in pocket).

lenticular sandstone bodies and mudrock. The existence of the Cuba Mesa Member as a sheet-like sandstone in the area west of the present study area suggests that the member pinches out to the northeast rather than simply to the north. The base of the Cuba Mesa Member may be on an unconformity below Manzanares Mesa and in the southern part of the study area, but is apparently conformable in the northeastern part of the study area where the Cuba Mesa intertongues with the Nacimiento Formation.

Regina Member—The Regina Member, the most widely distributed unit in the present map area (Figs. 5, 9), is composed of complexly interbedded mudstone, fine- to very coarse-grained sandstone, and minor amounts of shale. Sandstone beds are lenticular over scales ranging from a few meters to many kilometers. The sandstones are surrounded by mudrock and together form mesas and cliffs of medium- to very coarse-grained sandstone surrounded by badland slopes of fine sandstone and mudrock (Fig. 15). The lower contact of the Regina does not crop out in the map area but is conformable with the Cuba Mesa Member throughout the basin. The contact between the Regina Member and the overlying Llaves Member intertongues and is chosen at the base of an approximately 30 m thick sandstone-dominated sequence (after Baltz, 1967: pl. 1; Mytton, 1983).

Seven stratigraphic sections that include the Regina Member are shown in Fig. 16. Resistivity and SP electric logs from wells near four of these measured sections are correlated with parts of these sections (Fig. 7); lenticularity of sandstone beds is evident in these sections where beds do not directly correlate. The Regina Member in the stratigraphic sections is made up of 38% medium- to very coarse-

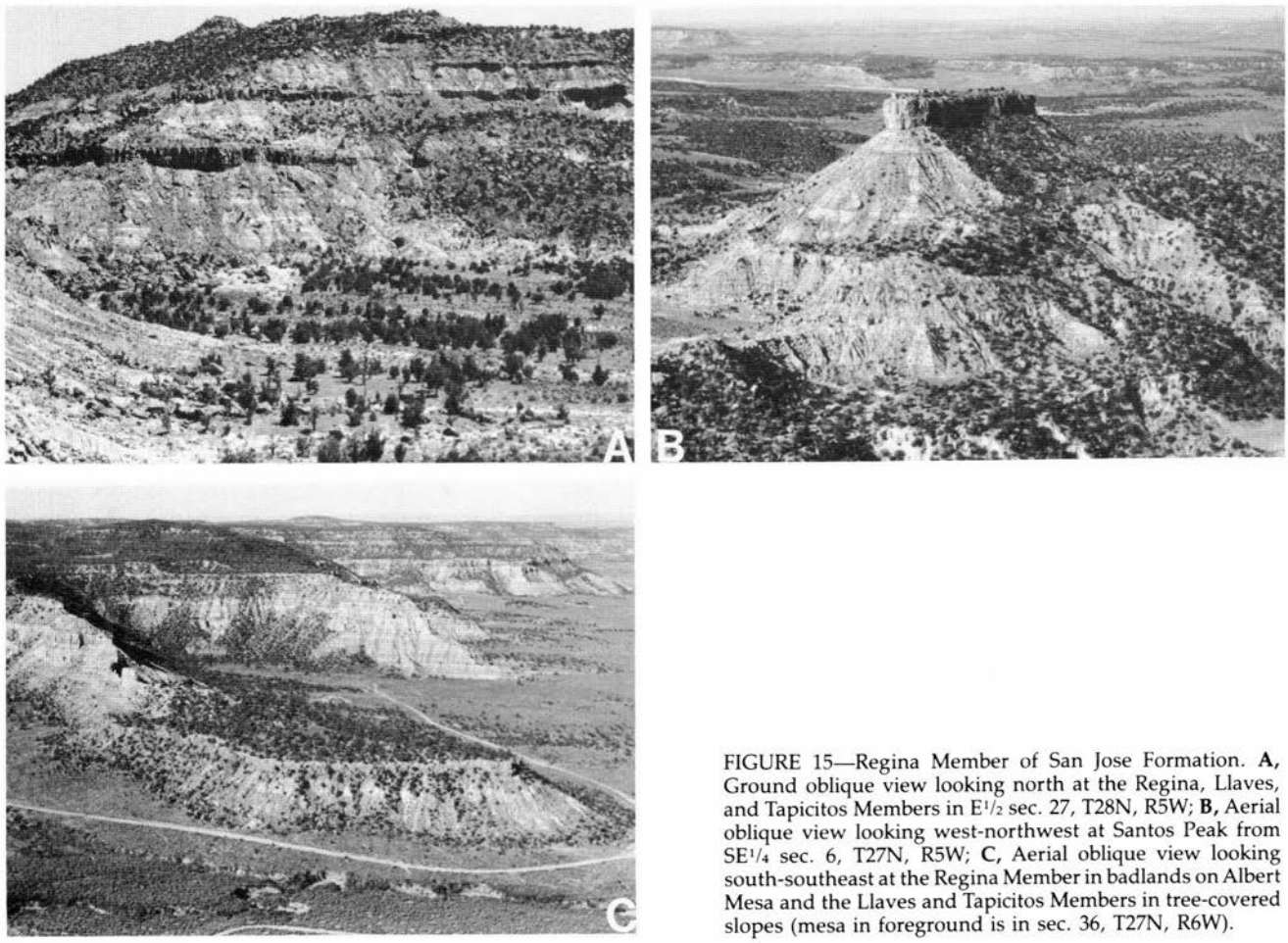

FIGURE 15—Regina Member of San Jose Formation. **A,** Ground oblique view looking north at the Regina, Llaves, and Tapicitos Members in E1/2 sec. 27, T28N, R5W; **B,** Aerial oblique view looking west-northwest at Santos Peak from SE1/4 sec. 6, T27N, R5W; **C,** Aerial oblique view looking south-southeast at the Regina Member in badlands on Albert Mesa and the Llaves and Tapicitos Members in tree-covered slopes (mesa in foreground is in sec. 36, T27N, R6W).

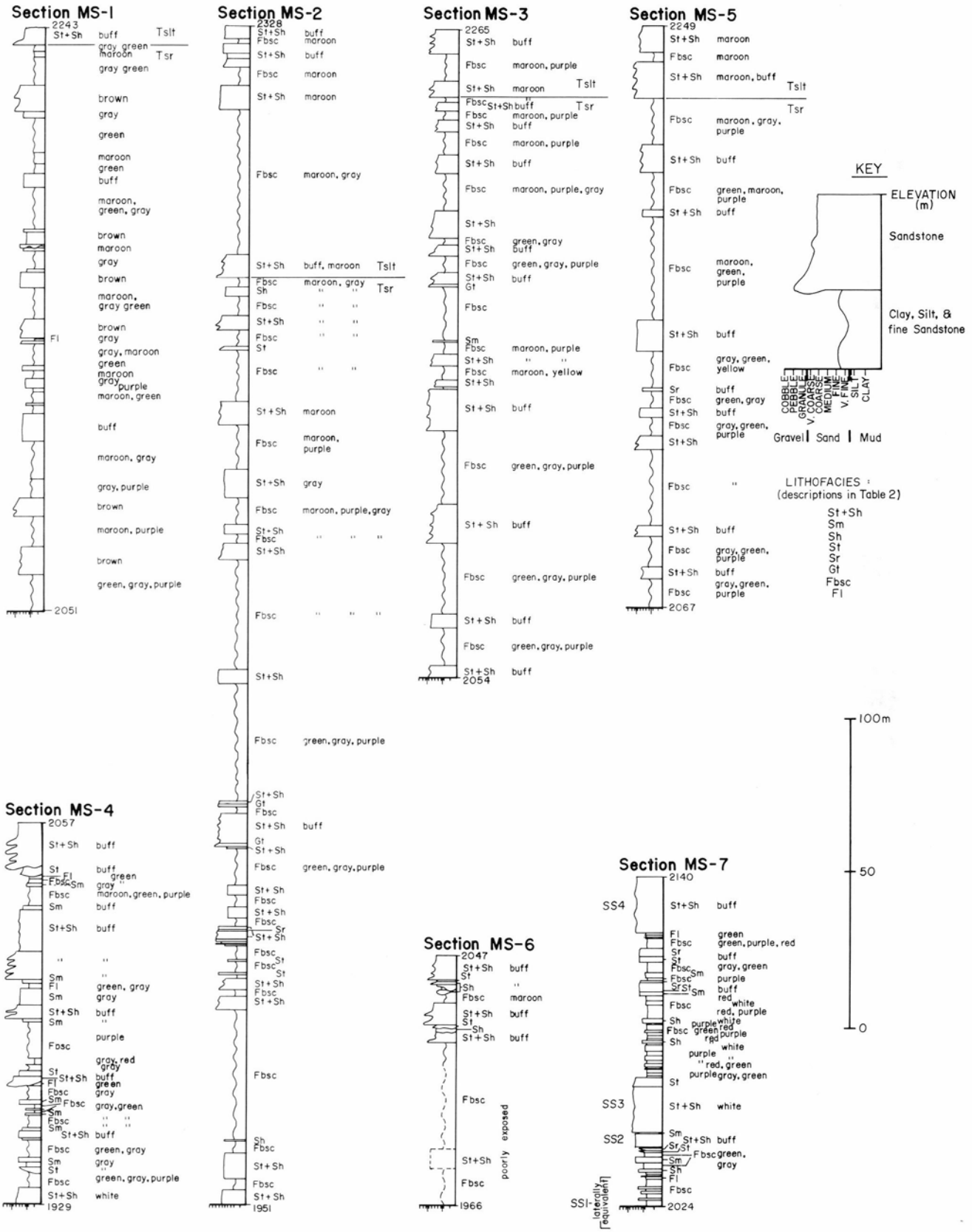

FIGURE 16—Stratigraphic sections of Regina Member and parts of Llaves and Tapicitos Members of San Jose Formation. Lithofacies designations are explained in the text and Table 2. Sections are located in Fig. 9.

grained, white and yellow sandstone. Grayish fine-grained sandstone and varicolored mudrock comprise 62% of the sections (Table 1). Mudrock intervals are dominated by lenticular to sheet-like varicolored bodies of claystone, silt-stone, and mudstone that are commonly sandy. Thinly to thickly bedded, fine- to medium-grained sandstone beds are contained in some mudrock intervals shown in the stratigraphic sections because they are poorly indurated and exposed. Sandstone beds are on the average thinner than mudrock intervals, although the ranges in thicknesses of both lithologies are wide (Table 1).

The average percentages of sandstone and mudrock in the Regina Member, calculated from all well logs employed in this study, are 34% and 66%, respectively. The similarity between values measured in surface and subsurface sections supports the contention that interpretations of subsurface logs accurately represent the stratigraphy of the Regina Member as exposed in outcrop.

The measured sections are included in cross sections 1, 2, and 3 of Pl. 1 (in pocket) for correlation. The Regina Member on the cross sections has few high-porosity sandstones that are correlative between well logs. However, a distictive bed, at approximately 2100 m, occurs on cross sections 1 and 2 and caps much of the Albert Mesa, Santos Peak, and Magdalena Butte (Pl. 1, Fig. 9). In addition, the upper part of the Regina Member in the northern part of cross section 3 contains some areally correlative sandstones in the upper part of the sequence.

The percentages of sandstone and mudrock in well logs suggest southward-coarsening of the Regina Member in the central portion of the San Juan Basin (Table 1). The least amount of sandstone in the Regina occurs north of La Jara Canyon along cross section 3. The Regina along cross section 2 has the greatest proportion of sandstone in the area. This northward fining of the Regina Member corresponds generally with the northeastward pinchout of the Cuba Mesa Member.

Little can be said about thickness trends in the Regina Member across the study area because of the absence of the Llaves Member in the west due to erosion, and the pinchout of the Cuba Mesa Member to the northeast. The upper contact of the Regina Member increases in elevation by 60 m from the south to the north (Pl. 1, Fig. 9). The Ojo Alamo Sandstone is essentially horizontal on this cross section. It is unclear whether the dip of the Regina-Llaves contact is due to a stratigraphic rise of the Llaves or a slight post-Ojo Alamo structural tilting.

Llaves and Tapicitos Members—The Llaves Member in the study area is a cliff-forming unit made up of red, yellow, and gray, very coarse- to medium-grained, locally conglomeratic, thickly bedded, arkosic sandstones. The Tapicitos Member is a slope-forming unit that is characterized by brick-red mudrock and light-red sandstone. The interval including the Llaves and Tapicitos Members is similar in bed thickness and overall character to, but somewhat less sandstone-dominated than, the Regina Member (Table 1). The Llaves and Tapicitos Members cap the high topography on the northern part of cross section 3, the Mestenas and Cabresto Mesas (Fig. 14, Pl. 1). North of these mesas, erosion along Cabresto Canyon and its tributaries has removed these members. The combined Llaves and Tapicitos Members reach a maximum thickness of 135 m in the study area. The interbedded and relatively thin nature of the sandstones and mudrocks (Fig. 16) makes separation of the Llaves and Tapicitos Members arbitrary and pointless in the study area.

Regional correlation of members of the San Jose Formation

Northward extension of stratigraphy of the San Jose Formation from the southern outcrop area is needed to understand the more poorly exposed strata of the formation's northern and northwestern outcrop area (Baltz, 1967: 56). Paucity of paleontological sites, dense vegetation cover, and sparse well logs in the region between the present study area and the northern outcrop limit of Paleogene strata in the San Juan Basin complicate understanding of the stratigraphy in northern New Mexico and southwestern Colorado.

Cuba Mesa Member—The Cuba Mesa Member is continuous from the present study area to the south and southeast (Baltz, 1967: pl. 5; Mytton, 1983). The member is expressed as both single and multiple sandstone sheets and numerous sandstone tongues, especially near its southeastern outcrops (Baltz, 1967: pls. 1, 2). The sheet-like nature of the member is consistent along its western and northwestern outcrops from Mytton's (1983) northern map boundary, along the Animas River valley, to the Mesa Mountains in southern Colorado (Barnes et al., 1954; Baltz,

TABLE 1—Summary of relative amounts and bed thicknesses of sandstone versus mudrock in the study area.

(A) Data from stratigraphic sections:

	Percent of section	Average bed thickness	Range in thicknesses	Number of beds
Regina Member				
Medium–coarse sandstone	38%	5.4 m	0.5–23 m	49
Fine sandstone and mudrock	62%	8.4 m	0.5–42 m	57
Llaves and Tapicitos Members				
Medium–coarse sandstone	34%	6.2 m	1.5–10.5 m	17
Fine sandstone and mudrock	66%	9.6 m	1.75–47.25 m	14

(B) Relative amounts of sandstone and mudrock in the Regina Member in well logs:

Well logs along cross sections	Sandstone	Mudrock
1	41%	59%
2	35%	65%
3 (south of La Jara Canyon)	35%	65%
3 (north of La Jara Canyon)	26%	74%

1967). Some intertonguing with subjacent and superjacent mudrock tends to split the member locally, between Cedar Hill and the Colorado state line (Stone et al., 1983; M. L. Gillam, written comm. 1985). West-to-east tracing of a distinct sandstone interval at the base of the San Jose in Colorado is difficult because of vegetation cover (Barnes et al., 1954). The lack of matching strata between the Mesa Mountains and the H-D Hills (Barnes et al., 1954) suggests a pinchout in this area of an otherwise continuous basal sandstone (Smith, 1988). This region lies near the north-northwest-trending structural axis of the San Juan Basin and may be laterally equivalent to the northwest-trending pinchout of the Cuba Mesa Member described in our report. The presence of a sheet-like sandstone at the base of the San Jose along the formation's eastern outcrop (Wasatch Formation of Dane, 1946, and Wood et al., 1948; Baltz, 1967) suggests that the Cuba Mesa Member is continuous around the eastern and northeastern sides of the basin and splits into lenticular bodies toward the Paleogene axis of the basin. Clearly, incorporation of many more well logs with data in this report is needed to test this hypothesis of the basin-wide stratigraphy of the Cuba Mesa Member.

Regina Member—The Regina Member in the study area is continuous in outcrop and subcrop with strata of the Regina Member to the south and southeast (Baltz, 1967: pls. 1, 5; Mytton, 1983). Erosion along Cabresto Canyon and its tributaries has exposed a somewhat finer-grained section of strata north of the present map area that correlates with the somewhat coarser-grained Regina Member strata to the south. In this area, Baltz (1967: 56) inferred that the Regina Member tongues out to the northeast into sandstones equivalent to the Llaves Member, as he showed it does near Llaves, New Mexico (Baltz, 1967: 50-51). Although his evidence is not stated, his inference may have been based on the apparent dominance of sandstone strata in the sequence exposed along La Jara Canyon (Fig. 17). The strata of La Jara Canyon are, however, clearly more like the Regina Member than the Llaves Member in surface sections and well logs (Fig. 16, Pl. 1). The continuity of the Regina Member along a north–south line through the present study area serves to show that the Regina and "unnamed" members of Baltz (1967: 56) are equivalent. The mudrock-dominated strata "in the northern third of the central basin in New Mexico and Colorado . . ." (Baltz, 1967: 56) should be referred to as Regina Member. Correlation of the Regina Member between the present study area and strata northwest of Navajo Reservoir is not clear at present.

FIGURE 17—Looking northeast in La Jara Canyon. Sequence appears to be dominated by sandstone beds, but in reality is dominated by mudrock (Fig. 16: MS-2, 3) (secs. 13, 14, and 24, T29N, R5W).

Llaves and Tapicitos Members—Sandstones of the Llaves and Tapicitos Members are distinguished from those in the Cuba Mesa and Regina Members only by their redder colors and higher stratigraphic positions. The relatively thin section of the Llaves Member exposed in the present study area is limited to the highest elevations. This sandstone-dominated interval correlates with the "persistent medial sandstone of the Llaves Member" of Baltz (1967: 50-51). Baltz (1967: 56) suggested that these strata correlate across Cabresto Canyon and its tributaries with a sandstone capping Carracas Mesa. The attitude and topographic position of the Llaves and Tapicitos Members on cross section 3 (Fig. 14, P1. 1), and the similar elevation of Carracas Mesa, support this correlation. Dominance of mudrock below the persistent medial sandstone of the Llaves Member in the study area indicates that the main body of the Llaves tongues out to the west and northwest into the Regina Member, much as it does to the south. The increase in percent sandstone in the Regina Member south of La Jara Canyon may reflect intertonguing of sandstones associated with the main body of the Llaves Member with mudrocks of the Regina Member. Preliminary study of the few available well logs east of the study area suggests that the main body of the Llaves Member is tongue-shaped and is replaced laterally by mud-rock north, west, and south of the member's type section. The Tapicitos Member decreases in thickness to the west, away from the continental divide, due to erosion; little can be said of its geometry.

Sedimentology of the San Jose Formation

The members of the San Jose Formation contain differing proportions of the same, or similar, lithofacies. The sedimentology of the San Jose is here treated by distinguishing and analyzing descriptive lithofacies (summarized in Table 2). Data come from measured sections, inspection of many outcrops, and photographic panoramas. After description and interpretation of lithofacies and sedimentary environments, the stratigraphic distribution of lithofacies in the study area is discussed.

The San Jose Formation contains sets of sandstone-dominated lithofacies and mudrock-dominated lithofacies. This distinction generally corresponds to the split between sandstone and mudrock recognized in measured sections and well logs (Figs. 7, 10, 13, Pl. 1, Table 1). Sequences of mud-rock typically contain nonresistant, very fine- to medium-grained sandstone beds that are difficult to distinguish from mudrock in outcrop. Thus, these nonresistant sandstone beds are included in the mudrock-dominated lithofacies.

Sandstone-dominated lithofacies

Sandstone-dominated lithofacies comprise 38% of the 1275 m of stratigraphic section measured in the study area. Lithofades are coded after the method of Miall (1978). Brief descriptions of these lithofacies are as follows (in order of decreasing prevalence in measured sections): (1) lithofacies St + Sh: large-scale trough cross-stratified and horizontally stratified, very thickly bedded, medium- to very coarse-grained sandstone; (2) lithofacies Sm: massive-bedded fine- to coarse-grained sandstone; (3)lithofacies St: large-scale trough cross-stratified, thick- to medium-bedded, medium-to fine-grained sandstone; (4) lithofacies Sr: small-scale trough cross-stratified (rippled) medium- to fine-grained sandstone; (5) lithofacies Sh: horizontally stratified medium- to very fine-grained sandstone; and (6) lithofacies Gt: trough cross-stratified conglomerate.

Description of lithofacies St + Sh—This is the dominant lithofacies in San Jose sandstones, comprising 87% of sandstone in measured sections (Fig. 16). A typical exposure of this lithology is shown in Fig. 18. The lithofacies typically

TABLE 2—Summary of lithofacies.

Lithofacies	Percent of sections	Grain-size	Sedimentary structures	Environment
Sandstone-dominated lithofaces – 38% of sections				
St + Sh	87%	medium–very coarse	large-scale troughs and horizontally stratified	channels; bars and bedforms
Sm	4%	fine–coarse	massive and some burrows	swale-fills and overbank
St	3%	fine–medium	large-scale troughs	crevasse channels
Sh	3%	very fine–medium	horizontal laminations	splay sheetfloods, channel-fills
Sr	2%	fine–medium	small-scale troughs and some ripples	crevasse splays, shallow swale-fills
Gt	1%	coarse–granules	large-scale troughs	channel thalwegs and channel lags
Mudrock-dominated lithofacies – 62% of sections				
Fbsc + Fl	97%	fine sand–clay	burrows, root traces, rare laminations, and small-scale troughs	paleosols, overbank deposits, levees, bioturbated back-swamps
Fl	3%	silt–clay	small-scale troughs, ripples, laminations	lacustrine; flood-basins, cutoffs

overlies a scoured surface cut into finer-grained lithologies. Lithofacies St + Sh is made up of poorly to moderately sorted medium- to very coarse-grained stratified sandstone and local lenses of conglomeratic sandstone. Gravels include granules of quartzite and granule- to cobble-sized, rounded mudrock ripups. These clasts are dispersed along, or at the bases of, stratification in sandstones and as thin lags at the bases of sandstones.

A diagrammatic stratigraphic section of lithofacies St + Sh is shown in Fig. 19. Thicknesses of individual fill-units, or stories, range from 1 m to nearly 6 m. Stories decrease in grain size upwards, typically from very coarse- or coarse-to medium-grained sand. Sandstone beds are typically multistoried, reaching thicknesses of 100 m, in sheet sandstones with width-to-thickness ratios of >15-300. Ribbon sandstones of lithofacies St + Sh, with width-to-thickness ratios of 5-15 (terminology after Friend et al., 1979), have single-story and multistoried fill.

Basal erosion surfaces include channel scours with smaller linear scours, longitudinal grooves, and flute marks (Fig. 19). Channel scours and planar erosion surfaces are covered by horizontal or low-angle (<10°) trough cross-stratified sandstones with mudrock-ripup and extrabasinal-clast conglomerates common at the base (Fig. 19). Structures present along the bases of some sandstones where they abruptly overlie claystone include: linear scours (Gibling and Rust, 1984), up to 1.5 m wide and 1 m deep U-shaped erosional features; longitudinal grooves (Allen, 1971), cylindrical casts 2-15 cm in diameter and as much as 1 m in exposed length; and flute marks. The flute casts are smooth-walled and reach lengths of 10 cm and depths of 1 cm. Small-scale erosional scours are filled by apparently unstratified, very coarse- to medium-grained sandstone rather than intraformational conglomerate, unlike those described by Plint (1986).

Beds of very coarse- to coarse-grained, horizontally stratified sandstone that are >2 m thick are commonly associated with mudrock ripups in the lower one-third of the beds (Fig. 19). Sets of horizontal stratification truncate low-angle trough cross-strata, are interstratified with thin beds of low-angle cross-strata, contain parting lineations along bedding surfaces, and locally steepen upward into large-scale, low-angle trough cross-strata. Horizontal stratification also occurs in some sections as thin sets stratigraphically high in very thick beds or in thinner beds, where they separate sets of trough cross-strata (Fig. 19).

Trough cross-strata in lithofacies St + Sh range from 10

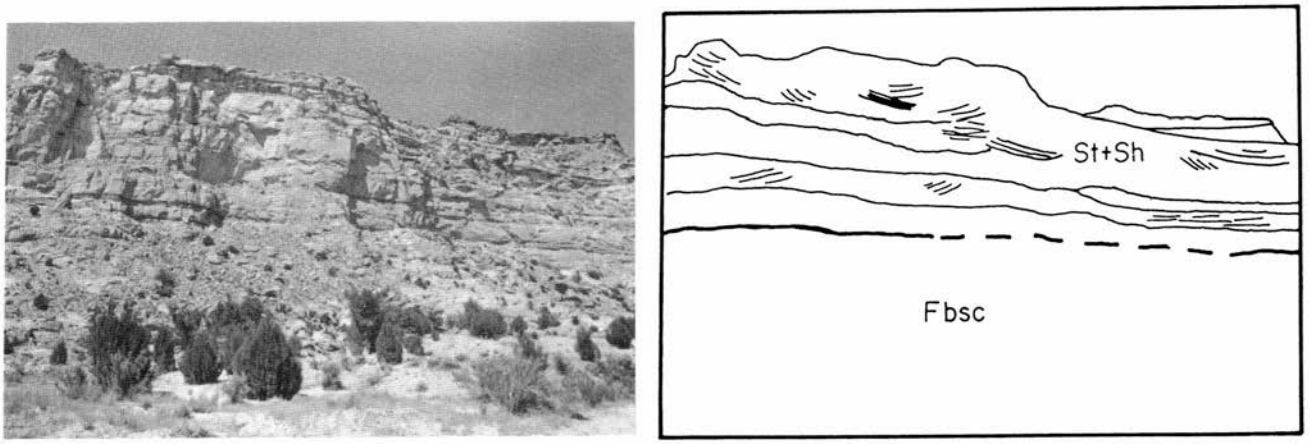

FIGURE 18—Lithofacies St + Sh overlying lithofacies Fbsc (looking northwest in NE¼ sec. 16, T27N, R6W). Trees in the foreground are approximately 3 m tall.

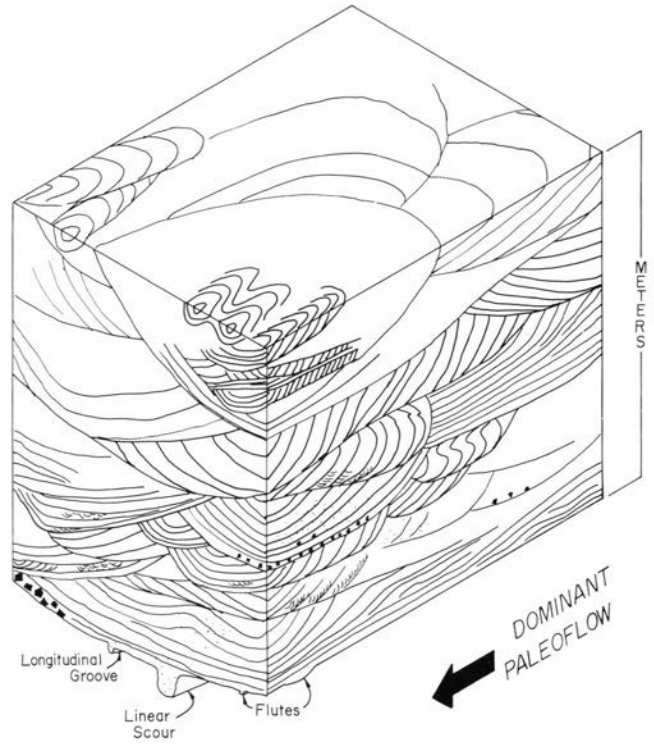

FIGURE 19—Block diagram of lithofacies St + Sh showing the nature of internal stratification in the lithofacies.

to 300 cm high and from 20 to >500 cm wide. The majority of sets are >20 cm in height. Many of the largest-scale sets are associated with horizontally stratified sandstone in channel sequences and have shallowly dipping (<10°) cross-strata. Basal bounding surfaces of trough cross-strata are typically trough- or scoop-shaped (Allen, 1982a: 348); upper bounding surfaces are erosional and locally depositional where small-scale cross-strata and horizontally stratified sandstone form topset beds. Outcrops of trough cross-strata resemble the grouped, subcritically climbing troughs of Allen (1982a: 360), except that the crosscutting troughs in the San Jose are typically oriented in a variety of directions.

Cross-strata in trough cross-stratified sets typically are concave-up and merge tangentially downward with the bed. Angular basal terminations are rare, occur in <10 cm thick beds, have 25-30° dip angles, and are associated with horizontally laminated sandstone relatively high in very thick sandstone beds (Fig. 19). Cross-strata commonly fill scours asymmetrically, have homogeneous texture, and are continuous between trough-bounding surfaces.

Cross-stratification that is meters in height is commonly difficult to classify because most outcrops of lithofacies St + Sh are not sufficiently large to allow differentiation of low-angle wedge-planar sets (simple cross-stratification of McKee and Weir, 1953; Xi cross-stratification of Allen, 1963) or of tabular sets (Allen, 1982a; Mu cross-stratification of Allen, 1963) from trough sets (McKee and Weir, 1953; Allen, 1982a; Pi cross-stratification of Allen, 1963) with low-angle limbs. The development of cross-stratification that is transitional between tabular and trough morphologies complicates classification and interpretation (Conolly, 1964, 1965) and may be important in the larger cross-strata of San Jose sandstones. Because most of the cross-strata and associated bounding surfaces observed in the study area show some curvature in plan view, they are considered to be trough cross-stratification in a general sense.

Measurements of dip directions and dip magnitudes of cross-strata were made in a few sandstones in the Santos Peak-Magdalena Butte area (Figs. 9, 16: MS-7) in order to quantify the orientations and dips of cross-strata in lithofacies St + Sh. Attitudes of cross-strata were measured on every three-dimensional exposure of large-scale cross-strata in one single-story sheet sandstone (SS1 in Figs. 16, 20A). These cross-strata do not represent paleocurrent measurements because no attempt was made to interpret trough axes; however, vector means of random cross-strata attitudes can indicate average paleoflow directions (DeCelles et al., 1983). The randomly collected attitudes of cross-strata and 13 paleocurrent measurements (orientations of trough axes and maximum-dip directions of cross-strata) from the same outcrop are shown in Fig. 20A (complete data and statistical treatments are included in the section on sediment dispersal below).

Of the 40 dip magnitudes, seven (17%) are oversteepened (here defined as having dip angles greater than 34°) and 10 (25%) are shallow (dip angles less than 11°) (Fig. 20A). Although there is a large dispersion of the data, the vector mean of the randomly collected cross-strata data that dip >10° is similar to that described by paleocurrent indicators; however, this vector mean bisects the bimodal paleocurrent data (Fig. 20A).

The orientations of various paleocurrent indicators show differences between paleoflow at the bases of beds and within sandstones of lithofacies St + Sh. Vector means of basal scour features, trough axes, and cross-strata dips in SS4 are similar in direction but not in magnitude (Fig. 20B). Cross-strata data show greater dispersion than, and are roughly bisected by, the scour data (Fig. 20B). The paleocurrent data from the SS2 and SS3 (Fig. 16: MS-7) sandstone bodies display complex orientations (Fig. 20C); basal scour data and cross-strata data display differing vector-mean directions and magnitudes. The basal scour and cross-strata dip-magnitude measurements and two trough-axis readings were made at one outcrop of SS2; the remaining data are a compilation of all measurements made over a 1 km^2 area and thus may record paleoflow from many channels that crosscut one another to form the sandstone bodies.

Some of the sets of cross-stratification have obviously undergone soft-sediment deformation (note the oversteepened dips in Fig. 20A). Soft-sediment deformation of litho-fades St + Sh is of two types: (1) oversteepened-to-recumbently folded large-scale cross-strata with dip angles that change from 20° to overturned along strike and upsection; and (2) anticlinal-to-domal structures with heights of 10 to >200 cm. Oversteepened-to-overturned cross-strata are overlain by undeformed large-scale trough sets that indicate paleoflow in the direction of overturning. Overturning apparently was entirely plastic. Anticlinal and domal structures are commonly faulted near their axes, have regions of massive sandstone near their cores, pass downward into undeformed cross-strata, are abruptly overlain by erosional scours, and are associated with diagenetic iron-rich concretions.

A few outcrops of 2 to 3 m high epsilon cross-strata occur in sheet sandstones of lithofacies St + Sh (Fig. 21). These cross-strata contain fining-upward packages of coarse- to fine-grained sandstone that dip 5 to 15° toward paleochannels. Epsilon cross-strata contain internally trough cross-stratified strata on the order of decimeters in thickness. They are restricted areally to the width of a few crossbeds and are commonly overlain or cut by very thick (>2 m) trough cross-stratified beds. Sets of epsilon cross-strata also occur within large scours that are filled dominantly by mudrock and disconnected beds of lithofacies St + Sh.

Interpretation of lithofacies St + Sh—The close association of low-angle trough cross-strata and thick accumulations of horizontal stratification with parting lineations suggests rapid deposition by decelerating, unsteady cur-

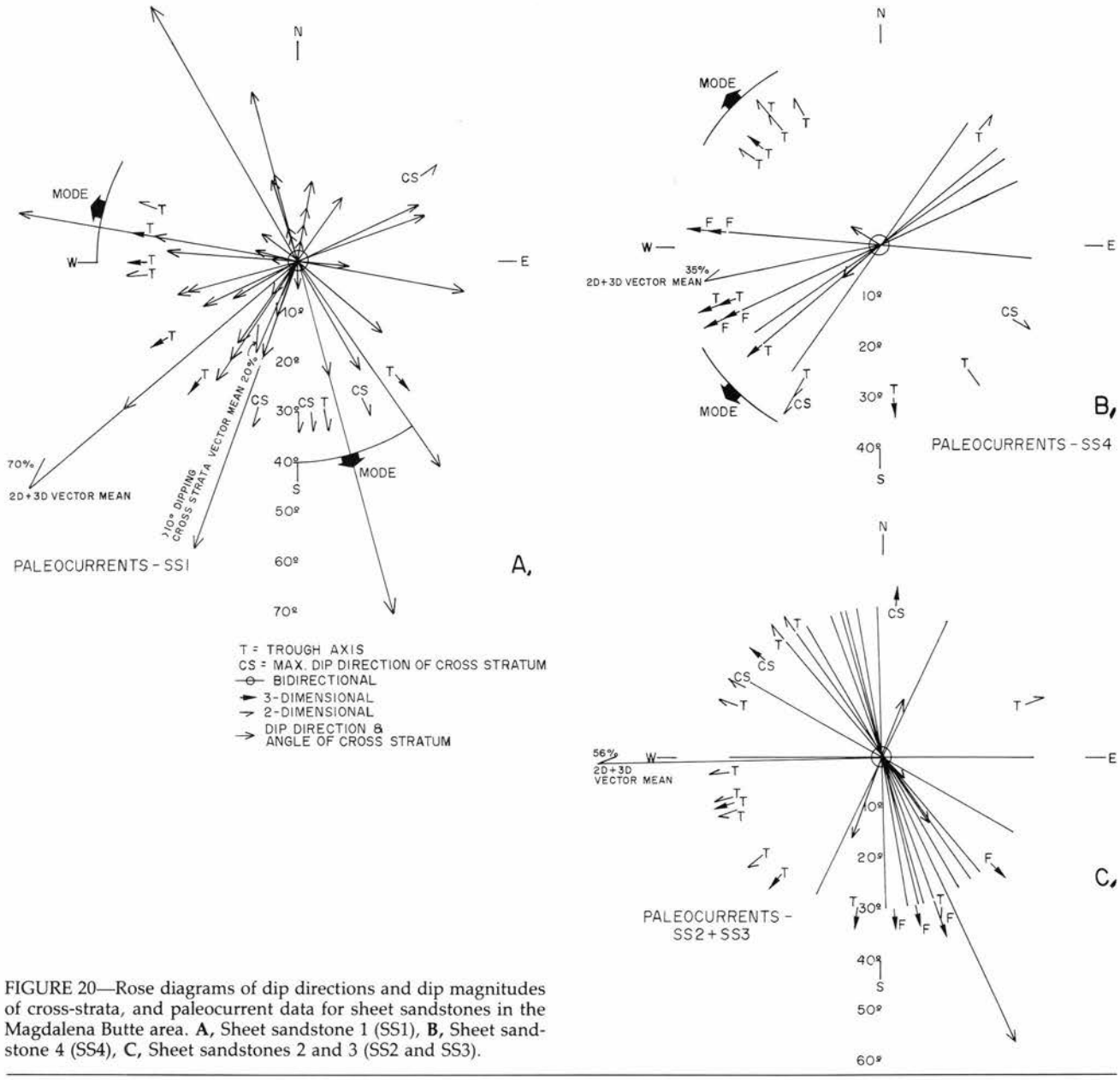

FIGURE 20—Rose diagrams of dip directions and dip magnitudes of cross-strata, and paleocurrent data for sheet sandstones in the Magdalena Butte area. **A,** Sheet sandstone 1 (SS1), **B,** Sheet sandstone 4 (SS4), **C,** Sheet sandstones 2 and 3 (SS2 and SS3).

FIGURE 21—Panorama showing epsilon cross-strata and bedding characteristics of sheet sandstones 2 and 3 (SS2 and SS3) in the Magdalena Butte area. Scale bar is 5 m long.

rents (Harms et al., 1982). The steepening-upward of horizontal stratification into trough cross-strata suggests local aggradation during bedform growth. Thin beds of cross-strata and gravel layers within horizontal sets indicate migration of sandy bedforms and gravel plane beds over sandy plane beds during fluctuations in flow.

Trough cross-stratification is generally associated with deposition in trough-shaped scours downstream of dunes of various shapes (Allen, 1982a: 360-366). The fine structure of cross-strata in lithofacies St + Sh suggests that many of the cross-strata were not formed by simple avalanching along lee slopes of bedforms. Cross strata of lithofacies St + Sh with tangential terminations, wide-ranging dip magnitudes, and laterally continuous laminae are similar to those termed accretionary cross-stratification by Imbrie and Buchanan (1965) and those produced experimentally during the transition of dunes to upper flat beds (Hand and Bartberger, 1988). The process of formation of these cross-strata may involve traction transport over both stoss and lee surfaces of bedforms (Imbrie and Buchanan 1965; Hand and Bartberger, 1988) and/or continuous avalanching (grain flow) accompanied by intense grain fall (Hunter and Kocurek, 1986). These processes are thought to involve higher bedform-migration velocities and higher depositional rates than normal grain-flow processes. Field evidence and sediment-transport theory suggest that so-called accretionary cross-strata are deposited under flowing water that is deep relative to the bedform height (Imbrie and Buchanan, 1965) and does not undergo flow separation from the bed at convex-up bedform crests (Hand and Bartberger, 1988). These processes are thought to involve higher bedform-migration velocities and higher depositional rates than normal grain-flow processes. Direct evidence in the San Jose Formation for transportation by traction processes along lee slopes of bedforms occurs locally where large-scale cross-strata are observed to be cosets of small-scale cross-stratification, and where clast imbrications occur along large-scale cross-strata. These small-scale paleocurrent indicators typically show that flow was locally at some acute angle to the dip directions of the large-scale cross-strata.

Paleocurrent data suggest that trough cross-strata formed from the progradation of bedforms that were oriented obliquely to the dominant, down-paleoslope flow, as determined by means of all data (Fig. 20A, B). The rarity of planar-tabular cross-strata suggests that most bedforms were associated with troughed scours and that straight-crested bedforms were uncommon or had poor preservation potential in comparison to sinuous-crested bedforms. Higher velocity (Harms et al., 1982) and more unsteady (G. A. Smith, pers. comm. 1987) currents may favor formation of three-dimensional dunes over two-dimensional dunes. The dominance of trough cross-strata suggests that much of lithofacies St + Sh was deposited by strong, unsteady flow along channel bottoms. The 10 cm high sets of cross strata that have 25 to 30° dips and angular basal terminations were likely deposited by subaqueous grain-flow processes (Hunter and Kocurek, 1986). The fine structure, stratigraphic position, and horizontal laminations associated with these cross-strata suggest deposition on sand flats (Cant and Walker, 1978) in water that was shallow compared to bedform height.

The scale and complexity of trough cross-strata and their relation to horizontally stratified sand in lithofacies St + Sh suggest deposition on sinuous-crested bars. Migration processes, dimensions, and geometries of these bedforms have not yet been assessed.

Epsilon cross-strata have been shown to form on convex sides of side-attached (point) bars (Allen, 1982b: 94-100) and mid-channel bedforms (Miall, 1977; Allen, 1983; Reading, 1986) during lateral accretion. The narrow width of epsilon cross-strata in thick-bedded San Jose sandstones suggests short-term lateral bedform migration, compared to high-sinuosity streams (Reading, 1986).

Oversteepening and overturning of cross-strata in the general direction of transport (Fig. 20A) and the lack of slippage planes that cut cross-strata suggest that fluid shear caused deformation of liquidized cross-strata (Allen 1982b: 389-392). Liquidization of cross-stratified sands can occur by increased pore-fluid pressure or seismic shaking (Allen and Banks, 1972). Because of the lack of association of liquidized sand and impermeable barriers in San Jose sandstones, it is likely that seismic activity liquidized the channel beds, which were subsequently deformed in downstream directions by normal stream flow.

Domal and anticlinal sedimentary structures display evidence of liquidization (massive sandstone in cores) and rupturing (faulting) due to fluid escape (Leeder, 1987). Liquidization and explusion of water from the sandstones may have been due to either seismic shaking and/or local overpressuring due to rapid burial. Small water-expulsion features (<20 cm amplitude) form during waning floods. However, larger features, such as those in the San Jose, are thought to be associated with seismic shaking (Leeder, 1987).

A model for lithofacies St + Sh (Fig. 22) is in some ways similar to the facies model proposed by Cant and Walker (1978) for the modern, sandy, braided South Saskatchewan River. Similarities include a dominance of trough cross-stratified sandstone, local deposits of tabular cross- and horizontal-stratified sandstone, a 90° + dispersion of current directions, and an association with muddy overbank deposits. Paleocurrent and cross-strata data suggest that the majority of lithofacies St + Sh was deposited along cross-channel bars and in channels in settings similar to those in the South Saskatchewan River. Differences are that the San Jose sandstones do not have as much tabular cross-strata as the South Saskatchewan model. The average flow depth, or flow velocity at a given depth, was possibly greater in the San Jose channels than in the South Saskatchewan, which can account for the dominance of sinuous-crested bedforms (both bars and dunes) in the San Jose. The rare occurrences of grain-flow and small-scale cross-strata suggest that the bars were only rarely emergent (in comparison to Cant and Walker, 1978). Thus, flow was likely less seasonal during deposition of the San Jose than in the modern South Saskatchewan River.

Description of lithofacies Sm—Lithofacies Sm occurs as 0.5 to 2 m thick beds below and above beds of lithofacies St + Sh and as solitary sandstones within mudrock sequences. This lithofacies comprises 4% of sandstone in the measured sections (Fig. 16) and is made up of poorly to moderately sorted fine- to coarse-grained massive sandstone. Most of the beds are poorly cemented at outcrop. Width-to-thickness ratios of beds range from 5 to >200; the more lenticular beds are characteristically associated with lithofacies St + Sh. Some of the better cemented beds display faint burrows.

Interpretation of lithofacies Sm—The massive nature of lithofacies Sm may be the result of any of a number of factors. These factors include either the lack of sufficient cementation or grain segregation to highlight stratification and destruction of stratification by bioturbation. Beds of lithofacies Sm in positions above lithofacies St + Sh suggest that stratification was disrupted along tops of channel sandstones by either bioturbation or compaction prior to cementation, after channel abandonment.

Description of lithofacies St—Lithofacies St is composed of medium- to fine-grained lithofacies that are entirely large-scale trough cross-stratified. The lithofacies comprises 3% of sandstone in the measured sections. Of the six beds of lithofacies St in the measured sections (Fig. 16), four are in finer-grained sequences and two are associated with coarser-

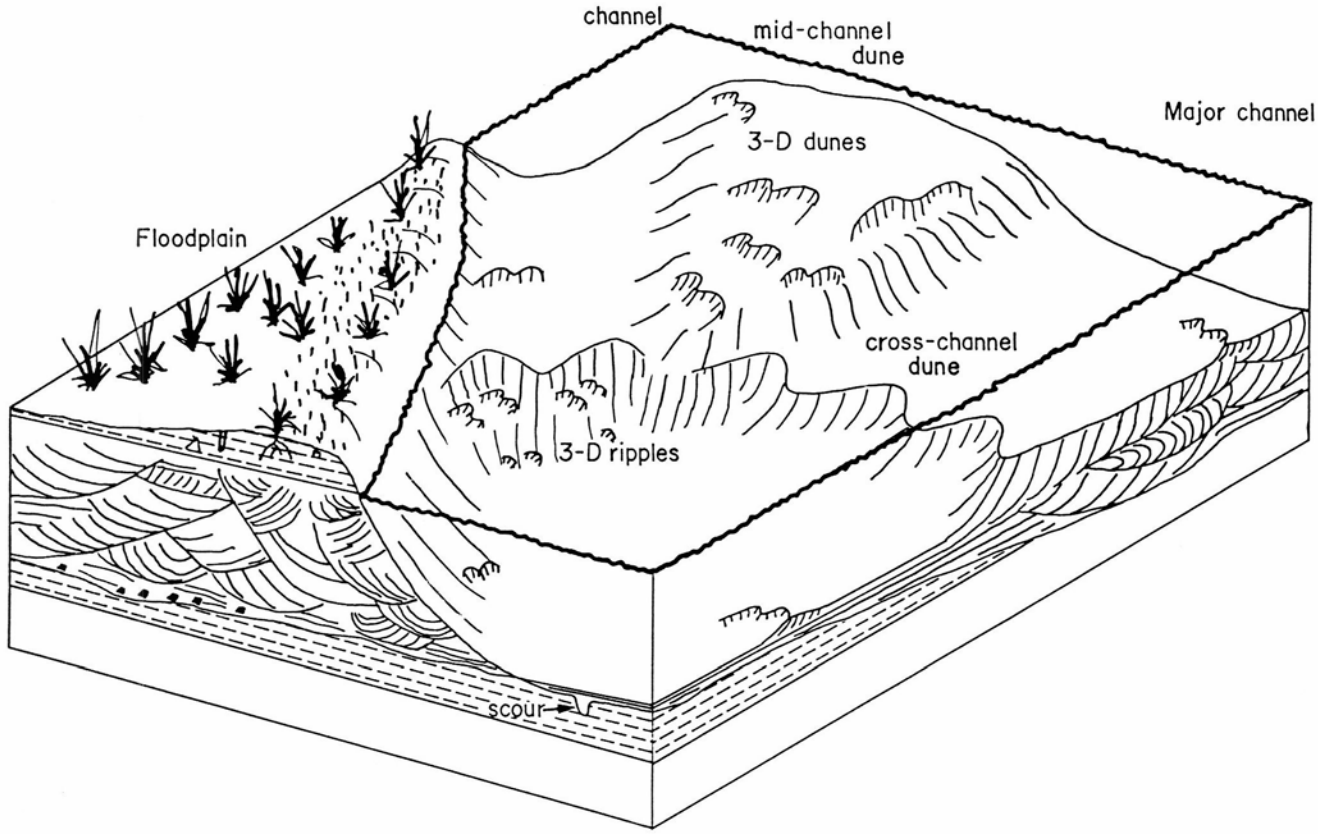

FIGURE 22—Cutaway representation of the facies model for lithofacies St + Sh. Only half of the channel is shown. Flow is from upper left to lower right.

grained channel sandstones of lithofacies St + Sh. Most of the lithofacies St beds are lenticular and have channelized basal contacts. The beds of lithofacies St in finer-grained sequences were deposited on siltstone or mudstone and were overlain by fining-upward sequences of fine sandstone to mudrock. One bed of lithofacies St represents a portion of a sequence that fines-upward from conglomerate (lithofacies St + Sh) through siltstone. Another bed is bounded by a channelized surface on shale at the base and an overlying channelized conglomerate, forming a coarsening-upward sequence.

Interpretation of lithofacies St—The cross-stratification of lithofacies St indicates deposition by three-dimensional dunes (Harms et al., 1982). Where the facies is underlain by mudrock and overlain by lithofacies Sr and/or mudrock, the sandstone sequence appears to have been deposited by a single flow event of waning strength. The scoured bases indicate high current velocities and channelized flow, possibly from a distributary channel of a crevasse in a levee. These sequences are interpreted to represent deposition on floodplains from distributary channels (relatively distal from main channels) and/or from small crevasse-splay channels (relatively proximal to main channels). The bed of lithofacies St in the upward-coarsening sequence suggests that crevassing which caused its deposition led to avulsion of the main channel onto the floodplain. The beds of lithofacies St in a fining-upward channel sequence indicate waning flow during aggradation. The fact that this is the only example in the measured sections of a protracted waning current suggests that it was a rare process in San Jose channels.

Description of lithofacies Sh—Lithofacies Sh is composed of very fine- to medium-grained, horizontally stratified sandstone, and comprises 3% of the sandstones measured in the study area. Six of the eight measured beds of lithofacies Sh are sheet-like, are overlain and underlain by mudrock, and range from 0.5 to 2.5 m thick; thinner beds occur in mudrock sequences but are typically poorly cemented and poorly exposed. Two beds of lithofacies Sh are 1.5 m thick and lenticular due to scouring along their bases, one of which contains mudrock ripups and is overlain by trough cross-stratified sandstone.

Interpretation of lithofacies Sh—Most of the beds of lithofacies Sh were probably deposited as lower plane beds of lower flow regime sheetflooding in overbank areas, as evidenced by their association with mudrocks. The wide range in grain size of different beds may reflect varying distances of transport from crevasses in channel levees. The thick accumulation of horizontally stratified sandstone suggests deposition by steadily flowing, sluggish, and probably shallow floodwaters.

The two lenticular beds of lithofacies Sh were likely deposited as upper plane beds of a lower flow regime. Incorporation of mudrock ripups into the horizontal stratification, associated basal scour surfaces, and their association with channel sequences suggest vigorously flowing water. These beds are similar to many of the basal beds of lithofacies St + Sh.

Description of lithofacies Sr—Lithofacies Sr is composed of medium- to fine-grained sandstones that display small-scale cross-stratification. The lithofacies comprises 2% of sandstones in the measured sections (Fig. 16). Medium-grained beds and most fine-grained beds are typified by small-scale through cross-stratification. Some fine-grained beds contain minor amounts of small-scale planar cross-stratification and rare climbing ripples.

Of the five beds of lithofacies Sr included in measured sections in Fig. 16, one is underlain and overlain by mudrocks, and the remaining four are underlain by beds of large-scale cross-strata. It is likely that more beds of lithofacies Sr occur in mudrock sequences but were not recorded in

the measured sections because of poor exposure of thin sandstones. Most of the recorded beds of lithofacies Sr occur as sheets near the tops of channel sequences of lithofacies St.

Interpretation of lithofacies Sr—The small-scale trough cross-stratification of lithofacies Sr was formed by the migration of three-dimensional ripples. The association of lithofacies Sr with mudrock and crevasse-channel and crevasse-splay deposits suggests that most of this lithofacies was deposited in overbank environments or in recently abandoned channels. The lithofacies and its stratigraphic position indicate deposition by shallow, waning sheet-flow.

Description of lithofacies Gt—Lithofacies Gt is composed of trough cross-stratified granule conglomerate. The unit comprises 1% of the total thickness of sandstones measured (Fig. 16). Clasts in the conglomerates are composed dominantly of quartzite with some other metamorphic rocks and chert. Lithofacies Gt is similar to lithofacies St except that granules are dominant over sand grains along cross-strata and that conglomerates occur as thin, crudely bedded, and poorly imbricated beds in troughs and at the bases of beds. Many clasts along cross-strata are surrounded by sand grains rather than gravel. Lithofacies Gt occurs interbedded with lithofacies St + Sh and at the bases of channel sequences.

Interpretation of lithofacies Gt—Trough cross-stratified conglomerates were likely deposited on three-dimensional dunes in channel thalwegs. The matrix-supported nature of the gravels along cross-strata suggests that clasts moved in a dispersed fashion along the bed and then were buried by sand. Crudely bedded and imbricated beds of conglomerate were likely formed by local scouring along thalwegs, winnowing of sand, and formation of lags.

The low percentage of extrabasinal gravel in the study area may be due to an insufficient supply of resistant clasts. Common mudrock-ripup clasts attest to sufficient flow velocities for gravel transport. Intraformational conglomerates are rarely thick enough and do not typically display characteristic sedimentary structures for classification and interpretation of lithofacies.

Mudrock-dominated lithofacies

Mudrocks are the prevalent rock type in the study area, comprising 62% of the 1275 m of stratigraphic section measured. The lithofacies are difficult to study in detail because of thick weathered mantles at outcrops and the paucity of sedimentary structures. Mudrock lithologies have been studied in one area near Magdalena Butte and Santos Peak (Fig. 9). The overall character and exposures of these strata are shown in Fig. 23.

Mudrock lithofacies are defined by primary sedimentary structures and grain-size trends in lithologic sequences. Study of polished slabs and thin sections indicates that horizontal laminae and crosslaminae are locally preserved in apparently massive, bioturbated strata; however, systematic micromorphologic analysis of mudrocks is beyond the scope of this study. Colors of the mudrocks are to some extent controlled stratigraphically rather than facies-controlled. Mudrocks of the Regina Member are dominantly green, gray, purple, and yellow, whereas Tapicitos Member mud-rocks are characteristically more red. Lithologies typically have gradational boundaries due to biogenic mixing of sediment; thus, most primary sedimentary facies are indistinct.

Detailed study of a 9.5 m long stratigraphic section (Fig. 24) and a more generalized description of 51.5 m of section (Fig. 16: MS-7) form the basis for data on the sedimentology of mudrocks in the area. Methods, terminologies, and the Munsell color scheme common to pedology (summarized in Birkeland, 1984) were used in the study of mudrocks because of the general similarity between compact mud-stones and some soil horizons. The location of the measured sections is shown in Fig. 23. Reconnaissance and detailed study elsewhere in the San Jose Formation suggest that lithofacies in these sections are representative of mudrocks in the Regina Member of the San Jose Formation in general (Smith, 1988).

Two mudrock-dominated lithofacies are distinguished on the basis of sedimentary structures observable at outcrop. These facies include (in order of decreasing prevalence in measured sections) (1) lithofacies Fbsc + Fl, bioturbated massive mudstone and minor sandstone with discontinuous and finely laminated and crosslaminated mudstone and sandstone; and (2) lithofacies Fl, finely laminated and crosslaminated shale and sandstone.

Description of lithofacies Fbsc + Fl—LITHOLOGY: The majority of beds of lithofacies Fbsc + Fl do not display primary stratification. Instead, the mudrocks display red and brown mottles, apparently massive blocky structure, and gradational-to-interpenetrating contacts between strata. This lithofacies comprises 97% of the 63 m of section measured. Dominant colors are green, gray, and yellow for the matrix of mudrocks. Mottle colors range from light olive brown (2.5Y 5/6) to dark yellowish brown (10YR 4/4) to strong brown (7.5YR 4/6) to reddish brown (5YR 3/2) to dusky red (10R 3/3) (Fig. 24).

Fig. 25A–C displays the cyclical lithologic nature of the mudrock sequences. Fig. 25B shows a typical lithologic se-

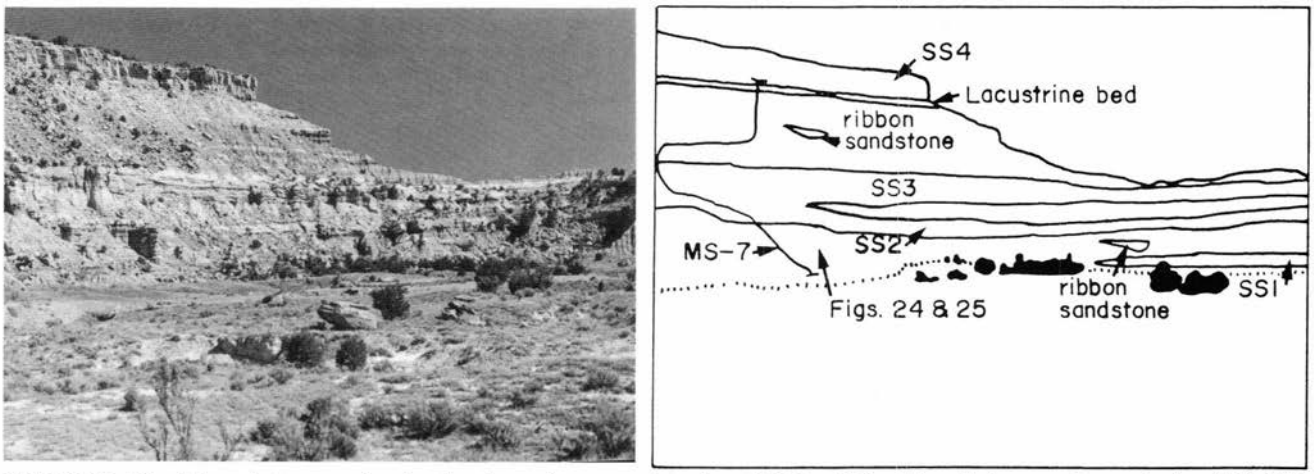

FIGURE 23—Magdalena Butte area showing locations of measured sections (MS-7 and Fig. 24) and sheet sandstone bodies (SS1–SS4) (looking northeast, NE¼ sec. 8, T27N, R5W).

quence, which fines-upward from light grayish-green and greenish-gray siltstone to a darker greenish-gray mudstone that contains an upward-increasing amount of reddish-brown mottles. The sequence is overlain by another greenish-gray siltstone. Siltstones and mudstones are locally laminated or crosslaminated. Primary sedimentary structures are cut or obliterated by cylindrical mottles (burrows).

Contacts between sandy, silty, and clayey sediments are typically gradational and interpenetrating over centimeterstodecimeters. Gradational and interpenetrating contacts and most mottles owe their morphologies to burrows and possibly to poorly preserved root casts.

STRUCTURE: Mudstone in the study area typically breaks into aggregates that are different from those produced in

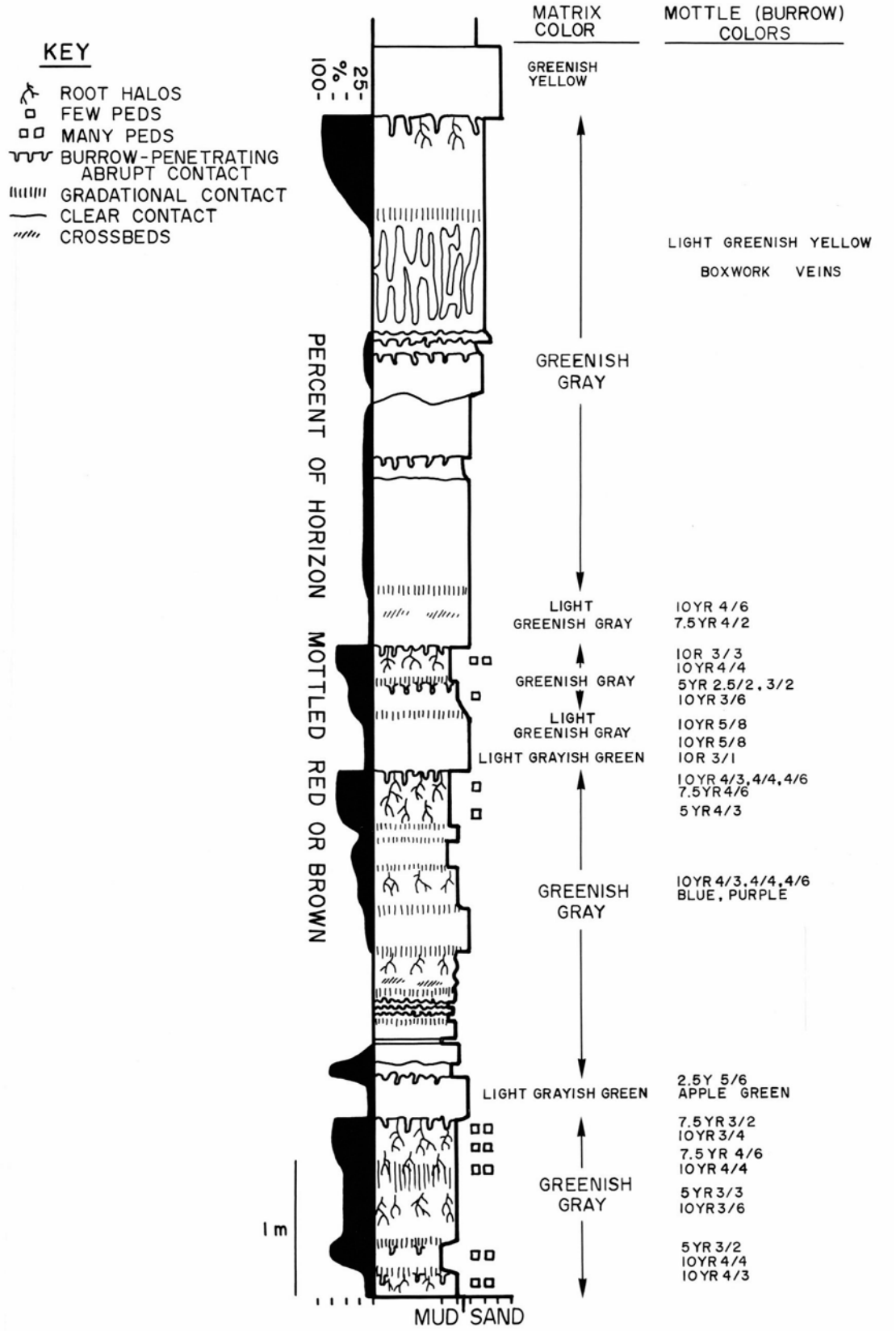

FIGURE 24—Detailed stratigraphic section of lithofacies Fbsc + Fl along Magdalena Butte (location in Fig. 23).

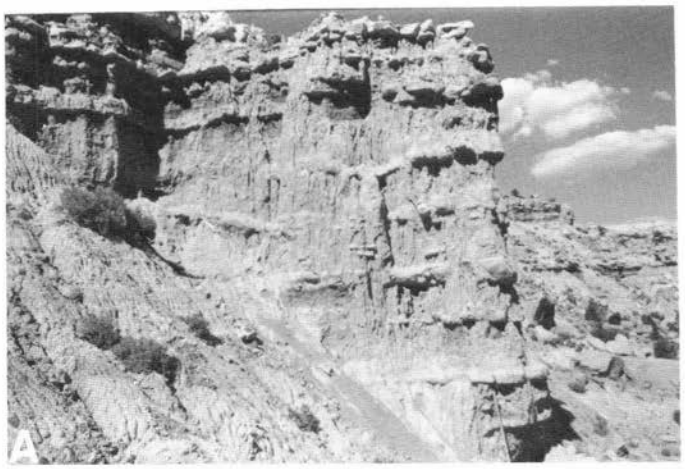

FIGURE 25—Lithofacies Fbsc + Fl (location in Fig. 23). Note multiple fining-upward sequences **(A)** that begin with a ledge-forming, fine-grained sandstone or siltstone **(B).** Interpenetrating contacts due to burrowing (Fig. 24) can be seen in **(C).**

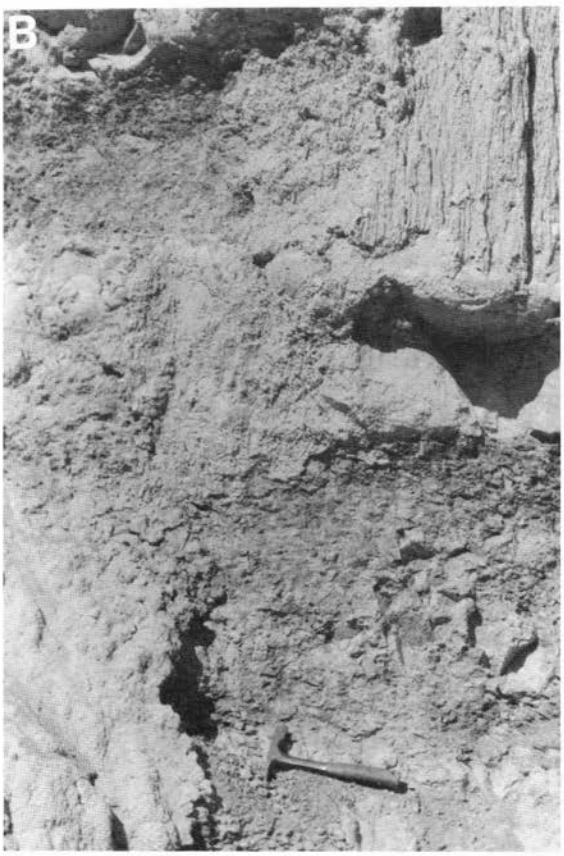

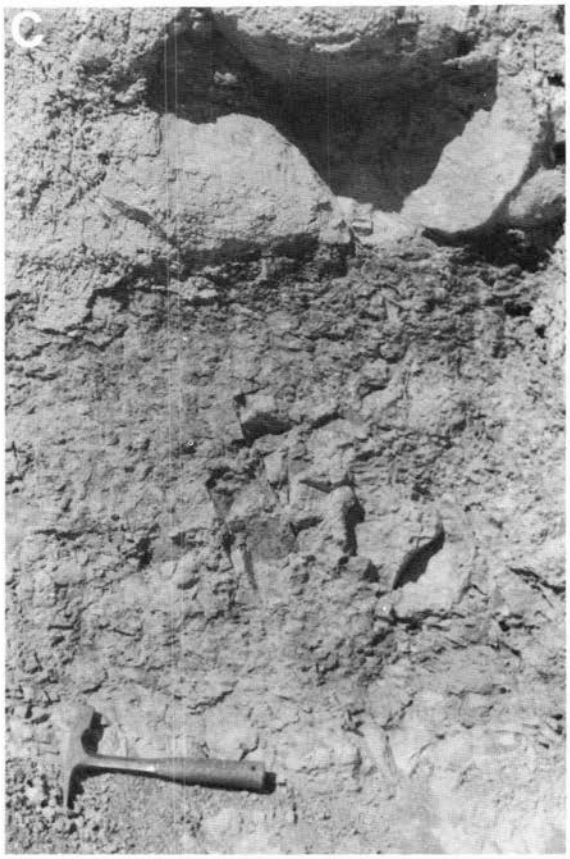

laminated sediment; this is the structure of the units, analogous in form to structure in modern soils. Most structure in the mudrock occurs in darker, finer-grained horizons. Fig. 25C displays typical medium, strong, subangular, blocky structure. The origin of this prevalent structure is likely related to post-burial compaction, the closing of pores, de-watering, and possibly cracking in Eocene soil environments. Some horizons (shown to have peds in Fig. 24) display few to many, strong, fine-granular, subangular-to-subrounded peds that are characterized by coatings of oriented clay and waxy appearances. These peds are cut by burrows and are thus a product of early diagenesis (probably clay illuviation during pedogenesis). Horizons containing these peds are also associated with many burrows and common root halos.

BURROWS: More than 95% of the section in Fig. 24 has been bioturbated. Burrows are recognized as nontapering, nonbranching cylindrical structures with smooth-to-irregular walls. Commonly occurring diameters are 2, 4-5, 7-9, and 12-17 mm, although all intermediate diameters have been observed. Burrows are commonly subvertical, and turn to horizontal, in lengths up to 15 cm. The fill is commonly coarser than neighboring matrix. Meniscate heterolithic fill is commonly observed in polished slabs of these burrows. Most of the burrows are redder than the matrix, indicating the presence of more oxidized iron in burrow fill than in the matrix. Interpenetrating abrupt contacts (Figs. 24, 25C) commonly occur where overlying lighter-colored siltstone or sandstone was brought down along burrows into underlying darker horizons.

ROOT TRACES: Such traces are evidenced by downward-branching and tapering light-colored, cylindrical halos, sometimes with thread-sized silty cores. Halos are typically 0.1 to 4 mm wide and up to 10 cm long (though more

typically 2 cm long) in exposure. Pieces of carbonized organic matter along some halo cores have been recognized in mudrocks studied in the field and under a microscope.

CHEMISTRY: Analysis of sequences of Regina Member and Tapicitos Member mudrocks within and outside of the present study area is summarized here (Fig. 24; Smith, 1988). Pedogenic carbonate has not been recognized to form distinct horizons in the Regina Member. Concretions of siderite(?) are prevalent in some horizons. Such concretions are a common post-burial diagenetic feature of many terrestrial mudrock sequences (Curtis and Colman, 1986).

Organic-carbon values range from 0 to 0.4 wt% and show a positive correlation with increasing ped development and decreasing color value. Dithonite-extractable iron (iron oxyhydroxide) values range from 0.4 to 4.7 wt% (as Fe_2O_3) and show a positive correlation with reddening and ped development. Dithonite-extractable manganese values range from 0.02 to 0.7 wt% (as MnO) and show a positive correlation with purple, blue, and red colors and ped development. Whole-rock chemistries of horizons suggest near-surface depletion of oxides of silicon, potassium, and sodium with respect to aluminum oxides in two of three paleosols analyzed.

Interpretation of lithofacies Fbsc + Fl—This lithofacies is interpreted to represent pedogenically modified overbank sediment. The cyclical nature of grain size in the section shown in Figs. 24 and 25 is due to relatively infrequent overbank events that brought silt and sand across the floodplain, followed by more frequent, clay-laden, overbank events. The finer-grained, bioturbated, and rooted portions of the cycles represent cumulic pedogenesis, although the entire sequence could be argued to be cumulic except where primary sedimentary structures are preserved over large lateral distances.

The floodplain environment must have been conducive to a soil fauna, as evidenced by the extensive bioturbation. The type of fauna is unclear; the burrows are similar in form and age to the types 5, 6, and 7 of Bown and Kraus (1983), who attributed them to worms, insects, and mollusks.

Recognition of distinct A horizons would be pure speculation in these paleosols because of the lack of distinct rooted horizons and characteristic structure. Many horizons show evidence of pedogenic accumulation of organic carbon, translocated clay, and oxides, suggesting the presence of B horizons.

Clay translocation evidenced by cutans on peds indicates that draining occurred in the soils. However, assessment of the hydrologic conditions of the floodplain is problematic because of the early and late diagenetic effects of cumulic pedogenesis, compaction, and associated dewatering.

The soils were probably surficially drained and oxygenated. Evidence for this includes (1) clay translocation, (2) extensive soil fauna, (3) the oxidized nature of burrow traces, and (4) the lack of preserved macroscopic organic matter. Post-burial decay of fine-grained organic matter was associated with reduction of iron in most of the horizons, except for strongly oxidized burrows, forming the overall greenish cast in the matrix. Further diagenetic modification likely took place during dewatering and compaction of the sediments (possibly with processes similar to those described by Kantorowicz, 1985). After compaction, permeabilities would have decreased to near zero, which may have hindered further diagenesis in mudrocks of the San Jose until fractures opened during Quaternary erosion.

It is possible that the paleosols were reduced (gleyed), producing the green colors essentially immediately after deposition. The silty and clayey nature of the sediment, low-relief topography, proximity to fluvial and lacustrine environments, and subtropical climate (inferred by fossil plants and invertebrate and vertebrate faunas; see below) suggest the possibility of developing poorly drained soils.

The relatively rare occurrences of cross-stratified facies in overbank environments indicate that sedimentation was rarely rapid enough to prevent bioturbation of overbank units. Further work is needed to understand soil environments and processes before any attempt can be made at interpreting floodplain microenvironments or the rates of soil development or subsidence required for preservation of these strata.

Description of lithofacies Fl—A thin but distinctive bed of laminated and crosslaminated siltstone and shale (lithofacies Fl) (Fig. 26) was first recognized at Santos Peak and has been traced and correlated over a large area (Fig. 27). Another thin and areally limited outcrop of this lithofacies was recognized in the study area (Fig. 16: MS-4). The unit in Figs. 26 and 27 is characterized by the anomalous occurrence in the San Jose Formation of preserved sedimentary structures in clay and silty units and carbonized fossil leaves and twigs (summarized below). The unit contains two coarsening- and thickening-upward sequences of sandy siltstone (Fig. 26). Shale samples have not yielded ostracodes, charophytes, or conchostrachans (K. Kietzke, oral comm. 1986).

Interpretation of lithofacies Fl—Sedimentary structures and fossil data indicate that lithofacies Fl was deposited in a locally anoxic, probably stratified, lacustrine environment. Paleocurrent measurements and channel orientations indicate that the silty units (Fig. 27) may represent fluvial incursion into the lake. Without exception, sheet sandstones overlie lacustrine sequences. Paleocurrents suggest that the stream(s) depositing the sandstones shifted into the ponds due to avulsion that was preceded by crevassing and deltaic incursion. Lithofacies Fl bed geometries are similar to carbonaceous beds of the Willwood Formation in the Bighorn basin, Wyoming (Wing, 1984). The Fl beds of the San Jose, however, are less abundant than those in the Willwood and are associated with channel sandstones rather than with mudrock.

Summary of the sedimentology of the San Jose Formation

Internally channelized sheet sandstones within the Regina and Llaves Members of the San Jose Formation are composed dominantly of lithofacies St + Sh. These sandstones and minor conglomerates were deposited in channels that included basal scours overlain by meter- and channel-scale 3D dunes that prograded down and across channels. The high-energy character of lithofacies St + Sh and abundant intraclasts of mudrock attest to a fluvial system in which high-energy channels shifted across, and eroded, low-energy mudrock facies. A diagrammatic portrayal of sedimentary environments of the San Jose Formation is shown in Fig. 28.

Paucity of epsilon cross-strata and vertically accreted mudrock channel fills and the broad cross-sectional channel profiles suggest a low-sinuosity, possibly braided, channel pattern (Bridge, 1985). Laterally discontinuous channel sandstones within floodplain deposits indicate channel belts shifted by avulsion in addition to bank erosion. Mudrock clasts and laterally restricted sets of epsilon cross-strata near the bases of some sheet sandstones suggest that channels may have had high sinuosities and steep banks where they eroded overbank mudrock, possibly in the initial development of a channel belt after avulsion. Continued deposition of sand and channel migration led to development of broad, sand-bed, braided mobile channel belts with shallow lateral pinchouts and subtle, flanking levees.

While direct evidence of levees, such as beds of overbank deposits with depositional dips away from channels, has

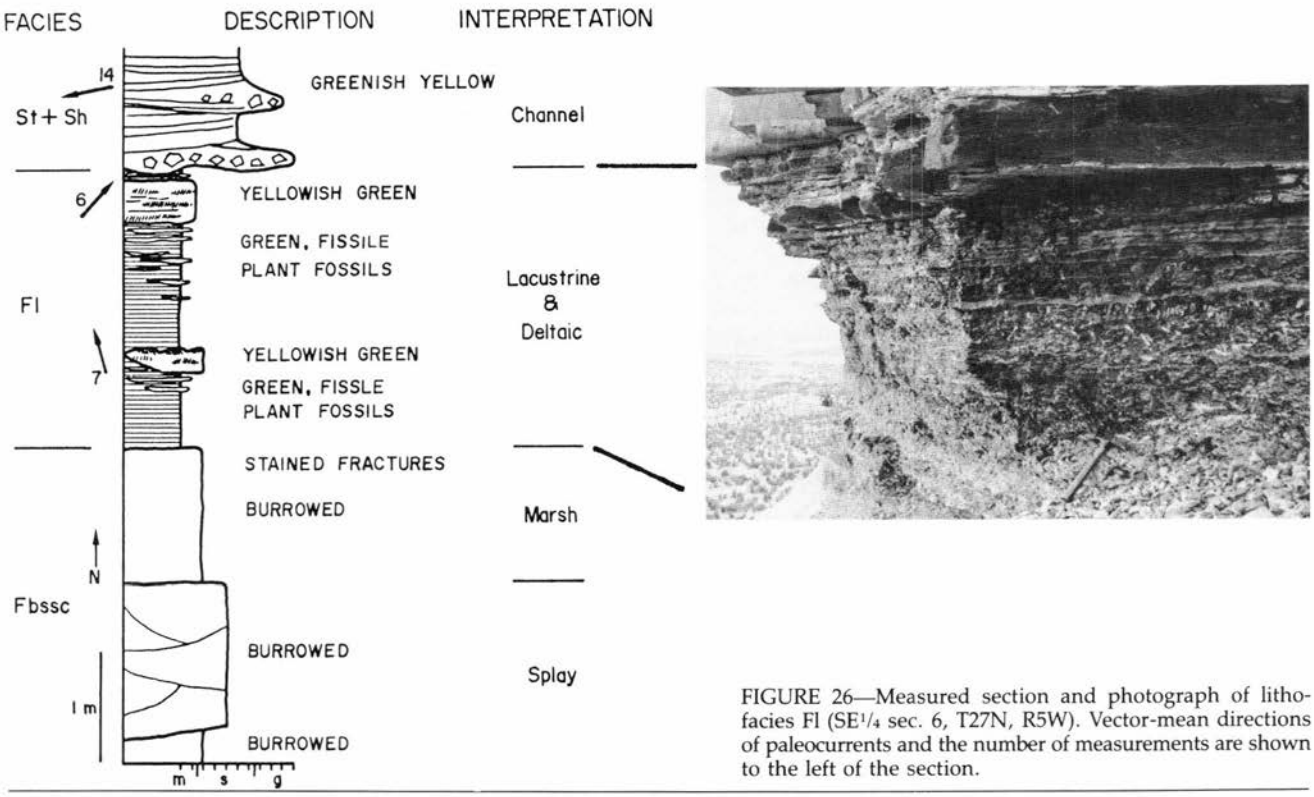

FIGURE 26—Measured section and photograph of lithofacies Fl (SE¼ sec. 6, T27N, R5W). Vector-mean directions of paleocurrents and the number of measurements are shown to the left of the section.

not been observed in outcrop, indirect evidence suggests the occurrence of topographic highs separating channels from lower floodplains. This evidence includes (1) the wide accumulation of continuous overbank sediment, and (2) ribbon-sandstone channels that are oriented at an angle to major sheet-sandstone channels (Fig. 23). The abrupt separation of channel and overbank environments suggests that levees acted as a barrier between in-channel flow and overbank flooding. Ribbon-sandstone channels must have cut through a topographic high (i.e. a levee) to reach a lower local base level (the main-stem channel itself or a floodplain or floodbasin).

Ribbon-sandstone channels are interpreted to be crevasse channels and their distributaries that formed during a single, or few, crevassing event(s) (Fig. 28). These channels probably fed sheet floods (splays) represented by lithofacies St, Sr, Sh, and Sm interbedded in mudrock sequences. Coarsening-upward sequences, mudrocks through fine- and coarse-grained sandstone below channel deposits, suggest that crevassing events occasionally led to channel avulsion. Abandoned channels were filled dominantly by sand deposited by the migration of large-scale bedforms and thin units of shallow sheetfloods. Relatively rare bioturbation of channel-fill sandstones suggests shallow rooting of vegetation and shallow bioturbation into sediment in areas of abandoned channels.

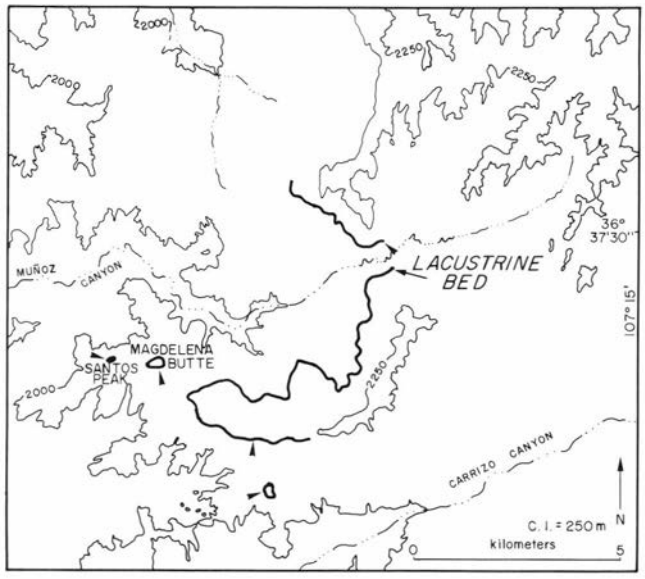

FIGURE 27—Map of outcrop extent of lithofacies Fl, indicated by arrows, at Santos Peak (Fig. 26).

Fining-upward sequences, extensive bioturbation, and pedogenic features in most of the overbank areas suggest sedimentation by overtopping of banks, flooding, vertical accretion, and cumulic pedogenesis. Laminated mudrocks represent shallow floodbasin lakes that accumulated plant debris. The rare occurrence of laminated mudrocks suggests either that much of the floodplain was subaerial or that bioturbation destroyed sedimentary structures in most lacustrine environments, making floodbasin environments difficult to recognize in outcrop. However, evidence for surficial drainage in much of the mudrock studied supports an interpretation of subaerial exposure of much of the flood-plains (Fig. 28). Mudrock cut-and-fill sequences outside of the study area (cf. Kraus and Middleton, 1987) indicate periods of floodplain erosion, although the areal extent and cause of incision are unclear (Smith, 1988).

Most of the sandstone bodies in all members of the San Jose Formation depicted in well logs (Figs. 7, 10, 13), along cross sections (Figs. 11, 12, 14, Pl. 1), and in measured sections (Fig. 16) are composed of lithofacies St + Sh. The more continuous nature of some sandstone sheets, for example the Cuba Mesa Member and the medial sandstone of the Llaves Member (Baltz, 1967: 50-51), is apparently due to great amalgamation of channels than in the more lenticular sandstones, for example those in the Regina and Tapicitos Members. Sheet sandstones throughout the members of the San Jose Formation were apparently deposited in similar channel environments.

Mudrock lithologies are apparently similar throughout

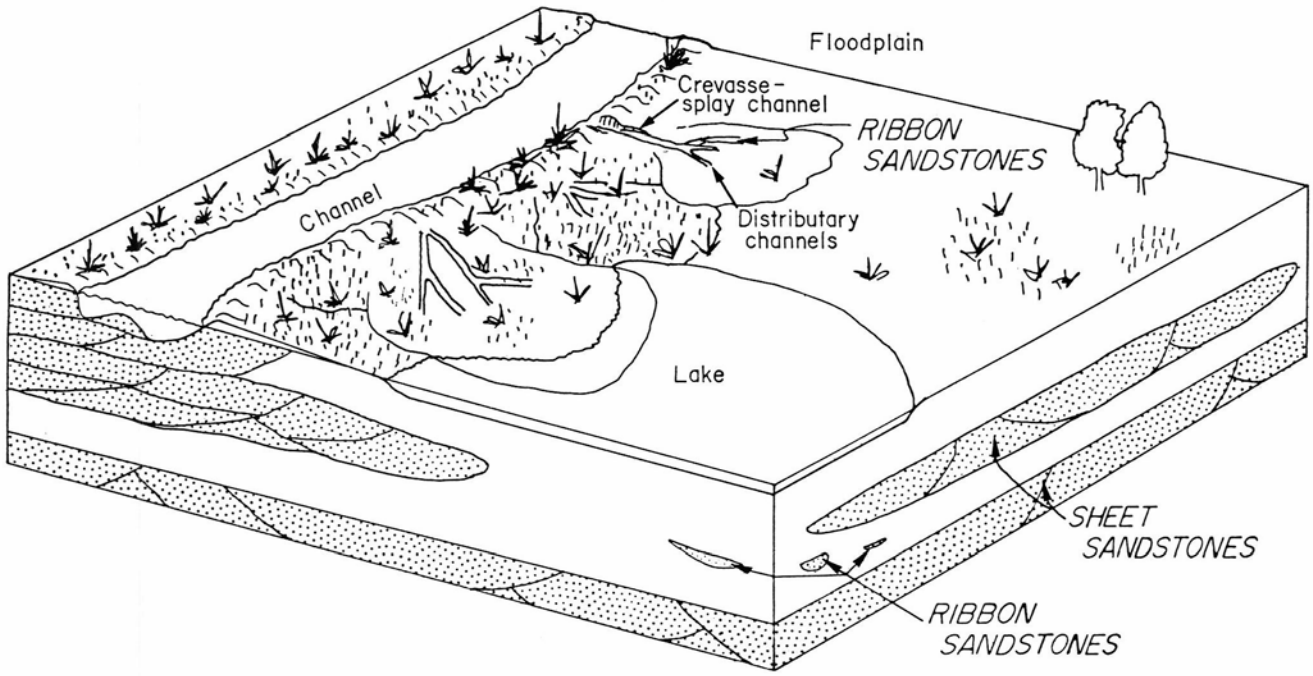

FIGURE 28—Diagrammatic portrayal of the sedimentology of the San Jose Formation. Approximate horizontal scale is hundreds of meters to a few kilometers.

the Regina Member in the study area, except for averaged percentages of mudrock-to-sandstone in vertical sections. Stratigraphic relationships depicted in Fig. 23 are representative of many of the mudrock and sandstone outcrops. Shales (lithofacies Fl) are everywhere overlain by sandstone beds, commonly lithofacies St + Sh, as they are in the Magdalena Butte—Santos Peak area (Fig. 23). Sedimentologic differences between the Regina and Tapicitos Members are unclear beyond the dominance of red colors in the Tapicitos.

Sediment dispersal

Introduction and methodology

Measurement of paleocurrent indicators of a variety of scales (Miall, 1974) was made in order to understand small-and large-scale flow patterns in channels in the San Jose Formation (Fig. 20). For the purpose of analyzing regional sediment dispersal, data from sedimentary structures that represent relatively high-energy fluid flow are discussed here. These structures include (in order of decreasing abundance) (1) axes of large-scale trough cross-strata, (2) maximum dip directions of large-scale trough cross-strata, (3) longitudinal groove and flute casts at channel bases, and (4) parting lineations.

Sandstone beds were chosen for study in order to have a wide geographic and stratigraphic spread of data. Paleocurrent measurements were collected from sheet sandstones of lithofacies St + Sh at stations that include one or more beds. The quality of exposure and type of paleocurrent indicator were recorded for each measurement made. For data from cross-strata, the trough axis or maximum dip direction was judged to be well exposed in either two (2D) or three (3D) dimensions. Three-dimensional data should be more precise and have less dispersion due to measurement error, but are less numerous. Because bedding is essentially horizontal, corrections for structural tilt did not have to be made. The existence of polymodal paleocurrent distributions, at 67% confidence levels for data in 30° groups (after High and Picard, 1971), was analyzed by the method of Tanner (1955). Vector means of 3D and 2D + 3D data from each station were calculated on a programmable calculator using the method described in Potter and Pettijohr (1977: 376-377). The Rayleigh test of whether the vector magnitude is likely due to pure chance was then applied to the vector means (after Curray, 1956).

Results

Vector means of paleocurrent data collected from large-scale sedimentary structures in the study area indicate paleoflow was from the northwest, northeast, and east, generally flowing toward the south (Fig. 29). Vector means of data from all paleocurrent indicators are compiled in Appendix 2. Data from six stations display bimodal distributions (Appendix 2). Four stations do not contain at least one significant paleocurrent vector mean (3D or 2D + 3D); of these four stations, one (station 23) displays a polymodal distribution, which likely accounts for its vector mean not passing Rayleigh's test of significance. Only vector means which are significant at the 95% level (following Curray, 1956), or are not significant due to bimodality, are shown on the maps of paleocurrent vectors. An enlarged map of paleocurrent vector means in the Santos Peak—Magdalena Butte area is shown in Fig. 30. Vector means of data from both 3D and 2D + 3D exposures are displayed in Figs. 29 and 30. Inclusion of data from 2D exposures with those from 3D exposures serves to raise the level of significance of vector means at 83% of the stations, while lowering, or having no effect on the level of significance of vector means, at 8.5% of the stations.

Discussion

Paleocurrent data suggest that streams were generally directed toward the study area from the northeast and northwest and exited to the south (Fig. 29). This is due to the Regina Member displaying south- to southeast-directed paleoflow in the western map area and southwest-directed paleoflow in the eastern map area. Paleocurrents in the Llavas and Tapicitos Members display west- to southwest-directed paleoflow. Work outside the present study area supports the occurrence of source areas to the northwest

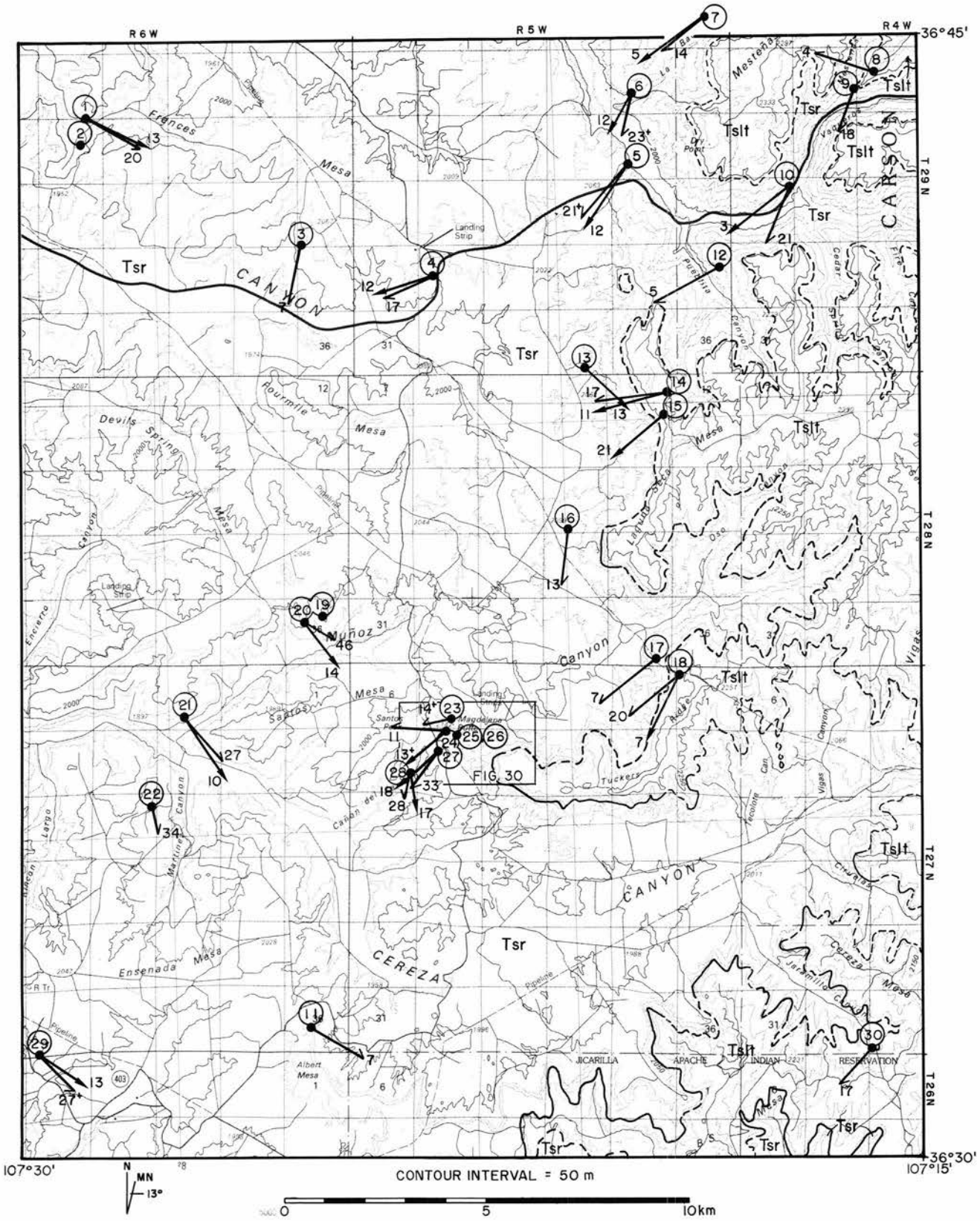

KEY

SAN JOSE FORMATION

Tslt — LLAVES and TAPICITOS MEMBERS

Tsr — REGINA MEMBER

PALEOCURRENT VECTOR MEANS

3D

2D+3D

LARGE-SCALE CROSS-STRATA

N = Number of readings

X = Station number

0 50 100%

FIGURE 29—Map of paleocurrent vector means and the members of the San Jose Formation in the study area. See Appendix 3 for data and text for explanation.

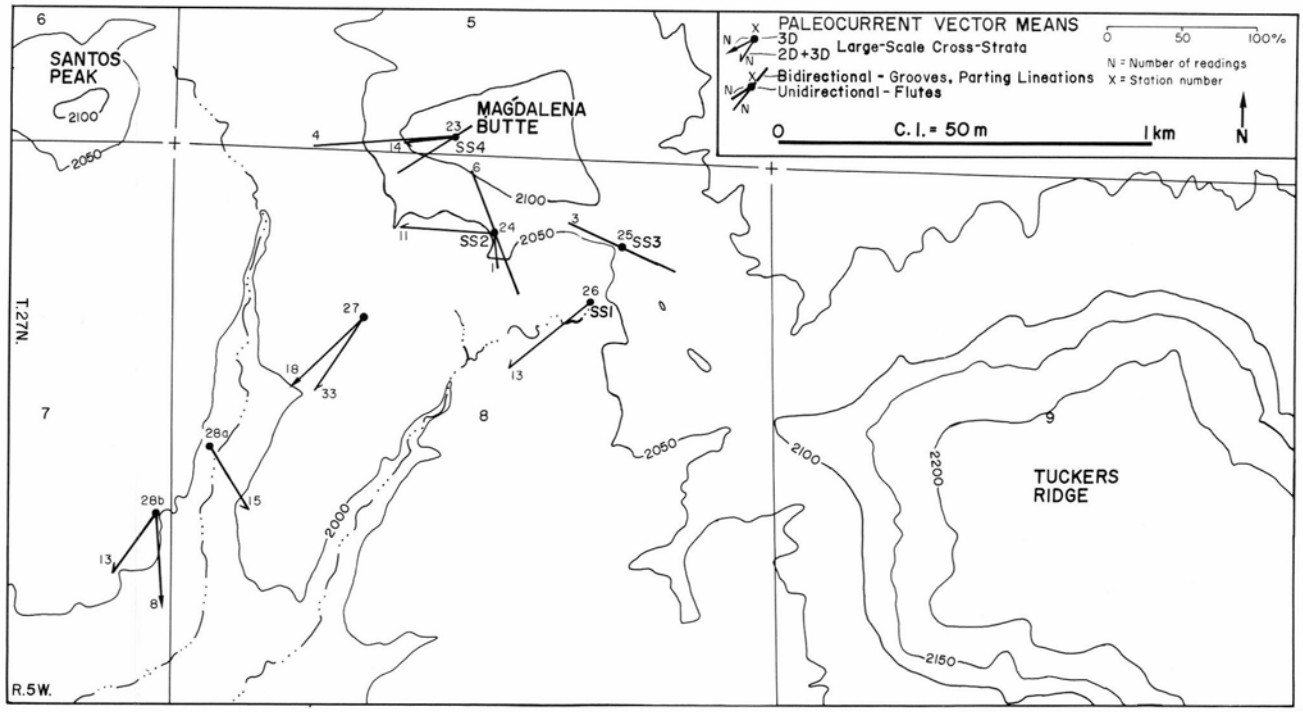

FIGURE 30—Detailed map of paleocurrent vector means in the Magdalena Butte–Santos Peak area (located in Fig. 29).

and east-northeast of the Eocene San Juan Basin (Smith, 1988).

Data from the Llavas and Tapicitos Members suggest that paleoflow was entirely from the northeast and east, in contrast to data from the Regina Member (Fig. 29). A change in paleoflow from more northwestern and northern to more northeastern sources is suggested by comparing data from different stratigraphic levels in the Regina Member. Paleocurrent data from the Santos Peak-Magdalena Butte area (Fig. 30) display a shift in orientation from south-southeast at the topographically and stratigraphically lowest station (28a), to west-southwest at the highest station (23) (SS4 in Fig. 23). The sandstone bed on Magdalena Butte and Santos Peak (SS4) has a similar lithology and paleoflow directions to sandstones of the Llaves Member.

Paleontology

Fossils of plants, invertebrates (nonmarine gastropods and unionids), and vertebrates (mostly mammals) were observed and, in most cases, collected at 46 localities in the study area (Fig. 9; Appendix 3). Most of these collections were made by two field parties as part of environmental-impact surveys contracted by the U.S. Bureau of Land Management. The first of these surveys, during 1977, produced fossils that are housed in the collection of the New Mexico Museum of Natural History and bear NMMNH accession numbers (Kues et al., 1977). The second survey, in 1979, produced fossils that are in the vertebrate-fossil collection at Brigham Young University, Provo, Utah, and bear BYU accession numbers (Ash et al., 1979).

Initial interest in collecting vertebrate fossils in the badlands of the San Jose Formation south of the settlement of Gobernador (Fig. 9) stems from 1976 when one of us (SGL) examined AMNH (American Museum of Natural History) 32660, a maxillary fragment of the early Eocene mammal *Phenacodus primaevus.* This specimen, found during the archaeological excavation of a pit house 1.2 km south of Gobernador, suggested the possibility of fossil-vertebrate occurrence in the San Jose Formation 35 km or more northwest of previously known occurrences. This locality and other localities described herein are the northernmost fossils yet found in the San Jose Formation. Thus, in a sense, the Kues et al. (1977) and Ash et al. (1979) surveys in the Gobernador-Vigas Canyon area followed this "lead." In addition to their collecting, one of us (SGL) also collected some fossils from the study area in 1983 and 1984. Here we review the fossils from the study area, identify them, and discuss their biochronologic significance.

Fossil plants

The only megafossil plants known from the San Jose Formation, except for the fossil logs common in the Cuba Mesa Member at various locales throughout the San Juan Basin, are from the study area. At locality 26, Tidwell et al. (1981) identified the following taxa: *Danaea?* sp., *Acrostichum hesperium, Taxodium olriki, Salix sp., Pterocarya-like* catkin, *Pterocarya-like* fruits, *Paleonelumbo macroloba?, Cinnamomum* cf. *C. hesperium, Lindera obtusata,* cf. *Persea coriacea, Sapindus dentoni, Eugenia americana, Araliophyllum* sp., *Leguminosites* sp., and *Carpites* sp. Based on this flora, Tidwell et al. (1981: 328) concluded that "the San Juan Basin during [early] Eocene time was in general a humid, forested region" because most of the living corollaries of the fossil plants "appear to characterize regions of ample rainfall and some probably grew in or near swampy areas."

Nonmarine invertebrates

Nonmarine invertebrates, unionids and gastropods, were collected at localities 3, 4, and 17 in the Regina Member (Fig. 9). These specimens (NMMNH 8552, 8853, and 8554), currently under study by J. H. Hartman of the North Dakota Geological Survey, considerably add to the small invertebrate fauna of the San Jose Formation. Hartman (1981) reviewed this fauna, which consists of two gastropod taxa originally reported by Cockerell (1915).

Vertebrates

Lepisosteidae—Gar scales were collected at localities 4 (NMMNH 8555), 5 (NMMNH 8556), 6 (NMMNH 8557), 8

(NMMNH 8558), 20 (NMMNH 8559), and 43 (BYU 4308). Precise identification of these specimens is not possible. Cope (1877) named two species of gars from the San Jose Formation: *Lepidosteus aganus* and *Clastes integer.* Wiley (1976) considered both taxa to be junior subjective synonyms of *Atractosteus simplex.* Thus, *A. simplex* is the only species of gar currently known from the San Jose Formation (Lucas et al., 1981).

Testudines—Although fragments of turtle shells were observed at many localities, virtually no specimens were collected. The only specimen collected is BYU 4264 from locality 41, shell fragments identified by J. H. Hutchison of the University of California, Berkeley (oral comm. 1987), as *Echmatemys* sp. This emydid genus is the most commonly encountered fossil turtle in the Eocene of Wyoming, first appears in the early Graybullian, and has previously been reported from the Regina Member of the San Jose Formation in the southeastern San Juan Basin (Hutchison, 1980; Lucas et al., 1981).

Crocodilia—Crocodilian fossils are limited to isolated bicarinate teeth, procoelous vertebrae, and deeply pitted, keeled scutes from localities 1 (NMMNH 8560), 4 (NMMNH 8561), 5 (NMMNH 8562), 6 (NMMNH 8563, 8564), 7 (NMMNH 8565, 8566), 20 (NMMNH 8567, 8568), 44 (BYU 4271), 45 (BYU 4232), and 46 (BYU 4232). We do not consider these fossils diagnostic at the generic level, though some workers (e.g. Bartels, 1983) readily attach the name *Leidyosuchus* to bicarinate teeth of early Cenozic crocodilians.

Phenacolemur praecox—NMMNH 8569 (Fig. 31-1) from locality 20 is a left-dentary fragment of a paromomyid primate bearing the roots of P_4, the talonid of M_1, the complete M_2, and the **M3** roots. Features of NMMNH 8569 that justify assignment to *Phenacolemur* (cf. Simpson, 1955; Bown and Rose, 1976; Szalay and Delson, 1979) include: dentary very deep under anterior cheek teeth, P4 as large or larger than M1 (judged from P4 roots), molar paraconids and metaconids closely appressed, no molar cingulids, molars low-crowned and with very shallow basins, and **M3** with expanded third lobe (judged from M_3 roots). M_2 size (L = 3.4 mm, W = 2.3 mm) and probably P_4 size (judged from the roots) indicate a very large *Phenacolemur,* unquestionably *P. praecox* (Simpson, 1955; Bown and Rose, 1976). This is the first report of *P. praecox* from the San Jose Formation. The smaller species *P. jepseni* is known from the Regina Member in the Llaves area of the east-central San Juan Basin.

Oxyaena forcipata—NMMNH 8570 (Fig. 31-2, 3) is a leftdentary fragment bearing $_{P4–M1}$ of *Oxyaena* from locality 15. We tentatively assign it to *0. forcipata* because of its relatively large size ($P4^L$ = 15.8 mm, W = 8.2 mm; M_1L = 16.3 mm, W = 9.7 mm) and massive **P4** which has a well developed anterior cuspid (Matthew, 1915: 49; Denison, 1938: 169). Clearly, *Oxyaena* is in need of taxonomic revision (cf. Bown, 1979: 85). *0. forcipata* has been reported previously from the Regina Member but not from the Tapicitos Member of the San Jose Formation (Lucas et al., 1981).

Ectoganus gliriformis—Schoch (1986: 74, pl. 38, figs. 5-20) described and illustrated taeniodont specimens from locality 13. He identified these specimens, NMMNH 8571, 8572, and 8573, as *Ectoganus gliriformis gliriformis,* a typical Wasatchian taxon to which belong all taeniodont specimens from the San Jose Formation (Schoch, 1986: table 1). We do not, however, use the trinominal nomenclature of Schoch (1986) and only identify these specimens as *Ectoganus gliriformis.*

Esthonyx bisulcatus—Two specimens of *Esthonyx bisulcatus* were collected, NMMNH 8574 at locality 19 and BYU 4248 at locality 28. BYU 4248 is a skull and lower-jaw fragments that include left P^4–M^3 (Ash et al., 1979: fig. 11A), right P^3 (Fig. 31-6), right M' (Fig. 31-7), and left **M1_2** (Fig. 31-8, 9). Measurements of these teeth (e.g. M_1L = 7.8 mm, W = 6.7 mm) and the fused mandibular symphysis support assignment to *E. bisulcatus* as that taxon was redefined by Gingerich and Gunnell (1979: 144) and Stucky and Krishtalka (1983: 379). All *Esthonyx* specimens known from the San Jose Formation pertain to *E. bisulcatus* (Lucas et al., 1981).

Coryphodon molestus—Fossils of the large pantodont *Coryphodon* dominated collections from the Regina Member, as they dominate all vertebrate collections from the Regina Member in the east-central San Juan Basin (Lucas, 1977). Most of the material is fragmentary and thus defies precise identification. The following localities produced such specimens: 6 (NMMNH 8575, upper-molar fragments), 7 (NMMNH 8576, limb fragments), 10 (NMMNH 8577, left C,), 11 (NMMNH 8578, left astragalus and other bone fragments), 14 (NMMNH 8579, incisor and lower-premolar fragments; NMMNH 8580, vertebrae and limb fragments), 16 (NMMNH 8581, tusk fragments), 19 (NMMNH 8582, part of right I_3), 20 (NMMNH 8583, upper-premolar fragments; NMMNH 8584, scapula fragment and a phalanx; NMMNH 8585 and 8586, upper-premolar fragments), 37 (BYU 4309, tooth and bone fragments), 38 (BYU 4290, two phalanges), and 46 (BYU 4259, lower-molar fragments and foot bones). NMMNH 8587 from locality 4 is an incomplete skeleton of a juvenile *Coryphodon* that is being described elsewhere. Specimens of *Coryphodon* from the study area that can be identified to species pertain to *Coryphodon molestus* as redefined by Lucas (1984b). They are: NMMNH 8588, a left **1²** from locality 20; BYU 4272, a right M_3 talonid from locality 44; and BYU 4354, isolated teeth that include a left M^2 (Fig. 31-4) and right **M3** (Fig. 31-5), from locality 23. **M3** talonid morphology (hypolophid transverse) and size (e.g. M_3 of BYU 4354 is 31.7 mm long and has a trigonid width of 19.6 mm and talonid width of 19.7 mm) justify referral of these specimens to *C. molestus. C. molestus* is the most abundant of the three species of *Coryphodon* known from the San Jose Formation (Lucas, 1984a).

Hyopsodus miticulus—Two localities yielded specimens of *Hyopsodus.* NMMNH 8589 from locality 14 is a left-maxillary fragment with M^{1-3}. BYU 4353 from locality 23 consists of four dentary fragments from a minimum of three individuals (a left-dentary fragment with M_{1_2} is shown in Fig. 31-10, 11). These specimens agree well with Gazin's (1968) concept of *H. miticulus* and are thus assigned to that species. Size of M1 (BYU 4353, M1L = 3.6 mm, W = 2.8 mm) plots near the lower end of the range of specimens from the Bighorn basin that Gingerich (1976: fig. 4) assigned to *H. latidens* and *H. lysitensis.* Clearly, San Juan Basin specimens cannot be placed into Gingerich's (1976) "stratigraphic" framework for *Hyopsodus* in the Bighorn basin. Therefore, the San Juan Basin *Hyopsodus* cannot be identified with respect to Gingerich's (1976) taxonomy which requires strati-graphic position of a specimen in the Bighorn basin, not just morphology, to undertake species-level identification.

Phenacodus primaevus—Specimens of *Phenacodus primaevus* were recovered from localities 9 (NMMNH 8590, an upper-molar fragment), 12 (NMMNH 8591, right M^3 [Fig. 31-13], left-dentary fragment with M_2 [Fig. 31-12], and other bone fragments), 20 (NMMNH 8592, a lower-molar fragment), and 23 (BYU 4352, a left-dentary fragment with incomplete M_3). The large bulbous teeth (M_2L = 13.3 mm, W = 12.8 mm; M^3L = 11.8 mm, W = 13.7 mm) justify referral to *P. primaevus* as redefined by West (1976) and Schankler (1981). *P. primaevus* is known from the Regina Member farther south, but has not been reported from the Tapicitos Member.

Hyracotherium angustidens—After *Coryphodon,* specimens of *Hyracotherium* are the most abundant mammalian fossils collected in the area. Collected specimens are: NMMNH 8593, lower-jaw and tooth fragments from locality

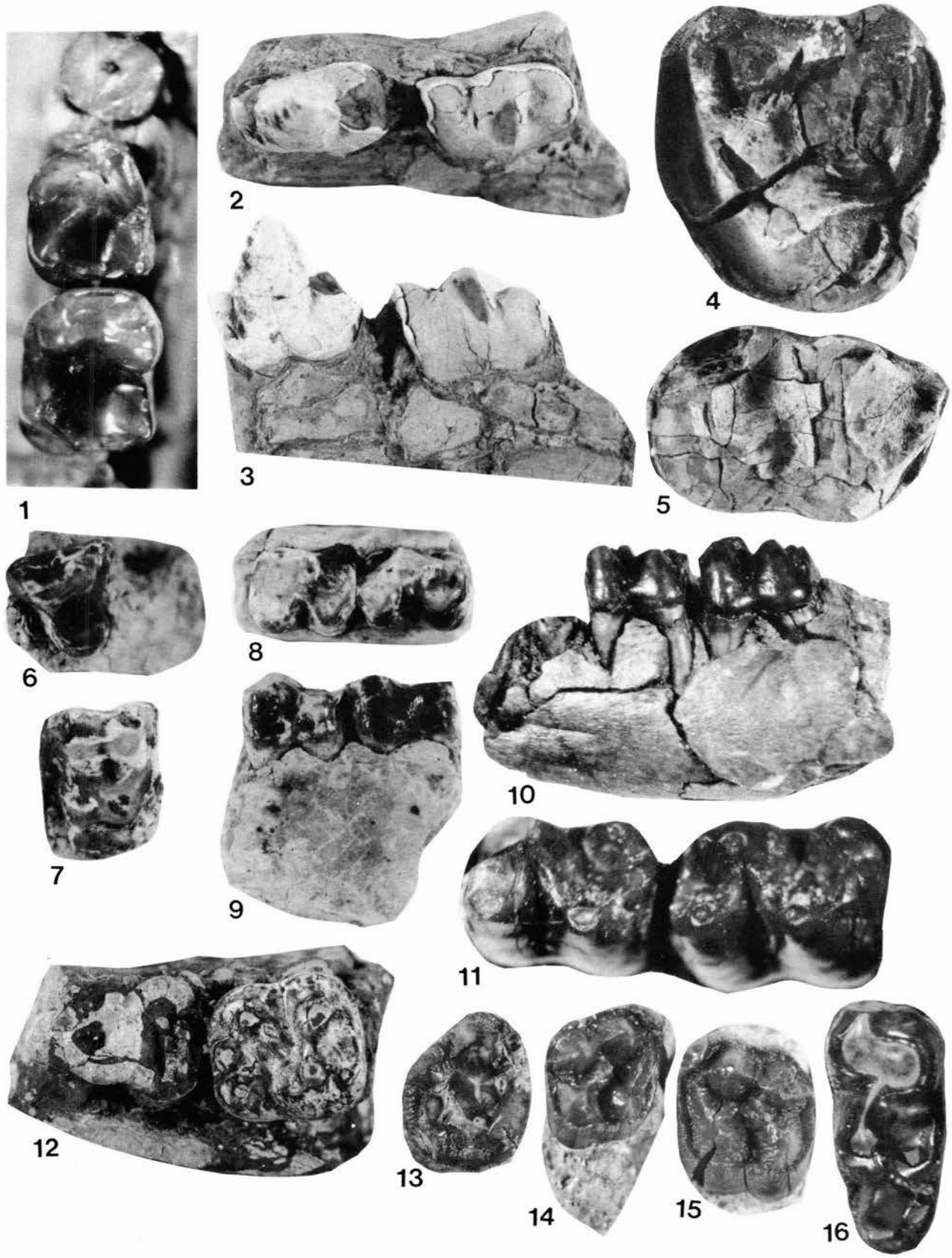

FIGURE 31—Some Wasatchian vertebrate fossils from the Regina Member of the San Jose Formation. **1,** *Phenacolemur praecox,* NMMNH 8559, left M_{1-2}, occlusal view, locality 20, ×20. **2–3,** *Oxyaena forcipata,* NMMNH 8570, left-dentary fragment with P_4–M_1, occlusal (2) and labial (3) views, locality 15, ×1.5. **4–5,** *Coryphodon molestus,* BYU 4354, left M^2 (4) and right M_3 (5), occlusal views, locality 59, ×1.7. **6–9,** *Esthonyx bisulcatus,* BYU 4248, right P^3 (6), right M^1 (7), left M_{1-2} (8–9), occlusal views (6–8) and labial view (9), locality 28, ×2. **10–11,** *Hyopsodus miticulus,* BYU 4353, left-dentary fragment with M_1–M_2, labial (10) and occlusal (11) views, locality 25, ×5 (10) and ×9 (11). **12–13,** *Phenacodus primaevus,* NMMNH 8591, right-dentary fragment with M_2, occlusal view (12), and right M^3, occlusal view (13), locality 12, ×2. **14–16,** *Hyracotherium angustidens,* NMMNH 8596, right M^1 (14) and left M^2 (15), and NMMNH 8594, left M_3 (16), locality 20, ×2.6 (14–15) and ×3.7 (16).

3; NMMNH 8594, a left-dentary fragment with damaged P2—M2 and complete M3 (Fig. 31-16) from locality 20; NMMNH 8595, left M_1 from locality 14; NMMNH 8596, a left M' (Fig. 31-14) and right M^2 (Fig. 31-15) from locality 20; NMMNH 8597, a left P4 and right M3 from locality 20; and NMMNH 8598, a left P3 from locality 20. Kitts (1956) published a complete revision of the species-level taxonomy of *Hyracotherium.* Information provided by P. D. Gingerich in 1980 on a then ongoing revision of the genus was used by Lucas et al. (1981), who listed three species of *Hyracotherium* for the San Jose Formation: *H. index, H. vasacciense,* and *H. tapirinum.* Gingerich has not yet published a taxonomic revision of *Hyracotherium,* though some information on its taxonomy has appeared in articles devoted to other subjects (Gingerich, 1980: fig. 6, 1981: fig. 1). Thus, our identification of the *Hyracotherium* specimens from the study area must rely primarily on Kitts (1956).

Measurements of these specimens suggest that a single species of intermediate-size *Hyracotherium* is represented. Indeed, these measurements (e.g. NMMNH 8596, M1L = 8.1 mm, W = 8.8 mm, M^2L = 9.5 mm, W = 11.2 mm; NMMNH 8594, M_3L = 12.2 mm, W = 6.7 mm) most closely match those of specimens that Kitts (1956: table 6) termed *H. angustidens etsagicum.* Like Bown (1979), we advocate abandonment of the trinominal nomenclature and thus refer the specimens to *H. angustidens.* The holotype of *H.*

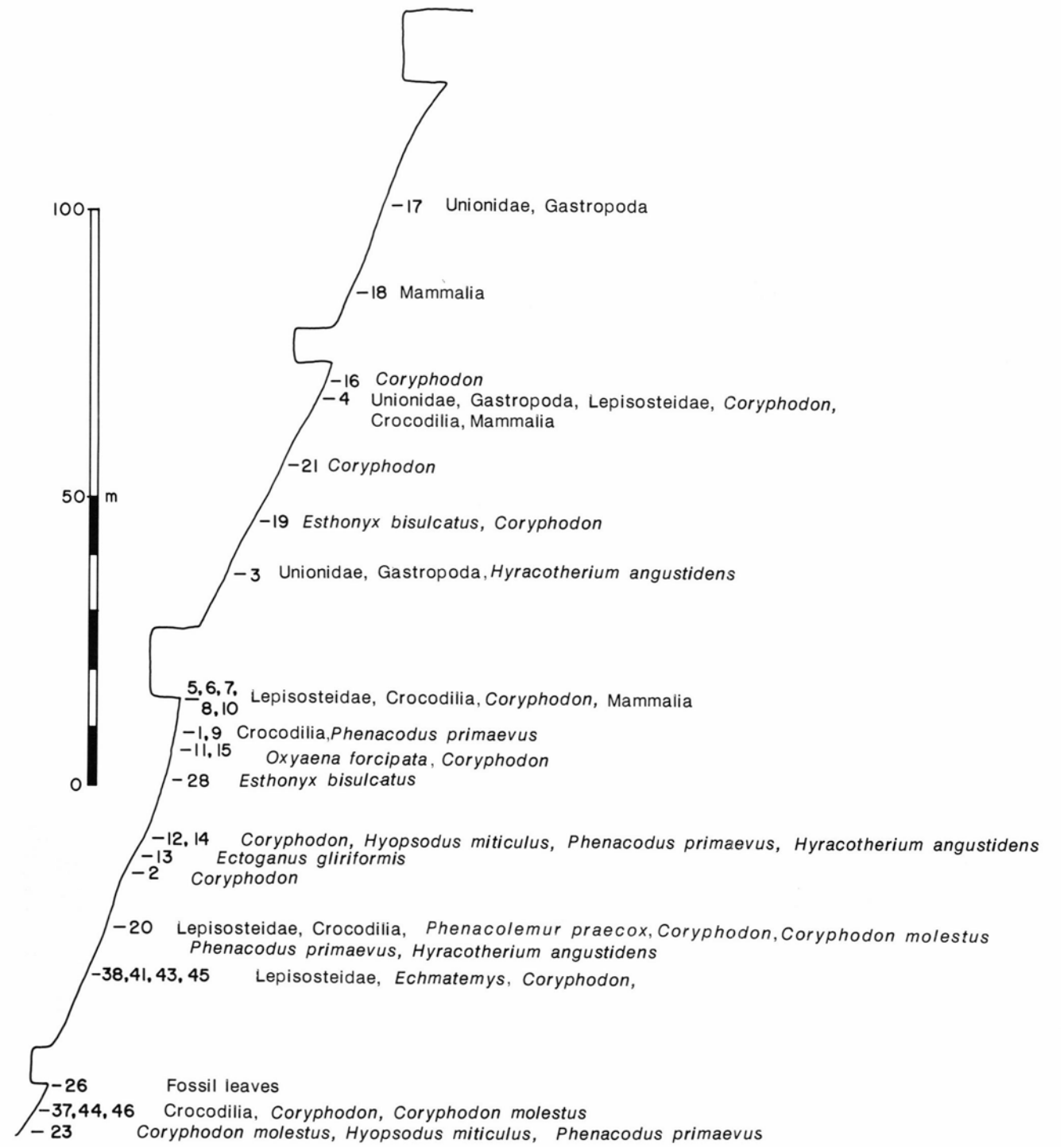

FIGURE 32—Composite stratigraphic section of Regina Member strata showing the positions of selected fossil localities and their fossil taxa with respect to locally correlative sandstone beds.

angustidens is from the Regina Member of the San Jose Formation in the southeastern San Juan Basin (Kitts, 1956).

Mammalia, indeterminate—Unidentifiable mammalian fossils were collected at several localities that are listed here for completeness: 4 (NMMNH 8599, tooth and bone fragments in the *Hyracotherium* size-range; NMMNH 8600, a coprolite), 5 (NMMNH 8601, glenoid of a scapula in the *Phenacodus* size-range; NMMNH 8602, long-bone fragment; NMMNH 8603 metapodial fragments in the *Phenacodus* size-range), 6 (NMMNH 8604, bone fragments), 18 (NMMNH 8605, vertebrae and limb-bone fragments in the *Hyracotherium* size-range), and 20 (NMMNH 8606, an edentulous-jaw fragment).

Biochronology

Fossil vertebrates were collected in the study area through a nearly 130 m thick interval of the Regina Member (Fig. 32). The occurrence of *Phenacolemur praecox, Oxyaena forcipata, Ectoganus gliriformis, Esthonyx bisulcatus, Coryphodon molestus, Hyopsodus miticulus, Phenacodus primaevus,* and H*yracotherium angustidens* in this interval is incontrovertible evidence of its Wasatchian (early Eocene) age (cf. Krishtalka et al., 1987). Furthermore, all of these mammals, except *Phenacolemur praecox,* are present in the Almagre local fauna of the Regina Member in the east-central San Juan Basin (Lucas et al., 1981). Indeed, two of these taxa, *Oxyaena forcipata* and *Phenacodus primaevus,* are not known from the Largo local fauna of the Tapicitos Member of the San Jose Formation in the east-central San Juan Basin. The absence in the study area of *Meniscotherium,* the dominant fossil mammal in collections from the Tapicitos Member, further emphasizes the conclusion that mammals from the study area represent a subset of the Almagre local fauna. This local fauna is of middle Wasatchian, Lysitean, age (Lucas et al., 1981; Krishtalka et al., 1987). We thus assign the mammal-producing interval of the Regina Member in the study area (Fig. 32) a Lysitean age. The small size of the collection from this interval prohibits us from attempting any finer age subdivision based on the stratigraphic presence/absence of taxa as shown in Fig. 32. The best available numerical calibration suggests an age of approximately 53 Ma for the Lysitean (Krishtalka et al., 1987). *Phenacolemur praecox,* first reported here from the Regina Member, is usually thought of as a Gray Bull taxon. However, it is known from the Hannold Hill Formation of Trans-Pecos Texas, a unit of Lysite age (Lucas, 1988). Thus, the stratigraphic range of *P. praecox* in New Mexico and Texas extends into the Lysite, whereas in Wyoming it apparently is restricted to the Gray Bull.

Summary

The lower Eocene San Jose Formation in the central portion of the San Juan Basin consists of the Cuba Mesa, Regina, Llaves, and Tapicitos Members. Well-log data indicate that the Cuba Mesa Member is as much as 100 m thick, thins towards the center of the basin, and pinches out to the northeast by latitude 36° 40' N, longitude 107° 19' W. The Regina Member crops out most extensively in the study area and decreases in sandstone-to-mudrock ratio to the north. The Llaves and Tapicitos Members occur only in the highest regions of the area, are thin due to erosion, and are not mappable as separate members.

Well-log data and approximately 1.2 km of measured sections in the Regina, Llaves, and Tapicitos Members indicate that stratigraphic sections are made up of approximately 35% medium- to coarse-grained sandstone and 65% fine-grained sandstone and mudrock. Six sandstone-dominated lithofacies (in order of decreasing predominance) include: (1) St + Sh, large-scale trough cross-stratified and horizontally stratified sandstone deposited in low-sinuosity braided channels; (2) Sm, sandstone in which primary stratification has been disturbed after deposition in channel or overbank areas; (3) St, large-scale trough cross-stratified sandstone deposited in overbank sheets and crevasse channels; (4) Sh, horizontally stratified sandstone deposited by sheet floods in channels and splays; (5) Sr, small-scale cross-stratified sandstone deposited in shallow channels and splays; and (6) Gt, trough cross-stratified granule conglomerate deposited in channel thalwegs and lags. Two mudrock-dominated lithofacies are recognized in the study *area:* (1) Fbsc + Fl, silt, clay, and fine-grained sandstone that were deposited in overbank areas, burrowed, and underwent pedogenesis; and (2) Fl, laminated silt and clay with plant fragments that accumulated in lacustrine environments on floodplains.

Sedimentology and paleocurrents of the study area suggest deposition by generally south-flowing streams that had sources to the northwest, northeast, and east. The streams had low-sinuosity, sand-bedded, braided channels that shifted laterally to produce sheet sandstones. Subtle levees separated channel environments from muddy overbank areas. Avulsion relocated channels periodically to areas on the floodplain, producing the typically disconnected sheet sandstones within muddy overbank sediments of the Regina Member.

Fossil plants, nonmarine invertebrates, and vertebrates were collected at 46 localities in the Regina Member of the San Jose Formation. The fossil plants suggest a humid, forested environment. The fossil vertebrates are mostly mammals that indicate a middle Wasatchian (Lysitean) age for the Regina Member, about 53 Ma.

References

Allen, J. R. L., 1963, The classification of cross-stratified units, with notes on their origin: Sedimentology, v. 2, pp. 93-114.

Allen, J. R. L., 1971, Transverse erosional marks of weakly cohesive mud beds: Journal of Sedimentary Petrology, v. 39, pp. 607-623.

Allen, J. R. L., 1982a, Sedimentary structures, their character and physical basis, volume 1: Elsevier Scientific Publishing Company, Amsterdam, 593 pp.

Allen, J. R. L., 1982b, Sedimentary structures, their character and physical basis, volume 2: Elsevier Scientific Publishing Company, Amsterdam, 663 pp.

Allen, J. R. L., 1983, Studies in fluviatile sedimentation: bars, bar complexes and sandstone sheets (low-sinuosity braided streams) in the Brownstones (L. Devonian), Welsh borders: Sedimentary Geology, v. 33, pp. 237-283.

Allen, J. R. L., and Banks, N. L., 1972, An interpretation and analysis of recumbent-folded deformed cross-bedding: Sedimentology, v. 19, pp. 257-283.

Ash, S. R., Lucas, S. G., and Tidwell, W. D., 1979, Paleontological survey of the San Juan planning unit and the Rio Puerco resource area. Part I, Report of investigations: Unpublished report to U.S. Bureau of Land Management, Albuquerque District Office, 91 PP.

Baltz, E. H., 1953, Stratigraphic relationships of Cretaceous and early Tertiary rocks of a part of northwestern San Juan Basin: Unpublished MS thesis, University of New Mexico, Albuquerque, 101 pp.

Baltz, E. H., 1967, Stratigraphy and regional tectonic implications of part of Upper Cretaceous and Tertiary rocks, east-central San Juan Basin, New Mexico: U.S. Geological Survey, Professional Paper 552, 101 pp.

Baltz, E. H., Ash, S. R., and Anderson, R. Y., 1966, History of nomenclature and stratigraphy of rocks adjacent to the Cretaceous—Tertiary boundary, western San Juan Basin, New Mexico: U.S. Geological Survey, Professional Paper 524-D, 23 pp.

Barnes, H., 1953, Geology of the Ignacio area, Ignacio and Pagosa Springs quadrangles, La Plata and Archuleta Counties, Colorado: U.S. Geological Survey, Oil and Gas Investigations Map OM-138, scale 1:63,360.

Barnes, Harley, Baltz, E. H., and Hayes, P. T., 1954, Geology and fuel resources of the Red Mesa area, La Plata and Montezuma

Counties, Colorado: U.S. Geological Survey, Oil and Gas Investigations Map OM-149, scale 1:62,500.
Bartels, W. S., 1983, A transitional Paleocene-Eocene reptile fauna from the Bighorn basin, Wyoming: Herpetologica, v. 39, **pp.** 359374.
Birkeland, P. W., 1984, Soils and geomorphology: Oxford University Press, New York, 372 pp.
Bown, T. M., 1979, Geology and mammalian paleontology of the Sand Creek facies, lower Willwood Formation (lower Eocene), Washakie County, Wyoming: Geological Survey of Wyoming, Memoir 2, 151 pp.
Bown, T. M., and Kraus, M. J., 1983, Ichnofossils of the alluvial Willwood Formation (lower Eocene), Bighorn basin, northwest Wyoming, U.S.A.: Palaeogeography, Palaeoclimatology, Palaeoecology, v. 43, pp. 95-128.
Bown, T. M., and Rose, K. D., 1976, New early Tertiary primates and a reappraisal of some Plesiadapiformes: Folia Primatologica, v. 26, pp. 109-138.
Bridge, J. S., 1985, Paleochannel patterns inferred from alluvial deposits: a critical evaluation: Journal of Sedimentary Petrology, v. 55, pp. 579-589.
Brimhall, R. M., 1973, Ground water hydrology of Tertiary rocks of the San Juan Basin, New Mexico; *in* Fassett, J. E. (ed.), Cretaceous and Tertiary rocks of the southern Colorado Plateau: Four Corners Geological Society, Memoir, pp. 197-207.
Cant, D. J., and Walker, R. G., 1978, Fluvial processes and facies sequences in the sandy braided South Saskatchewan River, Canada: Sedimentology, v. 25, pp. 625-648.
Clemons, R E., 1982, New Mexico highway geologic map: New Mexico Geological Society, scale 1:1,000,000.
Cockerel], T. D. A., 1915, Gastropod Mollusca from the Tertiary strata of the West: American Museum of Natural History, Bulletin, v. 34, pp. 115-120.
Conolly, J. R., 1964, Trough cross-stratification in the Hawkesbury Sandstone: Australian Journal of Science, v. 27, pp. 113-115.
Conolly, J. R., 1965, Large-scale cross-stratification in Triassic sandstones, Sydney, Australia: Journal of Sedimentary Petrology, v. 35, pp. 765-768.
Cope, E. D., 1877, Report upon the extinct Vertebrata obtained in New Mexico by parties of the expedition of 1874: U.S. Geological Surveys West of the 100th Meridian [Wheeler], v. 4, pt. 2, 370 PP.
Curray, J. R., 1956, The analysis of two-dimensional orientation data: Journal of Geology, v. 64, pp. 117-131.
Curtis, C D., and Coleman, M. L., 1986, Control of the precipitation of early diagenetic calcite, dolomite, and siderite concretions in complex depositional sequences; *in* Gautier, D. L. (ed.), Roles of organic matter in sediment diagenesis: Society of Economic Paleontologists and Mineralogists, Special Publication 38, pp. 23-33.
Dane, C. H., 1946, Stratigraphic relations of Eocene, Paleocene, and latest Cretaceous formations of eastern side of San Juan Basin, New Mexico: U.S. Geological Survey, Oil and Gas Investigations Preliminary Chart 24, scale 1:63,360.
Dane, C. H., and Bachman, G. **0.,** 1957, Preliminary geologic map of the northwestern part of New Mexico: U.S. Geological Survey, Miscellaneous Geological Investigations Map 1-224, scale 1: 380, 160.
Dane, C. H., and Bachman, G. **0.,** 1965, Geologic map of New Mexico: U.S. Geological Survey, scale 1:500,000.
DeCelles, P. G., Langford, R. P., and Schwartz, R. K., 1983, Two new methods of paleocurrent determination from trough cross-stratification: Journal of Sedimentary Petrology, v. 53, pp. 629642.
Denison, R. H., 1938, The broad-skulled Pseudocreodi: New York Academy of Sciences, Annals, v. 37, pp. 163-257.
Dresser-Atlas, 1975, Log interpretation fundamentals: Dresser Industries, Inc., Houston, Texas.
Dunn, D. E., 1964, Evolution of the Chama basin and Archuleta anticlinorium, eastern Archuleta County, Colorado: Unpublished PhD dissertation, University of Texas at Austin, 114 pp.
Fassett, J. E., 1968, Summary of geologic data obtained from borehole GB-1, Project Gasbuggy: New Mexico Geological Society, Guidebook 19, pp. 24-27.
Fassett, J. E., and Hinds, J. S., 1971, Geology and fuel resources of the Fruitland Formation and Kirtland Shale of the San Juan Basin, New Mexico and Colorado: U.S. Geological Survey, Professional Paper 676, 76 pp.
Friend, P. F., Slater, M. **J.,** and Williams, R. C., 1979, Vertical and lateral buildings of river sandstone bodies, Ebro Basin, Spain: Geological Society of London, Journal, v. 136, pp. 39-46.
Gazin, C. L., 1968, A study of the Eocene condylarthran mammal *Hyopsodus:* Smithsonian Miscellaneous Collections, v. 153, pp. 1-90.
Gibling, M. R., and Rust, B. R., 1984, Channel margins in a Pennsylvanian braided fluvial deposit; the Morien Group near Sydney, Nova Scotia, Canada: Journal of Sedimentary Petrology, v. 54, pp. 773-782.
Gingerich, P. D., 1976, Paleontology and phylogeny: patterns of evolution at the species level in early Tertiary mammals: American Journal of Science, v. 276, pp. 1-28.
Gingerich, P. D., 1980, Evolutionary patterns in early Cenozoic mammals: Annual Review of Earth and Planetary Science 1980, pp. 407-424.
Gingerich, P. D., 1981, Variation, sexual dimorphism, and social structure in the early Eocene horse *Hyracotherium* (Mammalia, Perissodactyla): Paleobiology, v. 7, pp. 443-455.
Gingerich, P. D., and Gunnell, G. F., 1979, Systematics and evolution of the genus *Esthonyx* (Mammalia, Tillodontia) in the early Eocene of North America: Contributions of the Museum of Paleontology, University of Michigan, v. 25, **pp.** 125-153.
Granger, W., 1917, Notes on Paleocene and lower Eocene mammal horizons of northern New Mexico and southern Colorado: American Museum of Natural History, Bulletin, v. 37, pp. 821-830.
Hand, B. M., and Bartberger, C. E., 1988, Leeside sediment fallout patterns and the stability of angular bedforms: Journal of Sedimentary Petrology, v. 58, pp. 33-43.
Harms, J. C., Southard, J. B., and Walker, R. G., 1982, Structures and sequences in clastic rocks: Society of Economic Paleontologists and Mineralogists, Short Course Notes, no. 9.
Hartman, J. H., 1981, Early Tertiary nonmarine Mollusca of New Mexico: a review: Geological Society of America, Bulletin, Part I, v. 92, pp. 942-950.
Haskin, R. A., 1980, Magnetic polarity stratigraphy and fossil Mammalia of the San Jose Formation, Eocene, New Mexico: Unpublished MS thesis, University of Arizona.
High, L. G., and Picard, M. D., 1971, Mathematical treatment of orientational data; *in* Carver, R. E. (ed.), Procedures in sedimentary petrology: Wiley-Interscience, New York, pp. 21-45.
Hunter, R. E., and Kocurek, G., 1986, An experimental study of subaqueous slipface deposition: Journal of Sedimentary Petrology, v. 56, pp. 387-394.
Hutchison, J. H., 1980, Turtle stratigraphy of the Willwood Formation, Wyoming: preliminary results: University of Michigan Papers on Paleontology, no. 24, pp. 115-118.
Imbrie, J., and Buchanan, H., 1965, Sedimentary structures in modern carbonate sands of the Bahamas; *in* Middleton, G. V. (ed.), Primary sedimentary structures and their hydrodynamic interpretation: Society of Economic Paleontologists and Mineralogists, Special Publication 12, pp. 149-172.
Kantorowicz, J. D., 1985, The petrology and diagenesis of Middle Jurassic clastic sediments, Ravenscar Group, Yorkshire: Sedimentology, v. 32, pp. 833-853.
Kitts, D. B., 1956, American *Hyracotherium* (Perissodactyla, Equidae): American Museum of Natural History, Bulletin, v. 110, pp. 1-60.
Knowlton, F. H., 1924, Flora of the Animas Formation: U.S. Geological Survey, Professional Paper 134, pp. 71-112.
Kraus, M. J., and Middleton, L. T., 1987, Dissected paleotopography and base-level changes in a Triassic fluvial sequence: Geology, v. 15, p. 18-21.
Krishtalka, L., Stucky, R. K., West, R. M., McKenna, M. C., Black, C. C., Dawson, M. R., Flynn, J. J., Golz, D. J., Lillegraven, J. A., and Turnbull, W. D., 1987, Eocene (Wasatchian through Duchesnean) biochronology of North America, in Woodbume, M. **0.** (ed.), Cenozoic mammals of North America, geochronology and biostratigraphy: University of California Press, Berkeley, California, pp. 77-117.
Kues, B. S., Froehlich, J. W., Schiebout, J. A., and Lucas, S. G., 1977, Paleontological survey, resource assessment, and mitigation plan for the Bisti-Star Lake area, northwestern New Mexico: Unpublished report to U.S. Bureau of Land Management, Albuquerque District Office, 1525 pp.
Leeder, M. R., 1987, Sediment deformation structures and the palaeotectonic analysis of sedimentary basins, with a case study from the Carboniferous of northern England; *in* Jones, M. E.,

and Preston, R. M. F. (eds.), Deformation of sediments and sedimentary rocks: Geological Society (U.K.), Special Publication 29, p. 137-146.
Lucas, S. G., 1977, Vertebrate paleontology of the San Jose Formation, east-central San Juan Basin, New Mexico: New Mexico Geological Society, Guidebook 28, pp. 221-225.
Lucas, S. G., 1984a, Biostratigraphic significance of *Coryphodon* species from the Regina Member (lower Eocene), San Jose Formation, San Juan Basin, New Mexico (abs.): New Mexico Geology, v. 6, p. 84.
Lucas, S. G., 1984b, Synopsis of the species of *Coryphodon* (Mammalia, Pantodonta): New Mexico Journal of Science, v. 24, pp. 33-42.
Lucas, S. G., 1988, *Coryphodon* (Mammalia, Pantodonta) from the Hannold Hill Formation, Eocene of Trans-Pecos Texas: The PearceSellards Series, no. 46, pp. 1-16.
Lucas, S. G., and Ingersoll, R. V., 1981, Cenozoic continental deposits of New Mexico: an overview: Geological Society of America, Bulletin, Part 1, v. 92, pp. 917-932.
Lucas, S. G., Schoch, R. M., Manning, E., and Tsentas, C., 1981, The Eocene biostratigraphy of New Mexico: Geological Society of America, Bulletin, Part I, v. 92, pp. 951-967.
Manley, K., Scott, G. R., Wobus, R. A., 1987, Geologic map of the Aztec 1° x 2° quadrangle, northwestern New Mexico and southern Colorado: U.S. Geological Survey, Miscellaneous Investigations Map 1-1730, scale 1:250,000.
Matthew, W. D., 1915, A revision of the lower Eocene Wasatch and Wind River faunas. Part I. Order Ferae (Carnivora). Suborder Creodonta: American Museum of Natural History, Bulletin, v. 34, pp. 1-103.
McKee, E. D., and Weir, G. W., 1953, Terminology of stratification and cross-stratification: Geological Society of America, Bulletin, v. 64, pp. 381-390.
Miall, A. D., 1974, Paleocurrent analysis of alluvial sediments: a discussion of directional variance and vector magnitude: Journal of Sedimentary Petrology, v. 44, pp. 1174-1185.
Miall, A. D., 1977, A review of the braided-river depositional environment: Earth-Science Reviews, v. 13 pp. 1-62.
Miall, A. D., 1978, Lithofacies types and vertical profile models in braided river deposits: a summary; *in* Miall, A. D. (ed.), Fluvial sedimentology: Canadian Society of Petroleum Geologists, Calgary, pp. 597-604.
Mytton, J. W., 1983, Geologic map of Chaco Canyon 30' x 60' quadrangle, showing coal zones of Fruitland Formation, San Juan, Rio Arriba, and Sandoval Counties, New Mexico: U.S. Geological Survey, Coal Investigations Map C-92A, scale 1:100,000.
Plint, A. G., 1986, Slump blocks, intraformational conglomerates and associated erosional structures in Pennsylvanian fluvial strata of eastern Canada: Sedimentology, v. 33, pp. 387-399.
Potter, P. E., and Pettijohn, F. J., 1977, Paleocurrents and basin analysis: Springer-Verlag, Berlin, 425 pp.
Reading, H. G. (ed.), 1986, Sedimentary environments and facies: Blackwell Scientific Publishers, Oxford, 615 pp.
Reeside, J. B., Jr., 1924, Upper Cretaceous and Tertiary formations of the western part of the San Juan Basin, Colorado and New Mexico: U.S. Geological Survey, Professional Paper 134, pp. 1-70.
Schankler, D. M., 1981, Local extinction and ecological re-entry of early Eocene mammals: Nature, v. 293, pp. 135-138.
Schoch, R. M., 1986, Systematics, functional morphology, and macroevolution of the extinct mammalian order Taeniodonta: Peabody Museum of Natural History, Yale University Bulletin 42, 307 pp.
Sikkink, P. G. L., 1987, Lithofacies relationships and depositional environment of the Tertiary Ojo Alamo Sandstone and related strata, San Juan Basin, New Mexico and Colorado: Geological Society of America, Special Paper 209, pp. 81-104.
Simpson, G. G., 1935a, The Tiffany fauna, upper Paleocene, 1. Multituberculata, Marsupialia, Insectivora, and ?Chiroptera: American Museum Novitates, no. 796, 19 pp.
Simpson, G. G., 1935b, The Tiffany fauna, upper Paleocene, 2. Structure and relationships of *Plesiadapis:* American Museum Novitates, no. 816, 30 pp.
Simpson, G. G., 1935c, The Tiffany fauna, upper Paleocene, 3. Primates, Camivora, Condylarthra, and Amblypoda: American Museum Novitates, no. 817, 28 pp.
Simpson, G. G., 1984, The Eocene of the San Juan Basin, New Mexico: American Journal of Science, v. 246, pt. 1, pp. 257-282; pt. 2, pp. 363-385.
Simpson, G. G., 1955, The Phenacolemuridae, new family of early primates: American Museum of Natural History, Bulletin, v. 105, pp. 415-491.
Sloan, R. E., 1987, Paleocene and latest Cretaceous mammal ages, biozones, magnetozones, rates of sedimentation, and evolution: Geological Society of America, Special Paper 209, pp. 165-200.
Smith, L. N., 1988, Basin analysis of the lower Eocene San Jose Formation, San Juan Basin, New Mexico and Colorado: Unpublished PhD dissertation, University of New Mexico, Albuquerque, 166 pp.
Smith, L. N., Lucas, S. G., and Elston, W. E., 1985, Paleogene stratigraphy, sedimentation, and volcanism of New Mexico; *in* Flores, R. M., and Kaplan, S. S. (eds.), Cenozoic paleogeography of west-central United States: Rocky Mountain Section of the Society of Economic Paleontologists and Mineralogists, Denver, Colorado, pp. 293-315.
Stone, W. J., Lyford, F. P., Frenzel, P. F., Mizell, N. H., and Padgett, E. T., 1983, Hydrogeology and water resources of San Juan Basin, New Mexico: New Mexico Bureau of Mines & Mineral Resources, Hydrologic Report 6, 70 pp.
Stucky, R. K., and Krishtalka, L., 1983, Revision of the Wind River faunas, early Eocene of central Wyoming. Part 4. The Tillodontia: Annals of Carnegie Museum, v. 52, pp. 375-391.
Szalay, F. S., and Delson, E., 1979, Evolutionary history of the primates: Academic Press, New York, 580 pp.
Tanner, W. F., 1955, Paleogeographic reconstructions from cross-bedding studies: American Association of Petroleum Geologists, Bulletin, v. 39, pp. 2471-2483.
Thaden, R. E., and Zech, R. S., 1984, Preliminary structure contour map on the base of the Cretaceous Dakota Sandstone in the San Juan Basin and vicinity, New Mexico, Arizona, Colorado, and Utah: U.S. Geological Survey, Miscellaneous Field Studies Map MF-1673, scale 1:500,000
Tidwell, W. D., Ash, S. R., and Parker, L. R., 1981, Cretaceous and Tertiary floras of the San Juan Basin; *in* Lucas, S. G., Rigby, J. K., Jr., and Kues, B. S. (eds.), Advances in San Juan Basin paleontology: University of New Mexico Press, Albuquerque, New Mexico, pp. 307-332.
Tsentas, C., Lucas, S. G., and Schoch, R. M., 1981, Lithofacies of the upper part of the Nacimiento Formation, San Juan Basin, New Mexico (abs.): Geological Society of America, Abstracts with Programs, v. 13, p. 229.
Tweto, O., 1979, Geologic map of Colorado: U.S. Geological Survey, scale 1:500,000.
West, R. M., 1976, The North American Phenacodontidae (Mammalia, Condylarthra): Milwaukee Public Museum, Contributions to Biology and Geology, no. 6, 78 pp.
Wiley, E. O., 1976, The phylogeny and biogeography of fossil and recent gars (Actinopterygii: Lepisosteidae): University of Kansas, Miscellaneous Publication 64, 111 pp.
Wing, S. L., 1984, Relation of paleovegetation to geometry and cyclicity of some fluvial carbonaceous deposits: Journal of Sedimentary Petrology, v. 54, pp. 52-66.
Wood, G. H., Jr., Kelley, V. C., and MacAlpin, A. J., 1948, Geology of the southern part of Archuleta County, Colorado: U.S. Geological Survey, Oil and Gas Investigations Preliminary Map 81, scale 1:63,360.

Appendices start on next page.

Appendix 1

Ownership and location of well logs used (see Fig. 9). * Location: quarter section-section-township-range; ** EPNG - El Paso Natural Gas Co., PNWP - Pacific Northwest Pipeline Co.; [1] near MS-4; [2] used by Baltz (1967); [3] log #218 of Stone et al. (1983); [4] near MS-1; [5] near MS-3; [6] near MS-2.

Number	Location*	Name**
1	NE1/4-13-27N-5W	EPNG San Juan Unit #9
2	SW1/4-12-27N-5W	PNWP San Juan 39-12
3	NE1/4-11-27N-5W	Pan American Pet. San Juan Unit #99
4	SW1/4-10-27N-5W	EPNG San Juan #171
5	SE1/4- 9-27N-5W	EPNG San Juan #173
6	NE1/4- 8-27N-5W	EPNG San Juan #176
7	SW1/4- 6-27N-5W	EPNG San Juan #45 PM
8	NE1/4-36-28N-6W	EPNG San Juan #94 (MD)
9	SW1/4-26-28N-6W	EPNG San Juan Unit #4
10	SW1/4-23-28N-6W	EPNG San Juan #76
11	NE1/4-16-28N-6W	PNWP San Juan #48-16[1]
12	SW1/4- 8-28N-6W	EPNG San Juan Unit #13
13	SW1/4- 7-28N-6W	EPNG San Juan Unit #12
14	SW1/4-31-29N-6W	PNWP San Juan Unit #51-31
15	SW1/4-36-29N-7W	EPNG San Juan #68
16	NE1/4-35-29N-7W	EPNG San Juan #30
17	NE1/4-27-29N-7W	EPNG San Juan #53
18	SW1/4-20-29N-7W	So. Union Gas Co. San Juan Unit #45
19	SW1/4-19-29N-7W	EPNG Marshall #1
20	NE1/4-24-29N-8W	EPNG Vanderwart #6-A
21	SW1/4-14-29N-8W	EPNG Roelofs 2-A
22	SW1/4-22-29N-8W	EPNG Roelofs 4-A
23	NE1/4-21-29N-8W	EPNG Hughes #6
24	NE1/4-20-29N-8W	Three States Nat. Gas Hughes #3
25	NE1/4-19-29N-8W	Three States Nat. Gas Hughes #2
26	SE1/4- 5-26N-8W	Huron Drilling Co. Davis #1
27	SE1/4- 4-26N-8W	John H. Hill Newsom A #2
28	SW1/4- 3-26N-8W	John H. Hill Newsom A #11
29	SW1/4- 2-26N-8W	J. Glenn Turner Turner State #13-2
30	NW1/4- 1-26N-8W	Ralph E. Davis Luthey #2
31	NE1/4- 5-26N-7W	Kingsley-Locke Oil Co. #4-15
32	NE1/4- 4-26N-7W	Compass Explor. Inc. Lindrith Fed. #1-4
33	NE1/4- 3-26N-7W	EPNG N.C.R.A. #1
34	SE1/4- 2-26N-7W	Southern Pet. Exploration Inc. State #2
35	SE1/4- 1-26N-7W	Johnston Oil & Gas Co. Rincon #12
36	NW1/4- 6-26N-6W	Johnston Oil & Gas Co. Rincon #13
37	NW1/4- 5-26N-6W	Robert E. Mead Federal Scott 1-B
38	NE1/4- 4-26N-6W	Caulkins Oil Co. Breech E #D-54
39	SE1/4- 3-26N-6W	Caulkins Oil Co. Breech E #112
40	SE1/4- 2-26N-6W	Caulkins Oil Co. State #116
41	SW1/4- 1-26N-6W	Caulkins Oil Co. Breech E #117

Appendix 1 continued

Number	Location*	Name**
42	SW1/4- 7-26N-5W	Northwest Prod. Co. W #1-7[2]
43	NE1/4- 5-26N-5W	Northwest Prod. Co. W #2-5
44	SW1/4- 4-26N-5W	Aztec Oil & Gas Co. Ariz. Jic. #1-B
45	SW1/4- 3-26N-5W	Continental Oil Co. AXI Apache K #4
46	SW1/4- 1-26N-5W	Southern Union Gas Co. Jic. #2-G
47	NE1/4- 6-26N-4W	Northwest Prod. Co. N #9-6
48	SW1/4- 5-26N-4W	Northwest Prod. Co. N #3-5
49	NE1/4- 4-26N-4W	Amoco Prod. Co. Jic. Apache 102 #19
50	NW1/4- 3-26N-4W	Amoco Prod. Co. Jic. Apache 102 #23
51	NE1/4- 1-26N-4W	Aztec Oil & Gas Co. Jic. 101 #1
52	18-26N-3W	J.P. McHugh Jic. 2-A[3]
53	NE1/4-36-27N-5W	EPNG San Juan #36 (PM)
54	SE1/4-25-27N-5W	EPNG San Juan #158
55	NE1/4-24-27N-5W	EPNG San Juan #31 (PM)
56	SW1/4- 1-27N-5W	EPNG San Juan #100
57	NE1/4-36-28N-5W	EPNG San Juan #47-36
58	NE1/4-26-28N-5W	EPNG San Juan #36
59	SW1/4-24-28N-5W	EPNG San Juan #37
60	SW1/4-13-28N-5W	EPNG San Juan #25
61	NE1/4-14-28N-5W	EPNG San Juan #26
62	SW1/4-11-28N-5W	EPNG San Juan #18
63	SW1/4-26-29N-5W	PNWP San Juan Mesa 9-26[4]
64	NE1/4-25-29N-5W	Northwest Pipeline Co. San Juan #100
65	SW1/4-23-29N-5W	EPNG San Juan #39-23
66	SW1/4-12-29N-5W	Phillips Pet. Co. Mesa #3-12[5]
67	SW1/4- 3-29N-5W	Dugan Prod. Co. Sherman Edwards #2
68	NE1/4-31-30N-5W	EPNG San Juan #28[6]
69	NE1/4-35-30N-5W	Phillips Pet. Co. Mesa #4-35
70	SW1/4-26-30N-5W	PNWP San Juan #16-26
71	SE1/4-20-30N-5W	EPNG San Juan #27
72	SW1/4-24-30N-5W	EPNG San Juan #21-24
73	SW1/4- 8-30N-4W	EPNG San Juan #12
74	SE1/4- 5-30N-4W	EPNG San Juan #15
75	SW1/4- 1-30N-5W	Aztec Oil & Gas Co. Carson #1
76	SW1/4-32-31N-5W	EPNG Rosa Unit #24
77	SE1/4-34-31N-5W	Amoco Prod. Co. Rosa Unit #55
78	NE1/4-29-31N-5W	PNWP Rosa Unit #15-29
79	SE1/4-22-31N-4W	Pan American Pet. Co. Rosa Unit #33
80	NE1/4- 8-31N-5W	Pan American Pet. Co. Sarah E. Lilly A
81	SW1/4-35-32N-5W	Stanolind Oil & Gas Co. San Juan #2
82	SW1/4-29-32N-4W	Phillips Pet. Co. Mesa #1-29
83	NW1/4-26-32N-5W	Belco Pet. Co. Carracas Mesa #1-26
84	SW1/4-21-32N-5W	Aztec Oil & Gas Co. Uells Canyon #1
85	SW1/4-14-32N-5W	Stanolind Oil & Gas Co. San Juan #1
86	SW1/4-16-32N-4W	Phillips Pet. Co. Mesa 2-16
87	SW1/4-10-32N-5W	Stanolind Oil & Gas Co. San Juan #3

Appendix 2

Paleocurrent vector means, Rayleigh statistics, and paleocurrent indicators for stations in the study area. Stations are located in Figs. 29 and 30. * Vector mean does not pass the Rayleigh test of significance; + data are bimodal at the 67% confidence level; N = number of measurements; mean = vector mean; L = vector magnitude (in percent); P = Rayleigh's probability that the vector represents random data.

	3D				2D + 3D					
Station	N	Mean	L	P	N	Mean	L	P	Indicator	Unit
1	13	117	86	<10-4	20	119	77	<10-5	lg. scale	Tsr
2	4	206*	62	>.1	16	205*	43	>.05	lg. scale	Tsr
"					8	251*	34	>.3	sm. scale	Tsr
"	2	227*	99	>.2					part. lin.	Tsr
3	2	199*	96	>.1	7	192	80	<.01	lg. scale	Tsr
4	12	253	75	<.01	17	249	69	<10-3	lg. scale	Tsr
5	12	215	89	<10-4	21	222+	87	<10-5	lg. scale	Tsr
6	12	207	56	<.03	23	193+	58	<10-3	lg. scale	Tsr
7	5	235	96	<.02	14	233	71	<10-3	lg. scale	Tsr
8	1	300*			6	303	73	<.03	lg. scale	Tslt
9	4	200*	78	>.05	18	199	56	<.01	lg. scale	Tsr
10	4	233	97	<.03	21	202	73	<10-4	lg. scale	Tsr
11	1	145*			7	121	76	<.02	lg. scale	Tsr
12	2	213*	99	>.1	5	242	91	<.02	lg. scale	Tsr
13	13	132	69	<.01	24	128*	33	>.05	lg. scale	Tsr
14	11	257	92	<10-3	17	264	91	<10-5	lg. scale	Tsr
15	11	231	85	<10-4	21	232	85	<10-5	lg. scale	Tsr
16	6	206*	67	>.05	13	187	71	<.01	lg. scale	Tsr
17	2	217*	99	>.1	7	232	87	<.01	lg. scale	Tslt
18	7	208	90	<.01	19	232	87	<10-5	lg. scale	Tslt
19	4	244*	4	>.99	11	218*+	9	>.9	lg. scale	Tsr
20	14	143	64	<.01	46	123+	43	<10-3	lg. scale	Tsr
"					6	145*	49	>.2	sm. scale	Tsr
21	10	145	90	<10-3	27	139	74	<10-3	lg. scale	Tsr
22	8	182*	49	>.1	34	168	34	<.02	lg. scale	Tsr
"	2	257*	84	>.1	8	118*	52	>.1	sm. scale	Tsr
23	5	243*	75	>.05	14	258*+	35	>.1	lg. scale	Tsr
"	4	260	97	<.03					flutes	Tsr
"	5	58-238	92	<.02					long. grov.	Tsr
24	4	284*	59	>.2	11	274	67	<.01	lg. scale	Tsr
"					5	240*	61	>.1	sm. scale	Tsr
"	1	175*							flute	Tsr
"	6	160-340	95	<.01					long. grov.	Tsr
25					3	142*	22	>.8	lg. scale	Tsr
"	1	90-270*							part. line.	Tsr
"	2	127-307*	99	>.1					long. grov.	Tsr
26	3	216*	56	>.3	13	230+	70	<.01	lg. scale	Tsr
"	8	151	85	<.01	11	139	83	<10-3	sm. scale	Tsr
27	18	227	65	<10-3	33	215	58	<10-4	lg. scale	Tsr
28a	9	139*	36	>.2	15	149	47	<.04	lg. scale	Tsr
28b	8	177	63	<.04	13	219	49	>.04	lg. scale	Tsr
28(both)	17	171	45	<.03	28	188	40	<.02	lg. scale	Tsr

Appendix 2 continued

	3D				2D + 3D					
Station	N	Mean	L	P	N	Mean	L	P	Indicator	Unit
29	13	125	63	<.01	27	137+	59	<10-4	lg. scale	Tsr
30	2	247*	98	>.1	16	222	63	<.01	lg. scale	Tslt

Summary of data totals: (TA = trough axes; CB = crossbeds)
3D TA+CB large scale = 220 2D+3D TA+CB large scale = 539
3D TA+CB small scale = 10 2D+3D TA+CB small scale = 38
flutes = 5; longitudinal grooves = 13; parting lineation = 3

Tests for polymodality of paleocurrent data. * Significant concentrations No > Ne + S; Ne = average number of readings in groups; S = standard deviation for readings in a group; No = threshold value for significance at 67% confidence; Polymodal = more than 2 measurements of a significant concentration separated by one or more groups.

	Station									
Interval	1	2	3	4	5	6	7	8	9	10
0-29	0	0	0	0	0	0	0	0	0	0
30-59	1	0	0	1	0	0	1	0	0	0
60-89	2	0	0	0	0	0	0	0	0	1
90-119	5*	0	0	0	0	2	0	1	2	1
120-149	7*	3*	1	0	0	2	0	0	3	1
150-179	3	3*	1	2	1	6*	2	0	1	2
180-209	1	3*	2*	1	8*	3	2	0	3	6*
210-239	0	2	2*	3	3	2	2	0	4*	7*
240-269	0	0	1	6*	7*	6*	5*	2*	3	2
270-299	0	2	0	3	2	1	2	0	2	1
300-329	0	1	0	1	0	0	0	1	0	0
330-359	1	2	0	0	0	1	0	2*	0	0
Total	20	16	7	17	21	23	14	6	18	21
Ne	1.67	1.33	0.58	1.42	1.75	1.92	1.17	0.5	1.5	1.42
S	2.27	1.3	0.79	1.83	2.86	2.15	1.53	0.8	1.51	1.83
No	3.93	2.64	1.37	3.25	4.61	4.07	2.69	1.3	3.01	3.25
Polymodal					X	X				

Appendix 2 continued

	Station									
Interval	11	12	13	14	15	16	17	18	19	20
0-29	0	0	2	0	0	0	0	0	1	4
30-59	1	0	1	0	0	0	0	0	2*	7*
60-89	1	0	3	0	0	0	0	0	0	3
90-119	0	0	5*	0	0	0	0	0	0	6
120-149	2	0	2	0	0	2	0	0	2*	8*
150-179	3*	0	2	0	1	4*	0	1	0	6
180-209 *	0	1	3	0	3	2	1	2	1	5
210-239 *	0	1	3	2	9*	2	3*	8*	2*	4
240-269	0	2*	1	9*	5*	2	2*	5*	1	2
270-299	0	1	0	4	3	0	1	3	1	0
300-329	0	0	1	2	0	1	0	0	1	0
330-359	0	0	1	0	0	0	0	0	0	1
Total	7	5	24	17	21	13	7	19	11	46
Ne	0.5	0.42	2	1.42	1.75	1.08	0.58	1.58	0.92	3.83
S	0.91	0.67	1.35	2.71	2.83	1.31	1	2.57	0.79	2.69
No	1.41	1.09	3.35	4.13	4.58	2.39	1.58	4.16	1.71	6.52
Polymodal										X

	Station										
Interval	21	22	23	24	25	26	27	28a	28b	29	30
0-29	1	2	0	1	0	0	0	1	0	0	0
30-59	0	2	1	0	0	1	0	0	0	1	1
60-89	1	3	0	0	1*	0	0	0	0	6*	0
90-119	4	2	0	0	0	0	2	2	1	6*	1
120-149	11*	5*	2	0	0	1	2	2	2	2	0
150-179	6*	5*	1	1	0	3*	4	5*	2	5*	1
180-209	2	4	0	0	0	2	7*	1	0	3	4*
210-239	1	4	3*	1	1*	1	6*	1	3*	3	4*
240-269	0	3	2	4	0	2	7*	1	2	1	4*
270-299	0	3	0	2	0	3*	1	0	2	0	1
300-329	1	0	4*	2	1*	0	2	0	1	0	0
330-359	0	1	1	0	0	0	2	2	0	0	0
Total	27	34	14	11	3	13	33	14	13	27	16
Ne	2.25	2.83	1.17	0.92	0.25	1.08	2.75	1.25	1.08	2.25	1.33
S	3.31	1.53	1.34	1.24	0.45	1.16	2.63	1.42	1.08	2.35	1.67
No	5.56	4.36	2.51	2.16	0.7	2.24	5.38	2.67	2.16	4.59	3.00
Polymodal			X			X				X	

Appendix 3

Fossil localities. * Section is truncated N-S; coordinates derived by treating as a complete section with northern boundary as reference line.

Locality number (this report)	Previous number	Map coordinates
1	NMMNH 600	NE1/4NE1/4NW1/4NW1/4
	UNM B 77-928	Sec. 26, T. 29 N. R. 5 W.
2	NMMNH 601	SE1/4NW1/4NW1/4NW1/4
	UNM B 77-929	Sec. 26, T. 29 N. R. 5 W.
3	NMMNH 602	SE1/4NE1/4NW1/4NW1/4
	UNM B 77-930	Sec. 26, T. 29 N. R. 5 W.
4	NMMNH 603	SW1/4SW1/4NE1/4SW1/4
	UNM B 77-927	Sec. 26, T. 29 N. R. 5 W.
5	NMMNH 604	NW1/4SW1/4SE1/4NE1/4
	UNM B 77-950	Sec. 27, T. 29 N. R. 5 W.
6	NMMNH 605	NE1/4SW1/4SE1/4NE1/4
	UNM B 77-944	Sec. 27, T. 29 N. R. 5 W.
7	NMMNH 606	SE1/4SW1/4SE1/4NE1/4
	UNM B 77-942	Sec. 27, T. 29 N. R. 5 W.
8	NMMNH 607	NW1/4SW1/4NE1/4SE1/4
	UNM B 77-943	Sec. 27, T. 29 N. R. 5 W.
9	NMMNH 608	SE1/4NE1/4SW1/4SE1/4
	UNM B 77-941	Sec. 27, T. 29 N. R. 5 W.
10	NMMNH 609	SW1/4NW1/4SE1/4SE1/4
	UNM B 77-945	Sec. 27, T. 29 N. R. 5 W.
11	NMMNH 610	NE1/4SE1/4NE1/4NE1/4
	UNM B 77-935	Sec. 34, T. 29 N. R. 5 W.
12	NMMNH 611	SE1/4NE1/4SE1/4NE1/4
	UNM B 77-937	Sec. 34, T. 29 N. R. 5 W.
13	NMMNH 612	NW1/4SE1/4SE1/4NE1/4
	UNM B 77-939	Sec. 34, T. 29 N. R. 5 W.
14	NMMNH 613	SE1/4SW1/4SE1/4NE1/4
	UNM B 77-936	Sec. 34, T. 29 N. R. 5 W.
15	NMMNH 614	SW1/4NE1/4NE1/4SE1/4
	UNM B 77-938	Sec. 34, T. 29 N. R. 5 W.
16	NMMNH 615	NE1/4NW1/4NW1/4SW1/4
	UNM B 77-940	Sec. 35, T. 29 N. R. 5 W.
17	NMMNH 616	NE1/4SE1/4SW1/4SW1/4
	UNM B 77-932	Sec. 35, T. 29 N. R. 5 W.
18	NMMNH 617	SE1/4SE1/4SW1/4SW1/4
	UNM B 77-931	Sec. 35, T. 29 N. R. 5 W.
19	NMMNH 618	SE1/4SE1/4NW1/4NW1/4
	UNM B 77-934	Sec. 11, T. 28 N. R. 5W*
20	NMMNH 619	SE 1/4SE1/4NE1/4NE1/4
	UNM B 77-933	Sec. 15, T. 28 N. R. 5 W.
21	NMMNH 620	SE1/4NW1/4NE1/4NE1/4
	UNM B 77-946	Sec. 27, T. 28 N. R. 5 W.
22	NMMNH 621	SE1/4NW1/4NE1/4SE1/4
	UNM B 77-947	Sec. 27, T. 28 N. R. 5 W.
23	Ash et al. (1979) loc. 58	NE1/4NW1/4NW1/4SE1/4 Sec. 29, T. 28 N. R. 5 W.

Appendix 3 continued

Locality number (this report)	Previous number	Map coordinates
24	no previous number	NW1/4SE1/4SE1/4SW1/4 sec. 21, T. 28 N. R. 6 W.
25	Ash et al. (1979) loc. 59	NE1/4SW1/4SE1/4SE1/4 sec. 6, T. 27 N. R. 5 W.
26	Ash et al. (1979) loc. 60	SW1/4SE1/4SE1/4SE1/4 sec. 6, T. 27 N. R. 5 W.
27	Ash et al. (1979) loc. 62	NE1/4NW1/4NE1/4NE1/4 sec. 7, T. 27 N. R. 5 W.
28	Ash et al. (1979) loc. 61	SW1/4SW1/4SW1/4SW1/4 sec. 5, T. 27 N. R. 5 W.
29	Ash et al. (1979) loc. 63	SW1/4SE1/4SE1/4SW1/4 sec. 5, T. 27 N. R. 5 W.
30	Ash et al. (1979) loc. 64	NE1/4NE1/4SW1/4NE1/4 sec. 8, T. 27 N. R. 5 W.
31	NMMNH 622 UNM B 77-1104	SW1/4SE1/4SE1/4NW1/4 sec. 3, T. 27 N. R. 5 W.
32	NMMNH 623 UNM B 77-1103 = Ash et al. (1979) loc. 65	NE1/4SW1/4SW1/4SE1/4 sec. 3, T. 27 N. R. 5 W.
33	Ash et al. (1979) loc. 66	SW1/4NE1/4SE1/4SW1/4 sec. 2, T. 27 N. R. 5 W.
34	Ash et al. (1979) loc. 67	SW1/4NE1/4SE1/4NE1/4 sec. 8, T. 27 N. R. 5 W.
35	Ash et al. (1979) loc. 68	NW1/4SW1/4SW1/4NW1/4 sec. 9, T. 27 N. R. 5 W.
36	Ash et al. (1979) loc. 70	SW1/4NW1/4SE1/4SW1/4 sec. 9, T. 27 N. R. 5 W.
37	Ash et al. (1979) loc. 69	NE1/4NE1/4SW1/4NW1/4 sec. 10, T. 27 N. R. 5 W.
38	Ash et al. (1979) loc. 78	NE1/4NW1/4SE1/4SW1/4 sec. 15, T. 27 N. R. 5 W.
39	Ash et al. (1979) loc. 71	center SW1/4SW1/4NE1/4 sec. 15, T. 27 N. R. 5 W.
40	Ash et al. (1979) loc. 72	SE1/4SE1/4NW1/4NE1/4 sec. 14, T. 27 N. R. 5 W.
41	Ash et al. (1979) loc. 73	NE1/4NW1/4SE1/4NE1/4 sec. 14, T. 27 N. R. 5 W.
42	Ash et al. (1979) loc. 74	SW1/4SE1/4NE1/4NE1/4 sec. 14, T. 27 N. R. 5 W.
43	Ash et al. (1979) loc. 75	NW1/4SE1/4SW1/4NW1/4 sec. 13, T. 27 N. R. 5 W.
44	Ash et al. (1979) loc. 76	NW1/4NE1/4SE1/4NE1/4 sec. 25, T. 27 N. R. 5 W.
45	Ash et al. (1979) loc. 79	SE1/4SW1/4SE1/4NE1/4 sec. 25, T. 27 N. R. 5 W.
46	Ash et al. (1979) loc. 77	SW1/4SW1/4NE1/4NE1/4 sec. 35, T. 27 N. R. 5 W.

Selected conversion factors*

TO CONVERT	MULTIPLY BY	TO OBTAIN
Length		
inches, in	2.540	centimeters, cm
feet, ft	3.048×10^{-1}	meters, m
yards, yds	9.144×10^{-1}	m
statute miles, mi	1.609	kilometers, km
fathoms	1.829	m
angstroms, Å	1.0×10^{-8}	cm
Å	1.0×10^{-4}	micrometers, μm
Area		
in^2	6.452	cm^2
ft^2	9.29×10^{-2}	m^2
yds^2	8.361×10^{-1}	m^2
mi^2	2.590	km^2
acres	4.047×10^{3}	m^2
acres	4.047×10^{-1}	hectares, ha
Volume (wet and dry)		
in^3	1.639×10^{1}	cm^3
ft^3	2.832×10^{-2}	m^3
yds^3	7.646×10^{-1}	m^3
fluid ounces	2.957×10^{-2}	liters, l *or* L
quarts	9.463×10^{-1}	l
U.S. gallons, gal	3.785	l
U.S. gal	3.785×10^{-3}	m^3
acre-ft	1.234×10^{3}	m^3
barrels (oil), bbl	1.589×10^{-1}	m^3
Weight, mass		
ounces avoirdupois, avdp	2.8349×10^{1}	grams, gr
troy ounces, oz	3.1103×10^{1}	gr
pounds, lb	4.536×10^{-1}	kilograms, kg
long tons	1.016	metric tons, mt
short tons	9.078×10^{-1}	mt
oz mt^{-1}	3.43×10^{1}	parts per million, ppm
Velocity		
ft sec^{-1} (= ft/sec)	3.048×10^{-1}	m sec^{-1} (= m/sec)
mi hr^{-1}	1.6093	km hr^{-1}
mi hr^{-1}	4.470×10^{-1}	m sec^{-1}

TO CONVERT	MULTIPLY BY	TO OBTAIN
Pressure, stress		
lb in^{-2} (= lb/in^2), psi	7.03×10^{-2}	kg cm^{-2} (= kg/cm^2)
lb in^{-2}	6.804×10^{-2}	atmospheres, atm
lb in^{-2}	6.895×10^{3}	newtons (N)/m^2, N m^{-2}
atm	1.0333	kg cm^{-2}
atm	7.6×10^{2}	mm of Hg (at 0° C)
inches of Hg (at 0° C)	3.453×10^{-2}	kg cm^{-2}
bars, b	1.020	kg cm^{-2}
b	1.0×10^{6}	dynes cm^{-2}
b	9.869×10^{-1}	atm
b	1.0×10^{-1}	megapascals, MPa
Density		
lb in^{-3} (= lb/in^3)	2.768×10^{1}	gr cm^{-3} (= gr/cm^3)
Viscosity		
poises	1.0	gr cm^{-1} sec^{-1} *or* dynes cm^{-2}
Discharge		
U.S. gal min^{-1}, gpm	6.308×10^{-2}	l sec^{-1}
gpm	6.308×10^{-5}	m^3 sec^{-1}
ft^3 sec^{-1}	2.832×10^{-2}	m^3 sec^{-1}
Hydraulic conductivity		
U.S. gal day^{-1} ft^{-2}	4.720×10^{-7}	m sec^{-1}
Permeability		
darcies	9.870×10^{-13}	m^2
Transmissivity		
U.S. gal day^{-1} ft^{-1}	1.438×10^{-7}	m^2 sec^{-1}
U.S. gal min^{-1} ft^{-1}	2.072×10^{-1}	l sec^{-1} m^{-1}
Magnetic field intensity		
gausses	1.0×10^{5}	gammas
Energy, heat		
British thermal units, BTU	2.52×10^{-1}	calories, cal
BTU	1.0758×10^{2}	kilogram-meters, kgm
BTU lb^{-1}	5.56×10^{-1}	cal kg^{-1}
Temperature		
°C + 273	1.0	°K (Kelvin)
°C + 17.78	1.8	°F (Fahrenheit)
°F − 32	5/9	°C (Celsius)

**Divide by* the factor number to reverse conversions.
Exponents: for example 4.047×10^{3} (see acres) = 4,047; 9.29×10^{-2} (see ft^2) = 0.0929.

Editor: Jiri Zidek

Typeface: Palatino

Presswork: Miehle Single Color Offset
Harris Single Color Offset

Binding: Saddlestitched with softbound cover

Paper: Cover on 12-pt. Kivar
Text on 70-lb white matte

Ink: Cover—PMS 320
Text—Black

Quantity: 1000

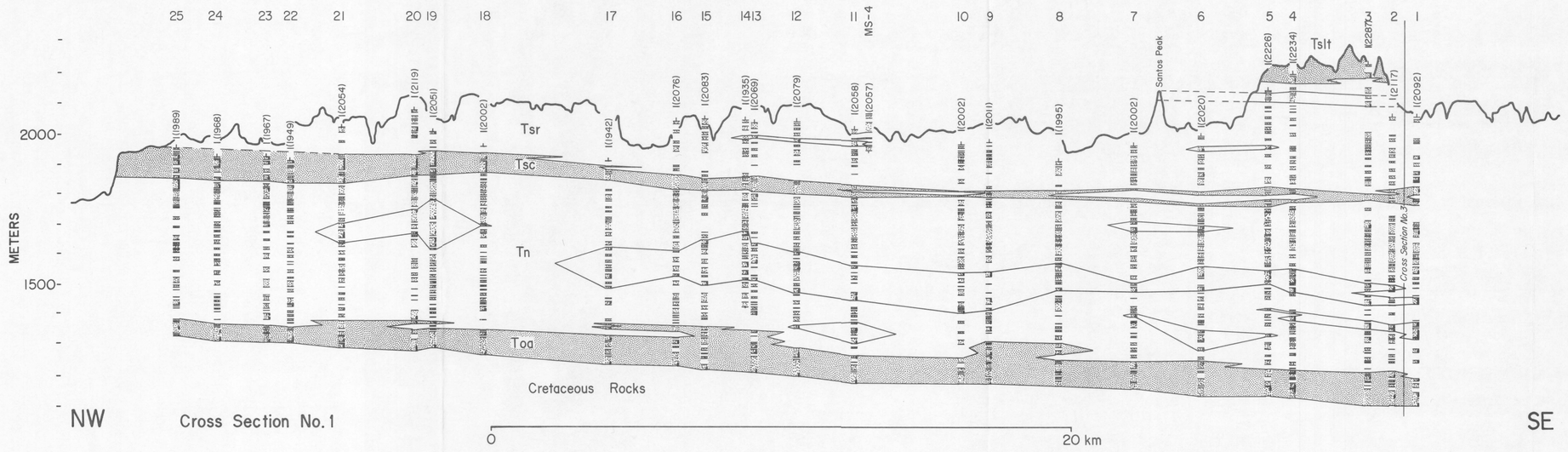

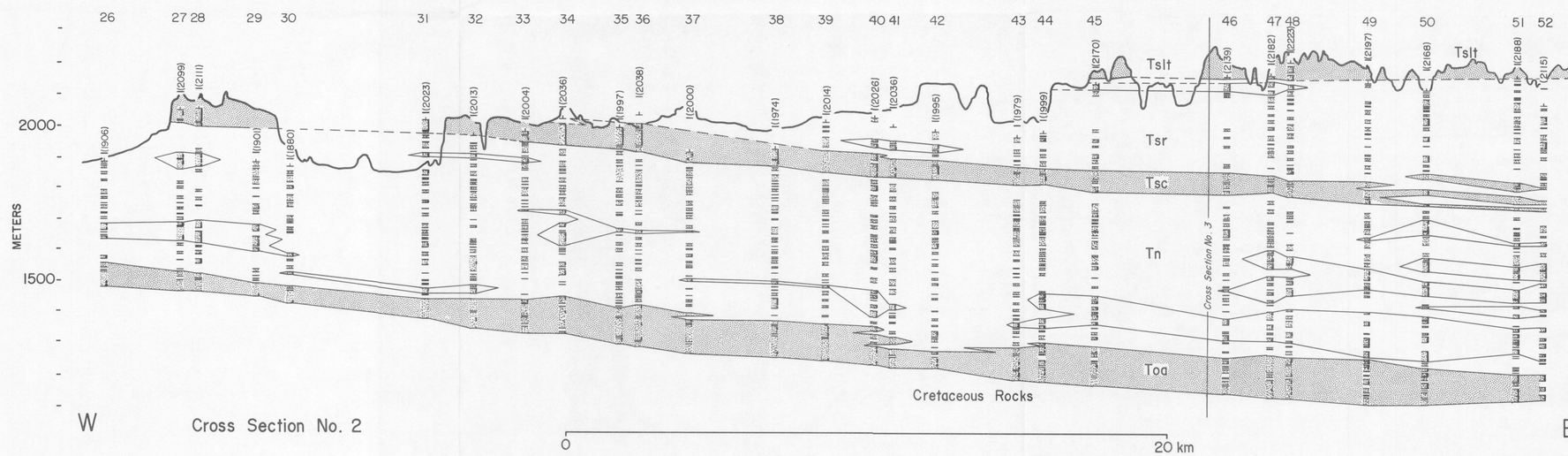

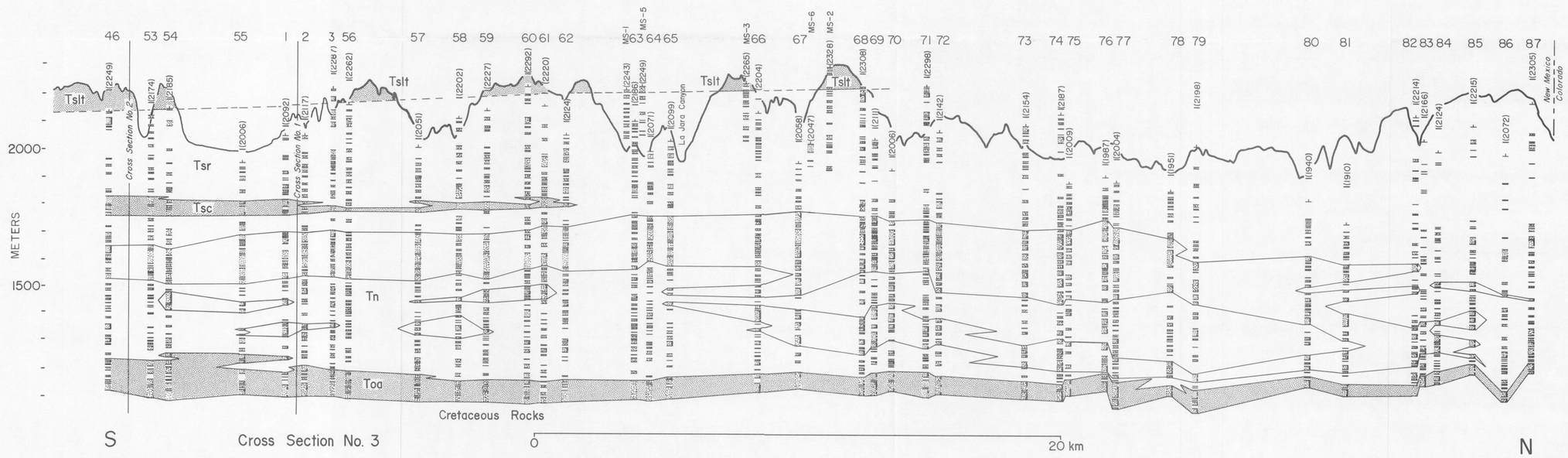

KEY

Well Log No.- 23

Ground Level Elevation

Top of Log

Present Topography

Sandstone

Mudrock

High Resistivity Interval of Sandstone

MS - Measured Section

SAN JOSE FORMATION

Tslt — Llaves and Tapicitos members

Tsr — Regina Member

Tsc — Cuba Mesa Member

Tn — NACIMIENTO FORMATION

Toa — OJO ALAMO SANDSTONE

Vertical Exaggeration = 10 X